REPORT NO. DOT-TSC-FAA-73-32

ATCRB ANTENNA MODIFICATION KIT - PHASE I

V. Mazzola
P.W. Hannon
E.M. Newman
P. Kendrick

APRIL TO JUNE 1973
INTERIM REPORT

Prepared for:

DEPARTMENT OF TRANSPORTATION
FEDERAL AVIATION ADMINISTRATION
Systems Research and Development Service
Washington DC 20591

Technical Report Documentation Pa

1. Report No.	2. Government Accession No.	3. Recipient's Catalog No.

4. Title and Subtitle
ATCRBS ANTENNA MODIFICATION KIT - PHASE I

5. Report Date

6. Performing Organization Code

7. Author(s) V. Mazzola, P.W. Hannan, E.M. Newman, P. Kendrick

8. Performing Organization Report No.
DOT-TSC-FAA-73-32

9. Performing Organization Name and Address
Hazeltine Corporation
Greenlawn NY 11740

10. Work Unit No. (TRAIS)
FA-419/R4102

11. Contract or Grant No.
DOT-TSC-598

12. Sponsoring Agency Name and Address
Department of Transportation
Federal Aviation Administration
Systems Research & Development Service
Washington DC 20591

13. Type of Report and Period Covered
Interim Report
April to June 1973

14. Sponsoring Agency Code

15. Supplementary Notes
*Under Contract to: Department of Transportation
Transportation Systems Center
Kendall Square
Cambridge MA 02142

16. Abstract This report presents the results of a study performed for Transportation Systems Center/DOT to establish the feasibility of an improved ATCRBS (Air Traffic Control Radar Beacon System) antenna with increased vertical aperture. The study concluded that a four-foot high array can be directly substituted for the existing ATCRBS antenna.

The array consists of a 4-foot by 26-foot structure with 252 dipole radiating elements. The wind loading on the array is minimized by using an open ground plane consisting of small aluminum tubes and specially designed tuned reflectors.

The report presents mechanical and electrical analyses of antenna performance, preliminary design results, experimental measurements on a small array section, and an estimate of the growth potential of the present design.

The study was performed under the cognizance of the Air Traffic Control Product Line of Hazeltine, with technical direction the responsibility of the Wheeler Laboratory antenna group.

17. Key Words	18. Distribution Statement
Antenna Radar Beacon Tuned Reflector Air Traffic Control	

19. Security Classif. (of this report)	20. Security Classif. (of this page)	21. No. of Pages	22. Price
Unclassified	Unclassified		

Form DOT F 1700.7 (8-72) Reproduction of completed page authorized

Engineering Report

Phase I

ATCRBS ANTENNA MODIFICATION KIT

Prepared by: V. Mazzola
V. Mazzola
Engineering Leader,
Antenna Design

P. W. Hannan
P. W. Hannan
Consultant, Antenna Design

E. M. Newman
E. M. Newman
Antenna Design, Sr. Engineer

P. Kendrick
P. Kendrick
Mechanical Engineer

Approved by: J. H. Gutman
J. H. Gutman
Program Manager

G. E. Vaupel
G. E. Vaupel
Wheeler Laboratory Head

H. Huebscher
H. Huebscher
Vice President, ATC

615

TABLE OF CONTENTS

TABLE OF CONTENTS (Cont)

TABLE OF CONTENTS (Cont)

LIST OF ILLUSTRATIONS

LIST OF ILLUSTRATIONS (cont)

LIST OF TABLES

SUMMARY

This report presents the results of a study performed for Transportation Systems Center/DOT to establish the feasibility of an improved ATCRBS (Air Traffic Control Radar Beacon System) antenna with increased vertical aperture. The study concluded that a four-foot high array can be directly substituted for the existing ATCRBS antenna.

The array consists of a 4-foot by 26-foot structure with 252 dipole radiating elements. The wind loading on the array is minimized by using an open ground plane consisting of small aluminum tubes and specially designed tuned reflectors.

The report presents mechanical and electrical analyses of antenna performance, preliminary design results, experimental measurements on a small array section, and an estimate of the growth potential of the present design.

The study was performed under the cognizance of the Air Traffic Control Product Line of Hazeltine, with technical direction the responsibility of the Wheeler Laboratory antenna group.

INTRODUCTION

General

The objective of the ATCRBS antenna program is to provide improved antenna performance in order to enhance overall system operation. The present antenna that is employed, or similar linear arrays, have serious performance limitations because of their limited vertical aperture. This limited vertical aperture produces vertical lobing in the presence of the ground which results in signal loss and in some cases over-interrogation of beacon targets. In addition, there are problems associated with the operation of the sidelobe suppression system. The conclusion that has been reached by many workers in the field is that a larger vertical aperture is required in the beacon system to provide the needed system reliability.

The ATCRBS antenna improvement program at Hazeltine has as its objective the achievement of maximum performance within the constraints imposed by the ASR and ARSR systems. We believe we have developed a simple low-cost antenna design which does not require any significant changes to these existing systems. To achieve our objective we have adopted the concept of direct replacement of the existing FA7202 antenna. We believe we can provide increased antenna performance utilizing a larger vertical aperture without increasing significantly the wind or weight loads on the existing ASR system.

For the ARSR case, we are proposing the identical antenna design mainly from the standpoint of commonality, and we believe that its attractive features are simplicity in installation and the reliability of overall system operation.

The Hazeltine approach uses a novel arrangement of an open ground plane consisting of tuned reflectors in which two thirds of the area is left open. Results of studies and pattern experiments

conducted prior to the Phase I study program and also during the Phase I program have lead us to conclude that the feasibility of this approach has been well established. Results of our study show that a four foot high aperture can be employed without increasing wind loads on the existing ASR system. An antenna of four foot height will provide substantial improvement over existing performance.

This report will cover the following subjects.

Summary of Phase I Study

This section discusses the overall objective of the program, namely, the achievement of improved antenna performance by utilization of a larger vertical aperture in the antenna. The basic ATCRBS antenna problem will also be discussed including calculated results and correlation with measurements of the vertical lobing patterns for the existing antenna. The design constraints imposed by the ASR and ARSR are also discussed and a description of the overall open-array approach is given. The concept of the open reflector is described and the manner by which the design is achieved. Also included is the method of installation on the ASR and ARSR systems. Finally, a summary of results and tasks performed during Phase I will be given.

ATCRBS Antennna Design

Electrical Design. System layouts including RF diagrams and calculated patterns are presented. The aperture design approach including the effects of mutual coupling in the open array and tuned rod design considerations is presented. RF component design is discussed, specifically, the design of the elevation networks and sum and difference networks, dipoles and cabling. Performance estimates are also presented and proposed specifications for Phase II of the development program are given.

Radiation Pattern Tests. This section includes a discussion of the objectives of these tests and a description of the test set-up and measured results on the partial array breadboard. Also described are various milestones and design changes, such as provision for chokes, incorporated during the design and testing of the ground plane to improve performance. Finally, estimates of pattern performance on the full array are made using the results of element patterns measured on the small array.

Mechanical Design. This section includes a description of the mechanical layouts of the open-array and the omni antenna. Cable and connector details are discussed as well as weight analyses, environmental protection and design specifications.

ATCRBS Structural Design for ASR

This section discusses the method of mounting the ATCRBS open-array on the ASR. Also presented are the results of the wind load analysis conducted for this antenna and the structural analysis of both the ATCRBS and ASR reflectors in the non-operating and operating conditions.

ATCRBS/ASR Interface Analysis

This section covers the study conducted on the ASR system and the impact the open-array will have on this ASR system. A summary of the existing information on the ASR is presented, including bearing design, allowable reflector deflections and information on the motor drive. The analysis includes the impact of the new antenna on the bearing and drive of the ASR. Also presented are the results of the analysis of the impact of the open array on the ASR reflector in both an operating and non-operating mode.

ATCRBS ARSR Structural Design

This section describes the mounting arrangement and the method of installation on the ARSR. Also presented are the results of

the deflection analysis carried out for the open array antenna and the limited deflection analysis carried out on the ARSR feedboom.

Cost Benefit Studies

This study has as its prime purpose the review of the selection of a four foot vertical aperture for the open array and considerations of requirements in terms of modifications to the existing ASR for increased vertical aperture of greater than four foot height.

Site Configuration Plan

This section discusses the specific changes that should be made to the ASR and ARSR in order to implement the open-array antenna on the sites. Included is a discussion of maximum downtime as well as the procedure for actual installation of the new antenna.

Long-Range Testing

This section discusses the plans for long-range testing of the antenna. Detailed developmental testing will be carried out at the Smithtown antenna test range. This test range will provide all of the information required to complete development and fabrication of the antenna. Final tests will be performed on a longer range. A long test range has been selected; this section discusses the plans for testing at this range.

Heater System

This section discusses the power required at the site for deicing the antenna. Also discussed is a review of existing heater approaches as well as a thermal analysis and method of implementing a heater system in the open-array antenna.

Growth Potential

This section discusses additional uses for the 4 x 26 open array, applications for an open array with a larger vertical aperture, and the possibility for the addition of difference SLS to the open array for use with the ARSR.

Deliverable Items

This section enumerates the hardware and reports to be delivered during the performance of Phase II. The section also includes an antenna performance specification and the planned program schedule for Phase II.

SUMMARY OF PHASE I STUDY

Description of the Overall Antenna Approach

The antenna consists of a 4 foot high by 26 foot long dipole array. It contains 36 columns of dipoles, with each full column containing 8 dipoles as shown in figure 2-1. The dipoles are mounted on two-inch diameter aluminum tubes which permit a majority of the area to be left open to the wind. Each column of dipoles is fed by an elevation network located immediately below the column in the lower portion of the structure. Semi-rigid cable (.141 dia) is used to connect each of the dipoles to the elevation networks. The azimuth distribution network is located at the central portion of the antenna in the lower structure. It is connected by 1/4" dia semi-rigid cables to the 36 elevation networks to provide the proper azimuth distribution.

Figure 2-2 shows a portion of the open-array configuration. The radiating elements are dipoles in columns 9 inches apart. Each column of dipoles is mounted on a 2-inch diameter metal pipe containing the coaxial cables feeding the dipoles. Midway between each of these pipes is a 5/8-inch diameter "tuned reflector" that reflects the radiation from the dipoles and prevents the array from radiating toward the rear.

The open-array structure shown is about 2/3 open to the wind. This permits the array to be four feet high while having about the same windage as the present FA-7202 antenna, which is about 20 inches high. Detailed calculations of wind effects, including overturning moment and azimuth torque, are discussed in Section IV.

It should be noted that the open space on each side of the tuned reflectors is quite wide. As a result, a thin coating of ice will cause only a small increase in windage. In contrast, a reflecting surface made of wire mesh or multiple metal rods would

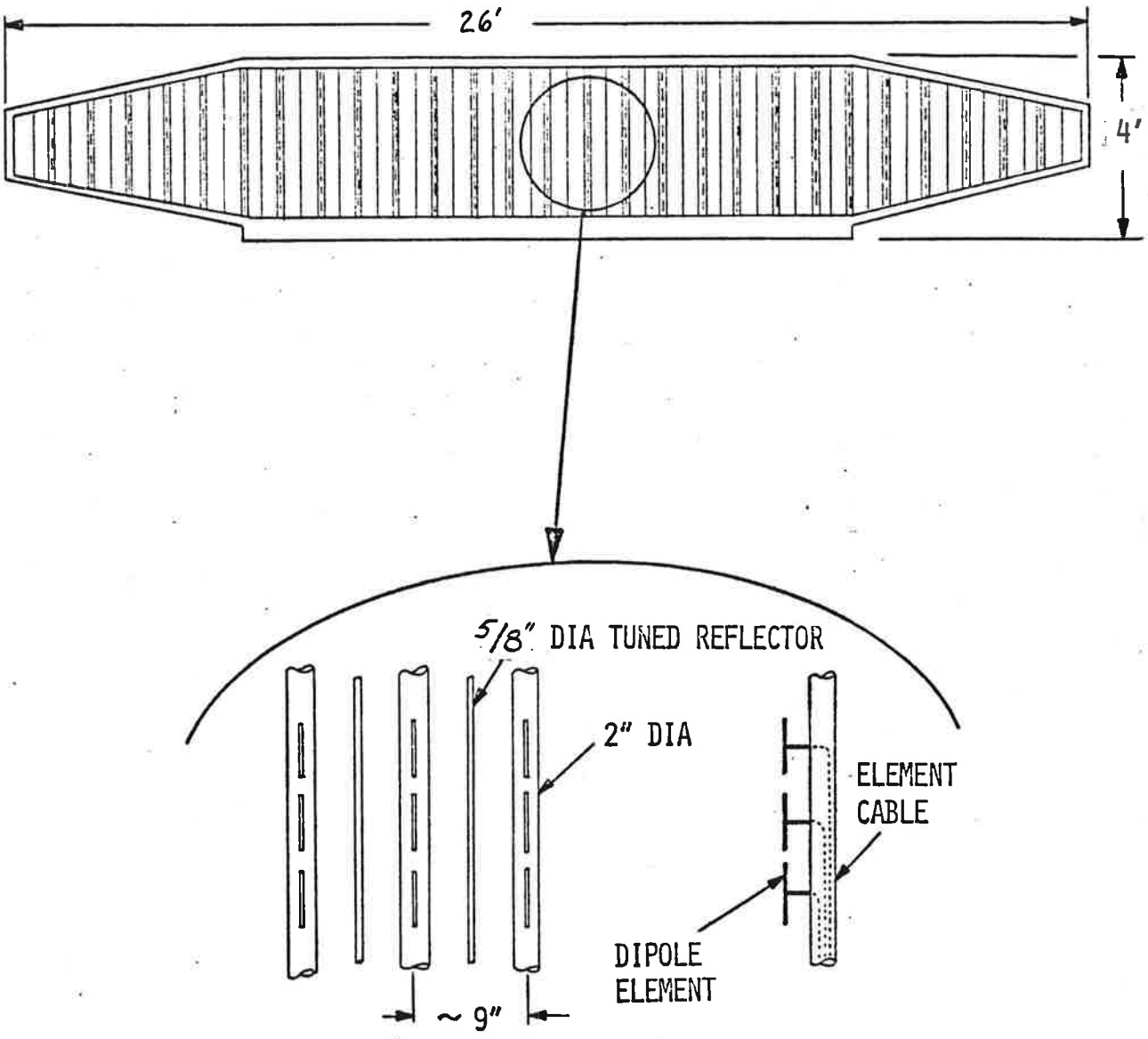

Figure 2-1. Descriptions of Open Array Antenna

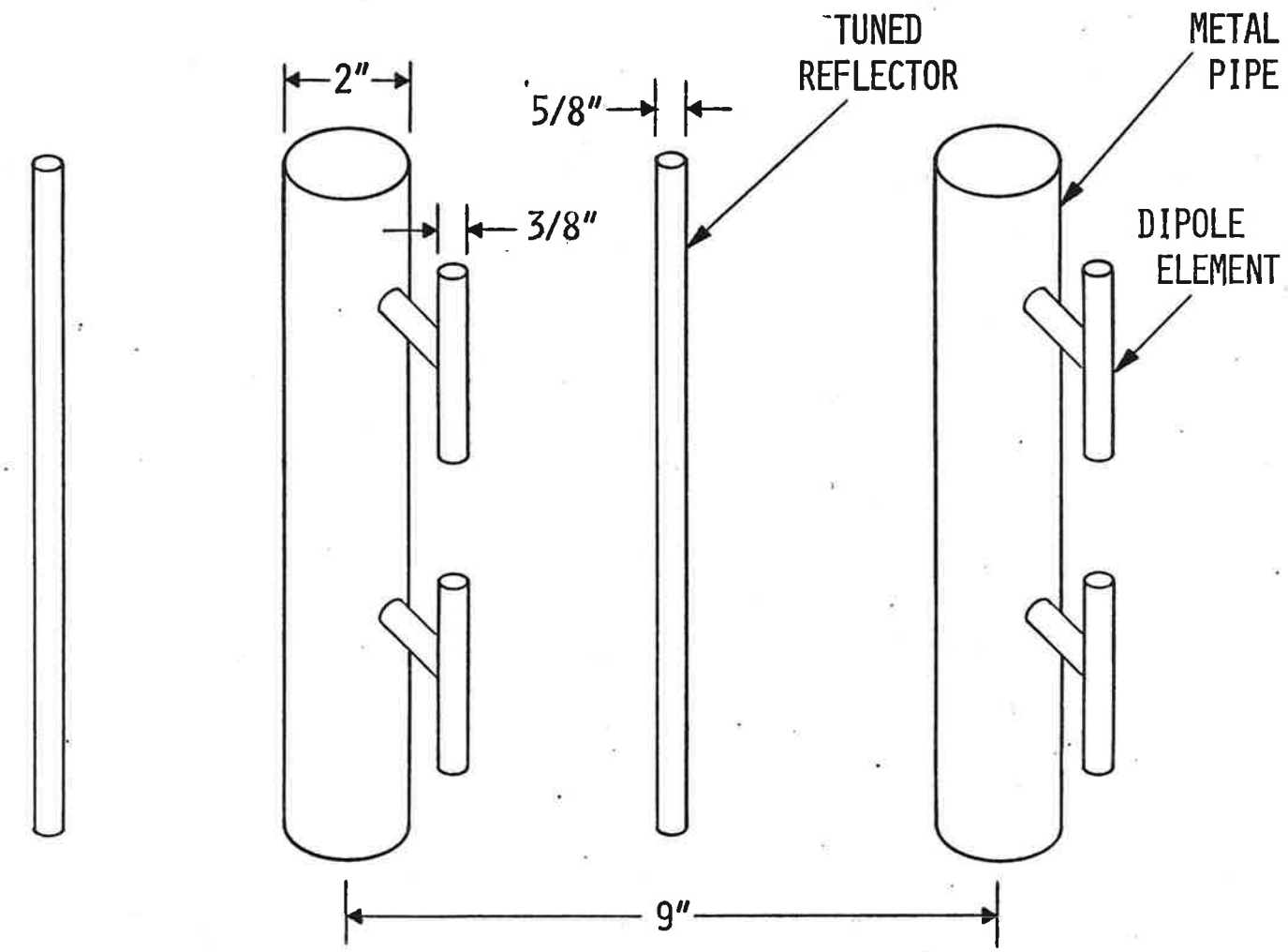

$$\frac{\text{OPEN AREA}}{\text{TOTAL AREA}} \approx \frac{2}{3}$$

Figure 2-2. Open Array

have to use smaller openings that would close up easily during iceing conditions. Even with no ice, such a reflecting surface would have less area open to the wind than the open array shown in figure 2-2.

The key component of the open array is the tuned reflector. Figure 2-3 indicates the basic principle of the tuned reflector, which consists of a series of metal rods separated by non-conducting gaps. Each metal rod acts like inductance and each gap acts like capacitance. This capacitance, which is in series with the inductance, tunes out the inductance to yield a resonant reflector that is much more effective as a reflector than a continuous metal rod would be. Detailed experimental verification of the tuned reflector in an open array configuration is described later in Section III.

Recommended Installation Configurations for ASR and ARSR

Figure 2-4 depicts the installation of the 4 foot open-array on the ASR. The antenna is mounted on top of the ASR reflector utilizing the mounting holes which are presently employed with the FA-7202 antenna. It is proposed that the omni antenna be placed on the existing pole at one corner of the tower platform. The omni antenna has an elevation pattern matched to that of the directive array, consequently, its height is also 4 feet.

Figure 2-5 depicts the installation of the open-array on the ARSR. Three possible mounting configurations have been studied; namely, on top of the reflector, back-to-back, and chin mounted. We have concluded that the chin mounted arrangement is most attractive. The companion omni antenna is shown installed below the radome roof. If it is decided that possible electrical degradation caused by proximity to the radome wall is serious, then an alternate configuration would be to mount the omni on top of the radome. A discussion of vertical lobing of the omni and open array antennas appears in Section XI.C.

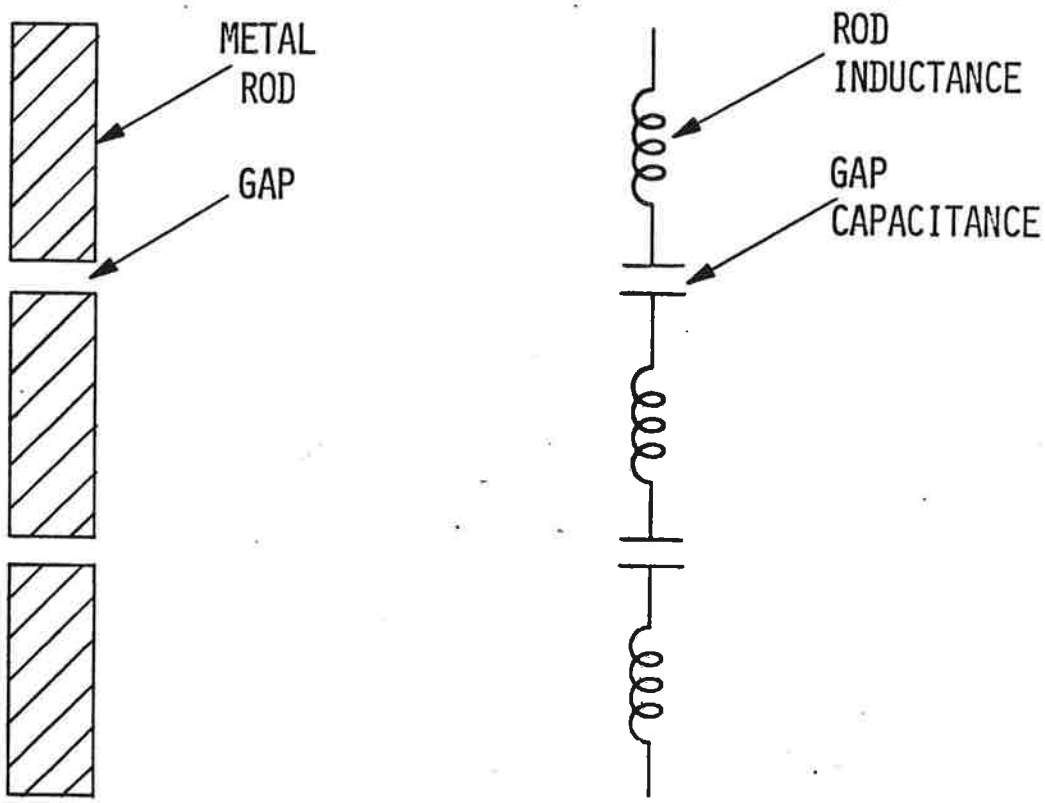

Figure 2-3. Basic Tuned Reflector

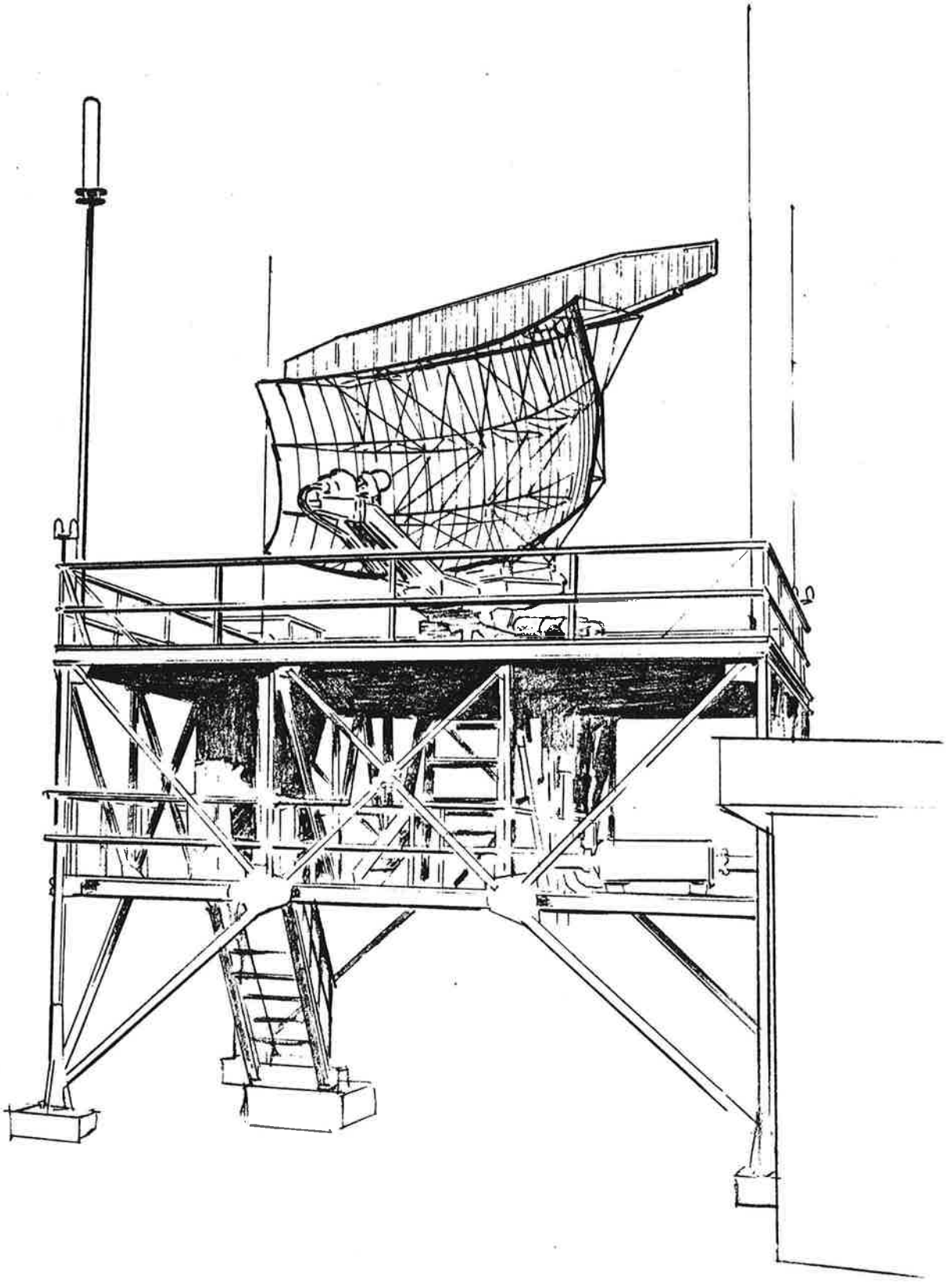

73333

Figure 2-4. Open Array on the ASR

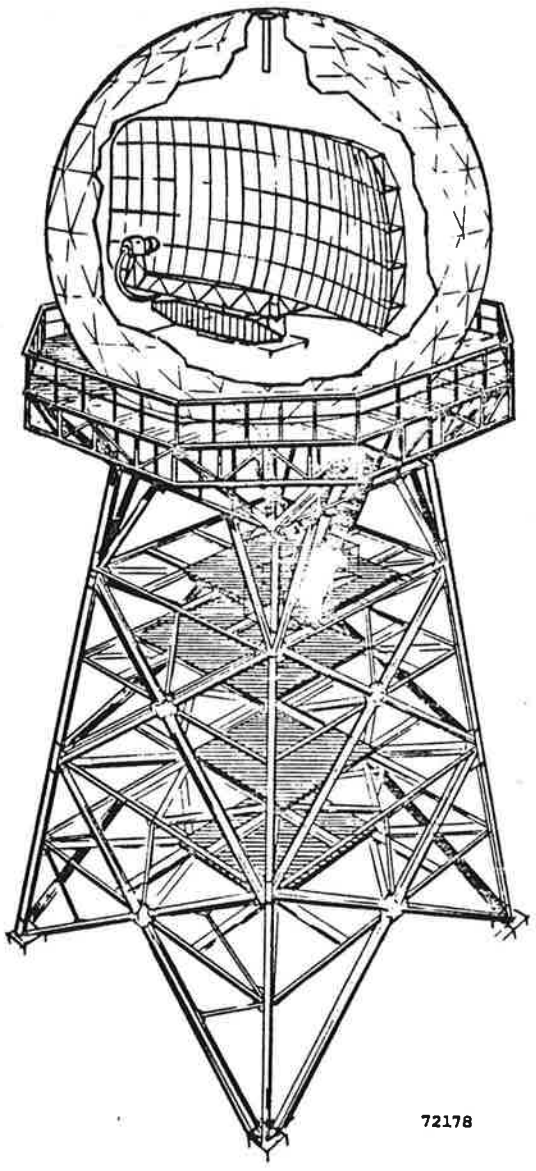

Figure 2-5. Open Array Under ARSR

Basic ATCRBS Antenna Limitations/Expected Improvements

Figure 2-6 depicts the present situation with regard to vertical lobing effects in the ATCRBS beacon system. The FA-7202 interrogator antenna has an antenna pattern as depicted in figure 2-6 (dotted line represents pattern in free-space). In the presence of ground, this pattern is perturbed as a result of reflections from the ground. The reflection adds with the direct signal to result in a lobing effect is detrimental to system performance because it results in a signal loss to some aircraft and over interrogation of other aircraft. The extent of this vertical lobing problem is dictated primarily by the size of the vertical aperture of the interrogator antenna. For very small vertical apertures, this lobing is quite significant because of the extensive amount of signal energy which is reflecting off the ground. Figure 2-7 shows actual measurements performed to verify the existence of this vertical lobing pattern. Shown on the figure is the vertical lobing pattern for the directional FA 7202 antenna and for the companion omni antenna. It is noted that several minima fall 20 dB below the peak level of the signal. The measurements shown here were performed over dry sandy loam and are taken from FAA report RD-67-59 entitled, "Analysis of SLS Capabilities at Joint-Use Radar Beacon Sites," August 1967, authored by George Spingler.

Figure 2-8 is a sketch of an elevation pattern which represents the ideal pattern for the beacon system. The lower limit of the pattern is slightly above the horizon, permitting illumination of targets at the maximum range but, having no signal energy below this angle, reflections from the ground are prevented. The pattern is more or less uniform up to some upper limit specified by the system at which a drop-off again occurs to prevent interrogation of targets immediately overhead. This ideal pattern can be exactly achieved only with an infinite vertical aperture.

Figure 2-9 shows the expected pattern performance of the 4-foot open array, as well as the pattern for the FA-7202 antenna. It

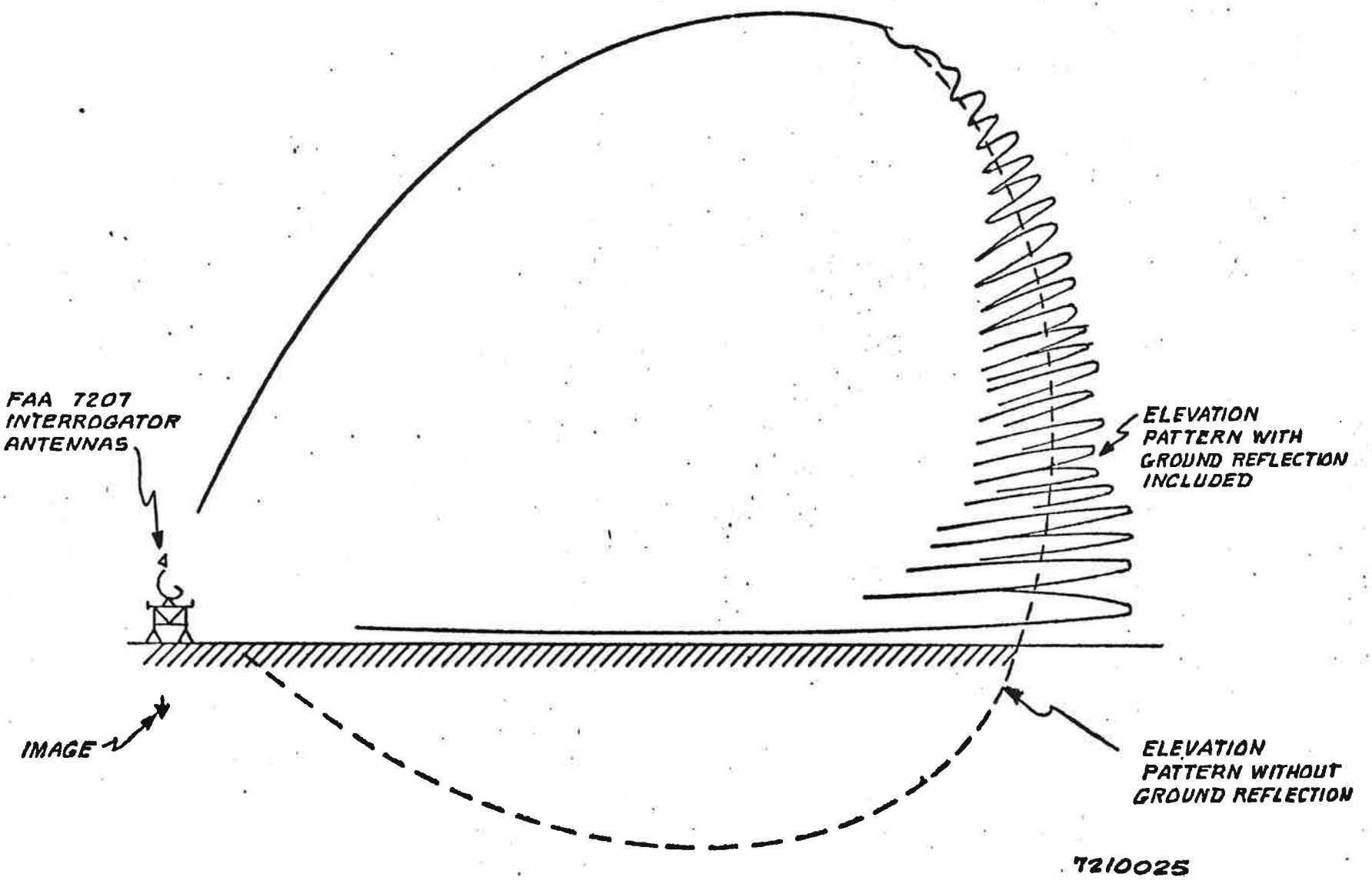

Figure 2-6. The Vertical Lobing Effect

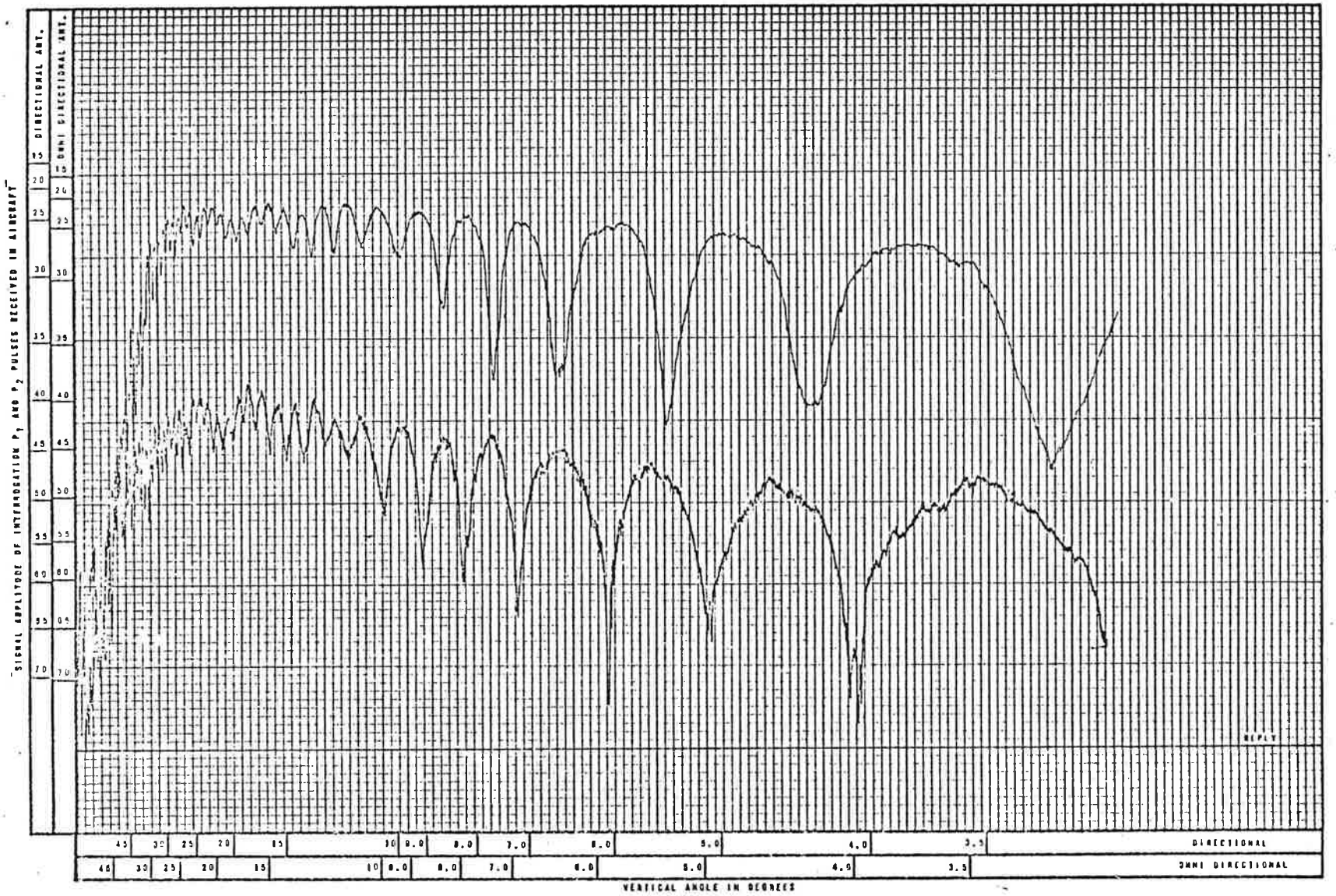

Figure 2-7. Vertical Radiation Pattern at 2,500 Feet Over Dry, Sandy Loam

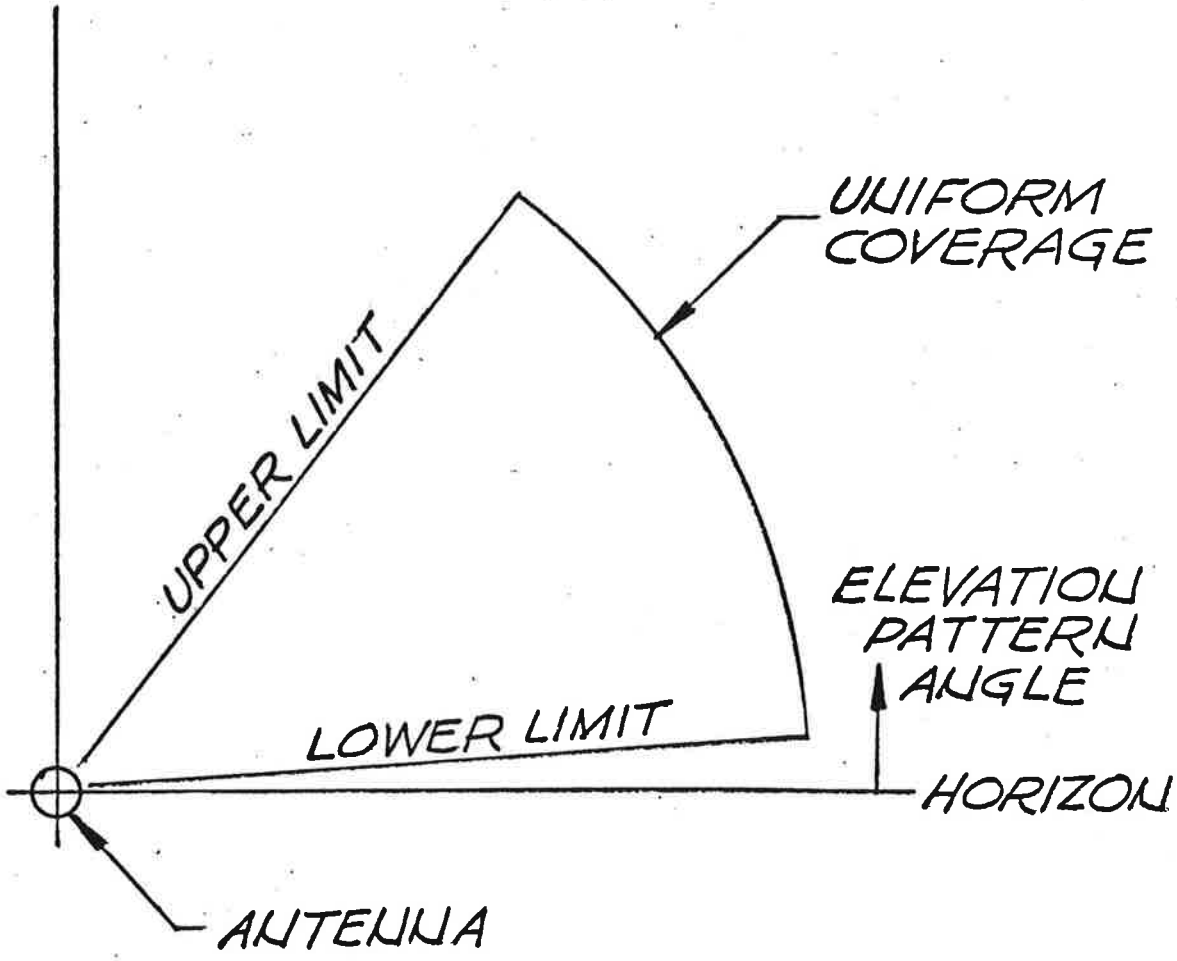

Figure 2-8. Ideal Elevation Pattern

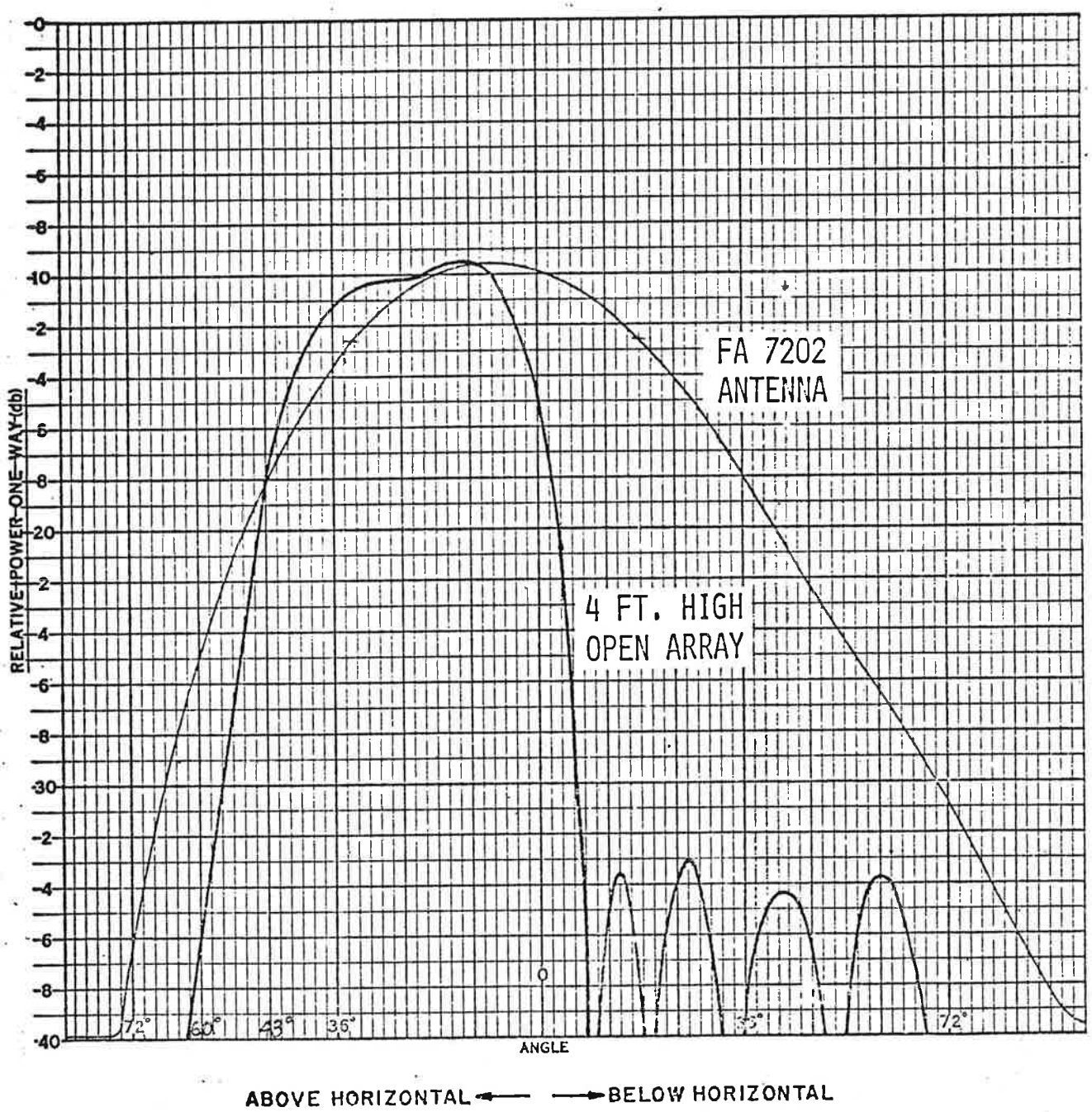

Figure 2-9. Typical Vertical Radiation Pattern, 1030 mc

should be noted that the four foot high array provides considerable reduction in signal strength below the horizon. In addition, the slope of the pattern at the horizon is considerably greater than the slope of the existing antenna. This increased slope will greatly reduce the vertical lobing that presently exists.

Figure 2-10 is a summary of the vertical lobing envelopes expected from the FA-7202, 4-ft open-array, and 8-ft E-scan cylindrical array antenna (normalized to an equal power basis). For each antenna, the two vertical lobing envelopes shown represent the maximum and minimum values in the vertical lobing pattern. The specific period of the ripple depends on the interrogator antenna height. The lower envelope determines minimum signal strength, while the upper envelope determines the extent of over-interrogation. The ideal case would be no separation between the upper and lower envelopes. As expected, the FA-7202, 4-foot and 8-foot antennas provide increasing performance in terms of envelope separation. The vertical lobing pattern of the FA-7202 antenna is significantly larger than either the 4-foot or 8-foot array. For example, at 2 degrees elevation angle, the maximum-to-minimum ratio for the FA-7202 is 19 dB, for the 4-foot open-array it is 10 dB, and for the 8-foot E-scan antenna it is 4 dB.

The vertical lobing envelope shown is calculated assuming a ground reflection characteristic of dry sandy loam. This type of ground represents nearly the highest reflection of any ground characteristic. We believe it is appropriate to represent the lobing patterns for this case since it represents a situtation where lobing problems will exist.

The points shown in the graph represent measured data taken from FAA report RD-67-59, entitled "Analysis of SLS Capabilities at Joint-Use Radar Beacon Sites," August 1967, authored by G. Spingler. Two sets of points are shown, consisting of measured data at a flight altitude of 2,500 feet and 1,000 feet. It is to be noted that these points cluster along the lower line

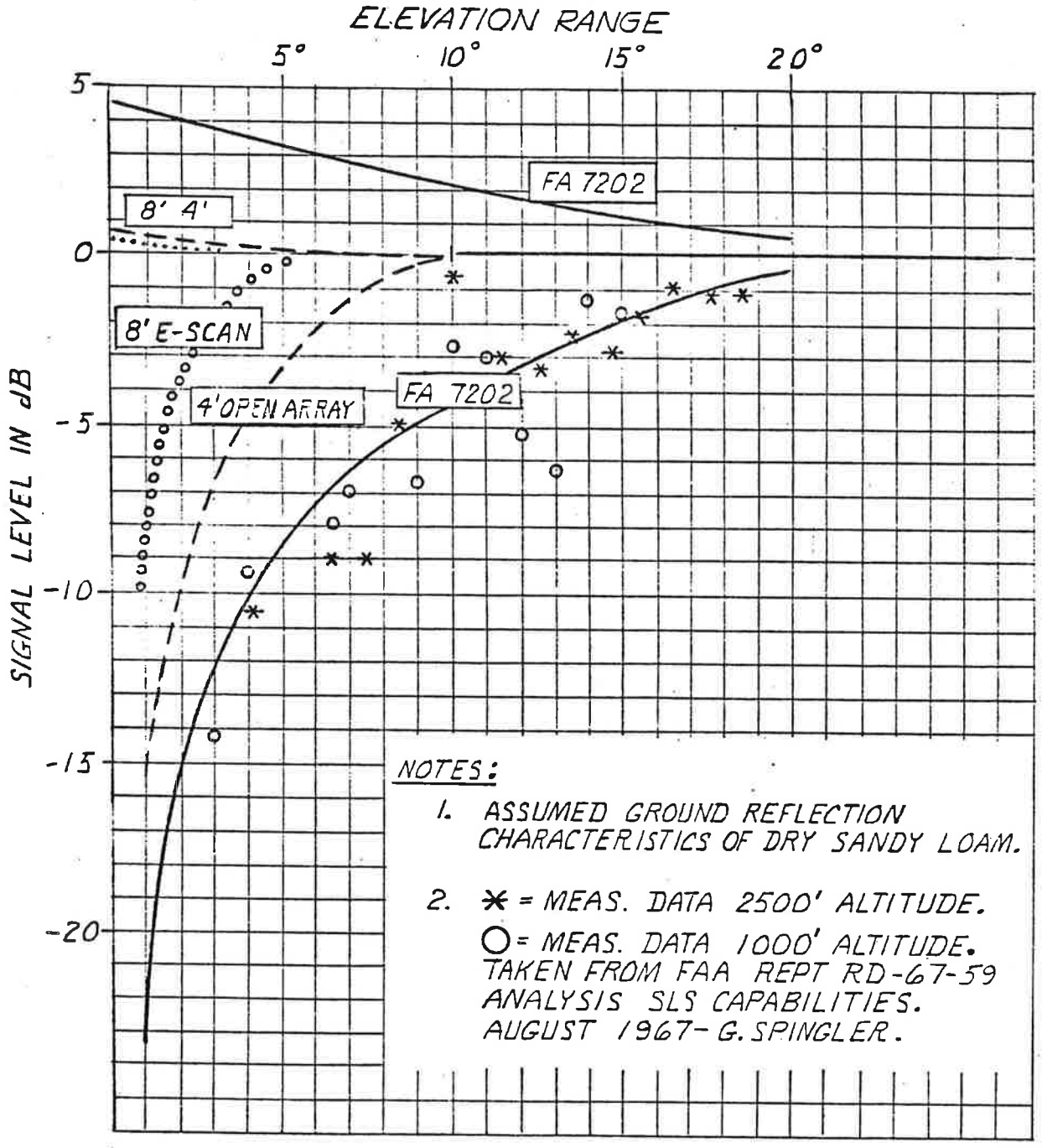

Figure 2-10. Vertical Lobing Envelopes

representing the minimum of the envelope of the FA-7202. These points have been plotted assuming that the measured lobing maxima correspond to the calculated upper envelope. The correlation between measured minimum points and calculated lower envelope indicates the degree to which pattern performance can be predicted from calculations assuming some particular ground characteristic, and measurements on a 4-foot open-array should indicate improvements comparable to those which are calculated.

The lobing envelope shown in the preceding figure is dependent on the elevation pattern location relative to the horizon. If the beam "nose" is too close to the horizon, the minimum signal level in the lobing pattern will be less, thus increasing the number of missed targets. If the beam "nose" is moved too far up in elevation angle, the lobing envelope will be reduced but so will the average signal level, again resulting in lost replies.

For the elevation pattern of the 4-foot array, figure 2-11 shows the level of the first peak and second null in the lobing pattern as a function of the location of the beam "nose". For the location of the 4' array on top of an ASR with a 17 foot tower, the first maxima comes at 0.5 degrees elevation and the second minima comes at 1.0 degrees.

The position of the beam peak has been selected so that the signal level in the second minimum is greatest. This criterion results in a beam peak at 13 degrees elevation. As shown in figure 2-11, the first peak of the lobing pattern is approximately equal to the nominal gain of the array (21 dB). This situation, it is felt, provides maximum gain in the minima to avoid lost targets, while also avoiding high gain peaks which could cause over-interrogation.

Summary of Results

Figure 2-12 is a summary of the open-array antenna characteristics. The antenna consists of a 4-foot by 26-foot dipole array with separate omni antenna. The array size permits azimuth beamwidth requirements to be met and also provides sufficient elevation

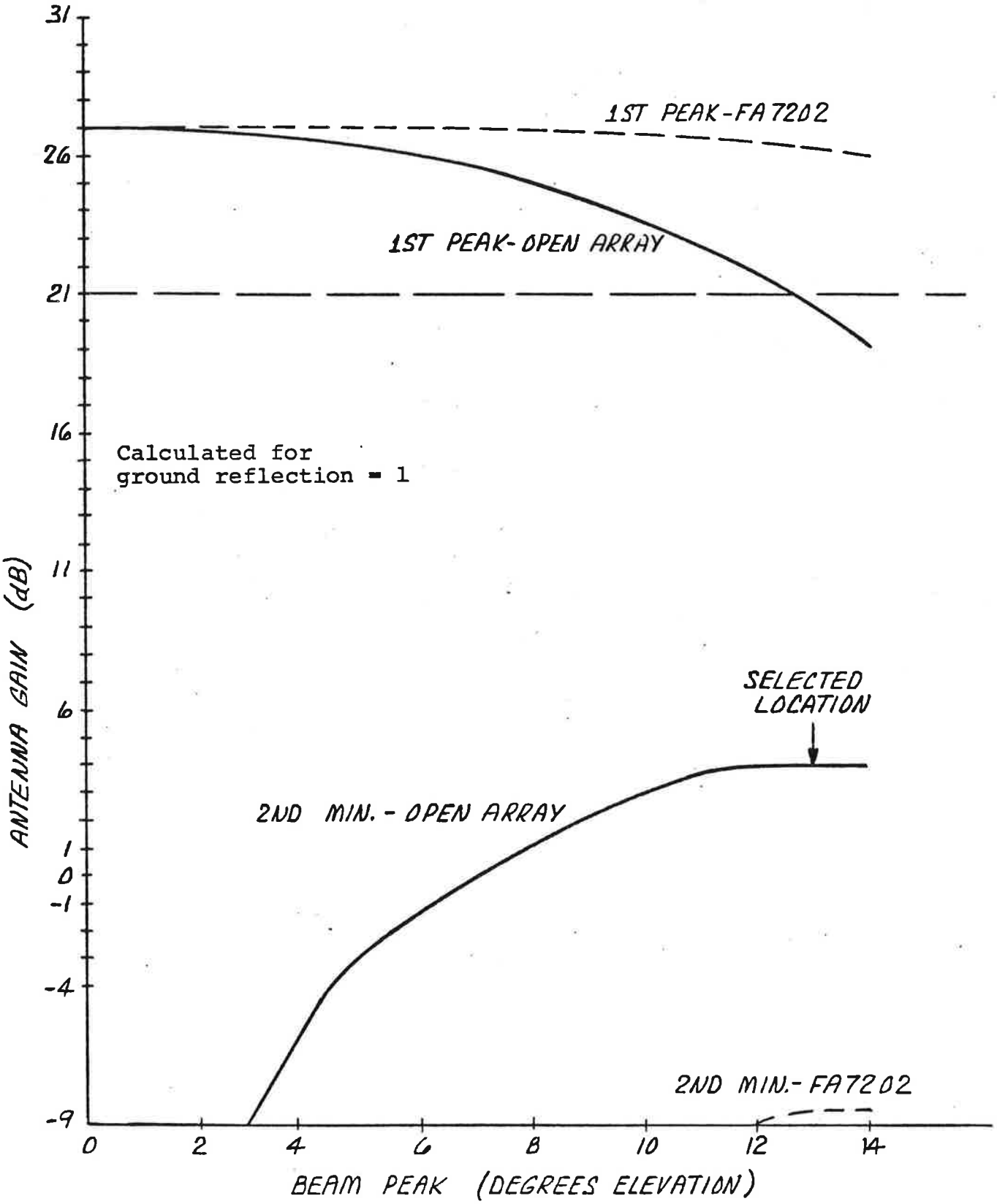

Figure 2-11. First Lobing Peak and Second Lobing Minima as a Function of Beam Peak Location

- 4' X 26' DIPOLE ARRAY WITH SEPARATE OMNI ANTENNA
- 2/3 OF AREA IS OPEN TO WIND
- WILL WEIGH 385 LBS.
- SHAPED ELEVATION BEAM WITH 1.25 DB/DEGREE SLOPE AT THE HORIZON
- GAIN GREATER THAN 21 DB
- AZIMUTH SIDELOBES LESS THAN 25 DB
- ELEVATION SIDELOBES LESS THAN 20 DB
- INDEPENDENTLY OPTIMIZED SUM AND DIFFERENCE PATTERN
- WILL INTERFACE WITH ASR & ARSR WITH MINIMAL CHANGES
- IS A DIRECT REPLACEMENT ON ASR FOR FA-7202 FROM THE STANDPOINT OF WEIGHT AND WIND LOADS
- LIGHTWEIGHT CHARACTERISTICS PERMIT INSTALLATION ON ARSR BOOM
- ASR/ATCRBS OPEN ARRAY WILL SURVIVE NON-OPERATING CONDITION OF 1-1/2" ICE & 150 MPH WITHOUT SUSTAINING PERMANENT DEFORMATION

Figure 2-12. Summary of TSC/Hazeltine Antenna Characteristics

pattern cutoff to minimize vertical lobing effects. The utilization of a separate omni antenna permits the existing system to be employed without any major changes to the equipment.

The antenna has a characteristic that permits a significant reduction of wind load; 2/3 of the area is open to the wind. The antenna will weight 386 lbs., permitting it to be installed on top of the ASR without imposing any additional weight loads.

The elevation pattern is a shaped beam with a 1.25 dB per degree slope at the horizon. This slope is a significant improvement over the existing antenna which has only about a 0.25 dB slope at the horizon. Gain of the antenna is expected to be greater than 21 dB. The azimuth sidelobes are less than 25 dB. Backlobes are also expected to be less than 21 dB by virtue of the shielded design of the open array reflector. The antenna will provide independently optimized sum and difference patterns.

The sum and difference patterns are independently optimized by use of a two line ladder network. This type of network has been designed in other applications at Hazeltine. We believe we have the design experience which permits extensive optimization within the stringent packaging requirements of space and weight in this antenna.

The open-array will interface with the ASR with minimum changes. Our recommendation is that the antenna will operate without any changes to pedestal, motor drive, or reflector on the ASR. From the standpoint of weight and wind loads, the open-array is a direct replacement on the ASR for the FA-7202. Finally, the open-array and the ASR will survive non-operating conditions of 1-1/2 inches of ice and 150-mile-an-hour winds without sustaining permanent deformation.

On the ARSR, the open-array is recommended as the antenna configuration to be used. However, its primary properties are determined from the ASR and its desirability in the case of the

ARSR stems largely from the desire for commonality of both ASR and ARSR. In the event that a larger vertical aperture is desirable in the ARSR, the 4 foot open-array can be easily modified with little design effort to provide increased vertical aperture.

The Phase I study has included a number of tasks. Figure 2-13 summarizes the objectives and conclusions of each of these tasks.

Task I - Pattern Feasibility Tests

The objective of these tests was to eliminate risks associated with the open-array ground plane design. We have concluded from the pattern feasibility tests conducted that the open-array ground plane is feasible, and that sufficient backlobe suppression can be obtained to achieve the desired system performance.

Task II - Wind Load Analysis

The objective of this task was to determine estimates of wind loads on the open array. In view of the larger vertical aperture employed in this array and the openness of the structure it was necessary to compute specific loads to determine on a sound basis, the equivalency to the existing FA-7202 antenna. From the results obtained, we have concluded that the loads are only slightly greater than the existing antenna. The actual wind pressure on the antenna surface is identical to that on the FA-7202, however, as a result of the higher center of force, the total overturning moment is proportionally greater.

Task III - ATCRBS Structural Design

The objective was to determine structural requirements and weight necessary to meet environmental specifications. A 386 lbs. total antenna weight, which includes components and cables will meet both operating and non-operating conditions.

Task	Conclusion
PATTERN FEASIBILITY TESTS	
ELIMINATE RISKS ASSOCIATED WITH OPEN ARRAY GROUND PLANE DESIGN	OPEN-ARRAY GROUND PLANE SUCCESSFULLY TESTED
WIND LOAD ANALYSIS	
DETERMINE CONSERVATIVE ESTIMATES OF WIND LOADS ON OPEN-ARRAY	LOADS ARE SLIGHTLY GREATER THAN EXISTING FA-7202 ANTENNA
ATCRBS STRUCTURAL DESIGN	
DETERMINE STRUCTURE AND WEIGHT	386 LB TOTAL ANTENNA WEIGHT WILL MEET OPERATING AND NON-OPERATING CONDITIONS
ATCRBS/ASR INTERFACE ANALYSIS	
ASSESS IMPACT OF OPEN ARRAY ANTENNA ON EXISTING ASR	OPEN ARRAY WILL NOT CAUSE ANY ADDITIONAL MECHANICAL OR ELECTRICAL DEGRADATION TO ASR EXCEPT FOR SOME EXTREME OPERATING CONDITIONS (OPTIONAL HEATER SYSTEM CAN BE USED)
HEATER SYSTEM	
TO ASESS CURRENT USAGE AND DETERMINE SUITABLE HEATER SYSTEM	IN VIEW OF INTERFACE ANALYSIS, COST-EFFECTIVENESS OF HEATER SYSTEM IS DOUBTFUL
ATCRBS ANTENNA DESIGN	
DETERMINE OVER-ALL ANTENNA LAYOUT AND FEASIBILITY PROVIDE PRELIMINARY INFORMATION ON COMPONENT DESIGN	REQUIRED COMPONENT PERFORMANCE EASILY ACHIEVED AND PACKAGING WITHIN CONSTRAINTS IMPOSED BY THE STRUCTURE IS FEASIBLE
ARSR STUDY	
STUDY ALTERNATE METHODS OF MOUNTING ATCRBS AND RECOMMEND AN APPROACH	CONCLUDED THAT MOUNTING UNDER ARSR FEED BOOM (CHIN MOUNT) IS MOST ATTRACTIVE

Figure 2-13. Phase I Results

Task IV - ATCRBS ASR Interface Analysis

To assess impact of the open-array antenna on the existing ASR, this task included gathering of information and also a preliminary analysis of the ASR reflector to determine specifically the loads applied. We have concluded from these analyses that the open-array will not cause any additional mechanical or electrical degradation to ASR except for some extreme operating conditions consisting of a maximum wind of 100 mph and 1-1/2 inches of ice. In the event these extreme operating conditions are required to be met precisely, an optional heater system can be deployed to de-ice the antenna under these extreme conditions.

Task V - Heater System

The objective was to assess current usage of such heater systems and to determine a suitable heater system for this application. Both electrical wire heaters and hot air heaters were considered. Heater sizing and method of implementation was studied. In view of the interface analysis performed for the ASR, we have concluded that the heater system is not cost effective.

Task VI - ATCRBS Antenna Design

To determine overall antenna layout and feasibility and to provide preliminary information on component design, this task included electrical and mechanical design, packaging, and environmental considerations for all components and cables. We have concluded that the required component performance is easily achieved and packaging within constraints imposed by the structure is feasible.

Task VII - To Study Methods of Mounting ATCRBS and Recommended Approach

We have concluded that mounting under the ARSR feed boom (chin mount) is most attractive.

ATCRBS ANTENNA DESIGN

Electrical Design

The detailed electrical design consists of synthesizing the desired aperture illuminations, designing the radiating element and configuring the power dividing network which feeds the radiating elements.

Figure 3-1 shows a sketch of the radiating aperture, which includes 252 radiating elements. A simple, inexpensive dipole design was selected for the radiating element. Details of the dipole design are included in a later section. The dipoles are arranged with 24 columns of eight dipoles in the central section of the array, tapering at each side to six dipoles in the next three columns and four dipoles in the outermost three columns.

The power dividing network comprises 36 elevation networks, one azimuth network, and two coaxial hybrids used to feed the azimuth network.

As shown in figure 3-2, each dipole is connected to its associated elevation network by a length of .141 inch diameter semi-rigid cable. The semi-rigid cable and stripline elevation network together supply suitable excitations to each dipole in the column such that the desired elevation pattern is radiated. The electrical path length through the elevation network and cable is the same for each cable, except for a phase length of ±90 degrees. This cable length, in conjunction with a 180 degree phase shift achieved by physically rotating the dipole 180 degrees, is used as required to achieve the desired phase at each element.

The result of this equal line length design is that the elevation pattern will not scan with frequency. The pattern will remain at the same level at the horizon over the 1030-1090 band, and only the non-critical upper roll-off will vary with frequency.

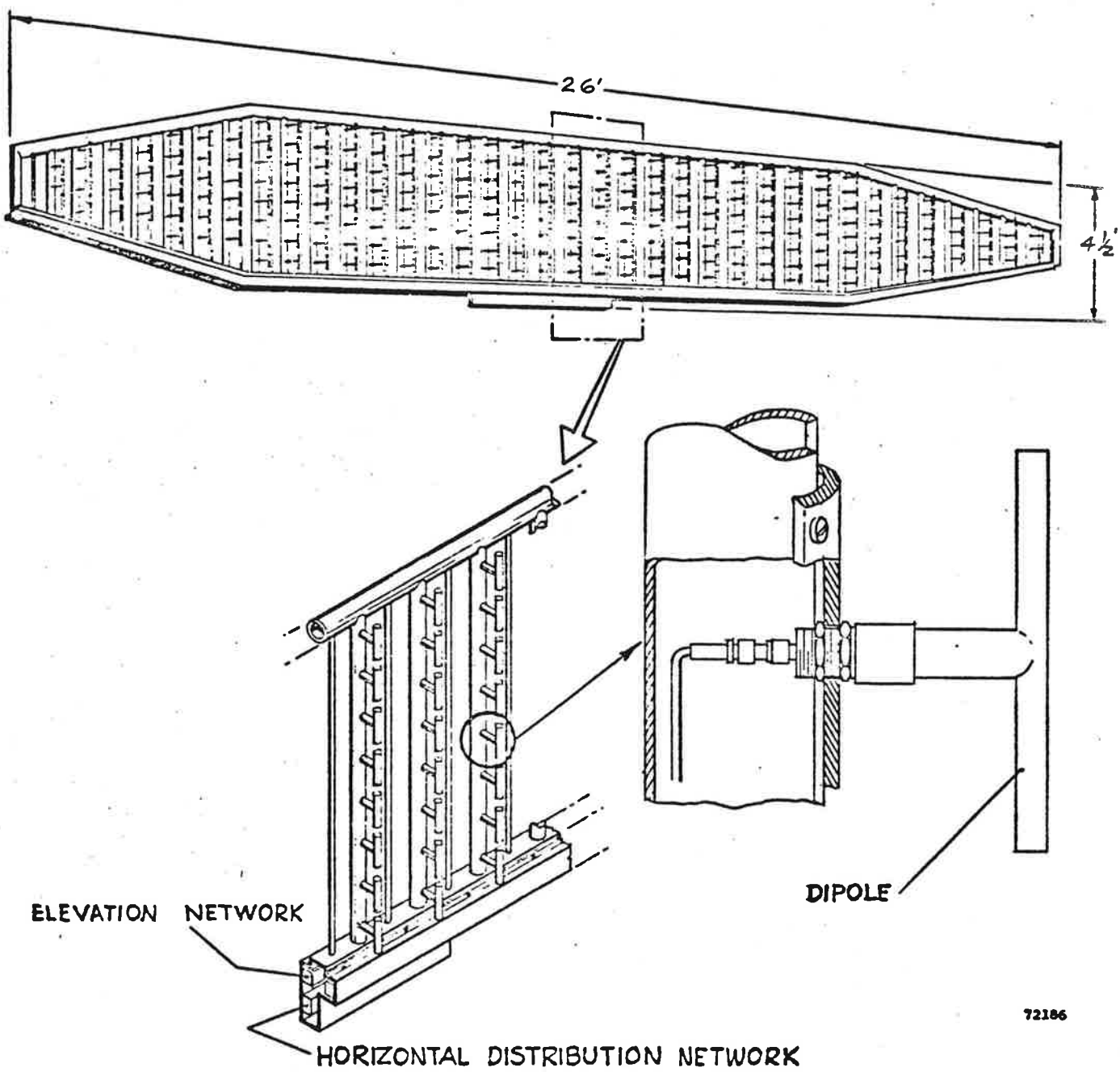

Figure 3-1. Four-Foot Open Planar Array

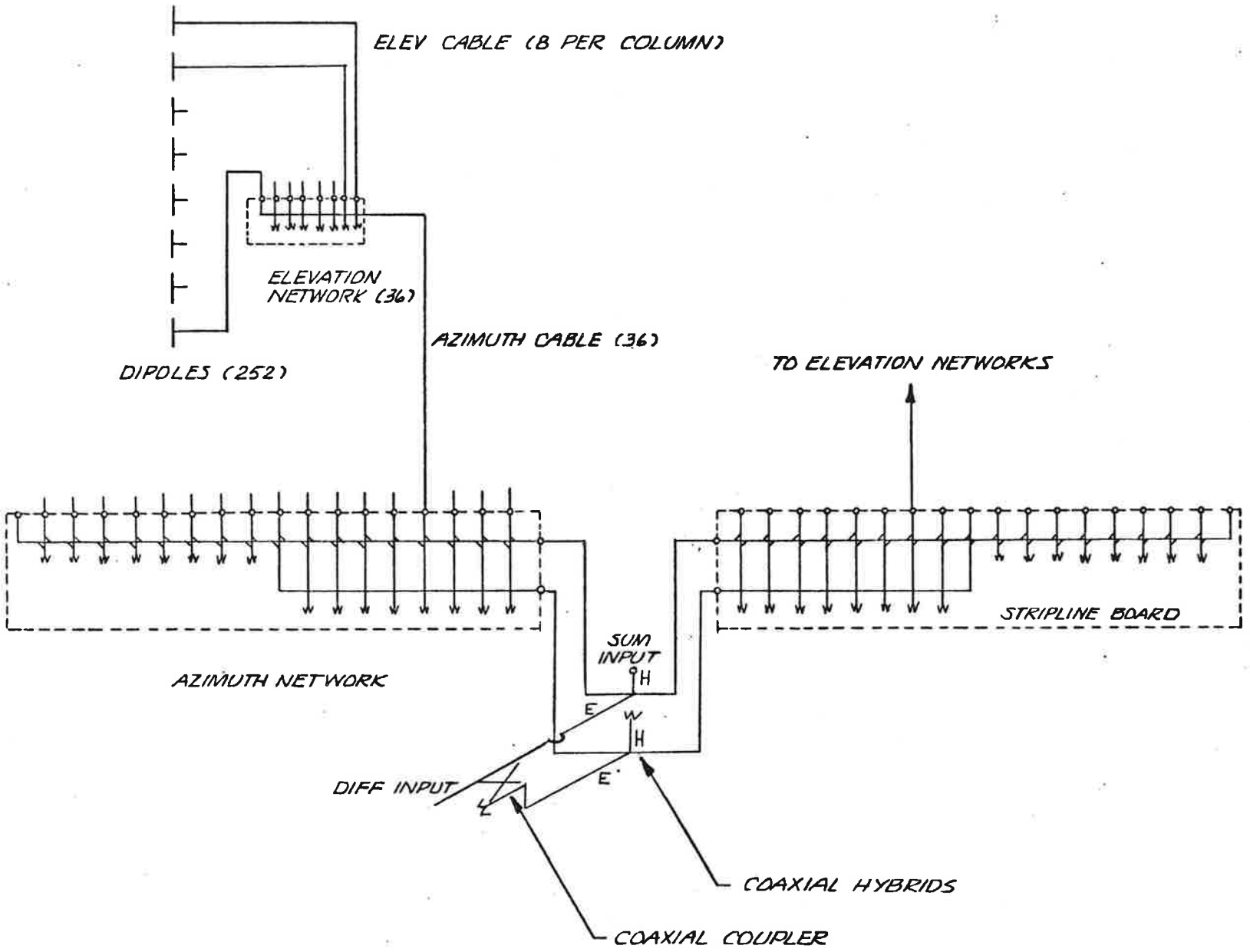

Figure 3-2. Array Schematic

In the columns containing less than eight dipoles, the unused outputs of the elevation networks will be terminated. This results in negligible loss (.02 dB).

Each of the elevation networks is then connected to an azimuth dividing network, as shown in figure 3-2. As shown, the azimuth network consists of two identical stripline networks, two coaxial hybrids, one coaxial coupler, and their associated cables. Using two networks permits the array to be split in half with only two cables to disconnect, rather than the eighteen connections which would be required with a single network.

The azimuth network is required to form both a sum illumination and a simultaneous indepedent difference illumination. To accomplish this, a two-line ladder network is used. The forward line of the stripline networks, fed by the in-phase output of the first hybrid, forms the sum illumination. A series of 17 stripline couplers form the desired azimuth amplitude taper. The difference illumination is obtained by feeding both lines of the stripline networks via both of the coaxial hybrids. The hybrids in turn are fed with a single power divider and phase correcting cables. The two-line stripline network is required to achieve a simultaneous independent difference illumination.

One quarter inch foamflex cable has been selected for the azimuth cables. This aluminum jacketed cable combines light weight with an acceptable loss per foot.

As with the elevation cables, the azimuth cables will be trimmed so that there is an equal electrical path length from the azimuth network input to each of the elevation networks. Provision will be made in each elevation network for a final phase trimming.

Azimuth Patterns. The nominal azimuth patterns are shown in figure 3-3. Both patterns have near-in sidelobe levels of -35 dB and both patterns are very close to optimum in the sense that the sum pattern has

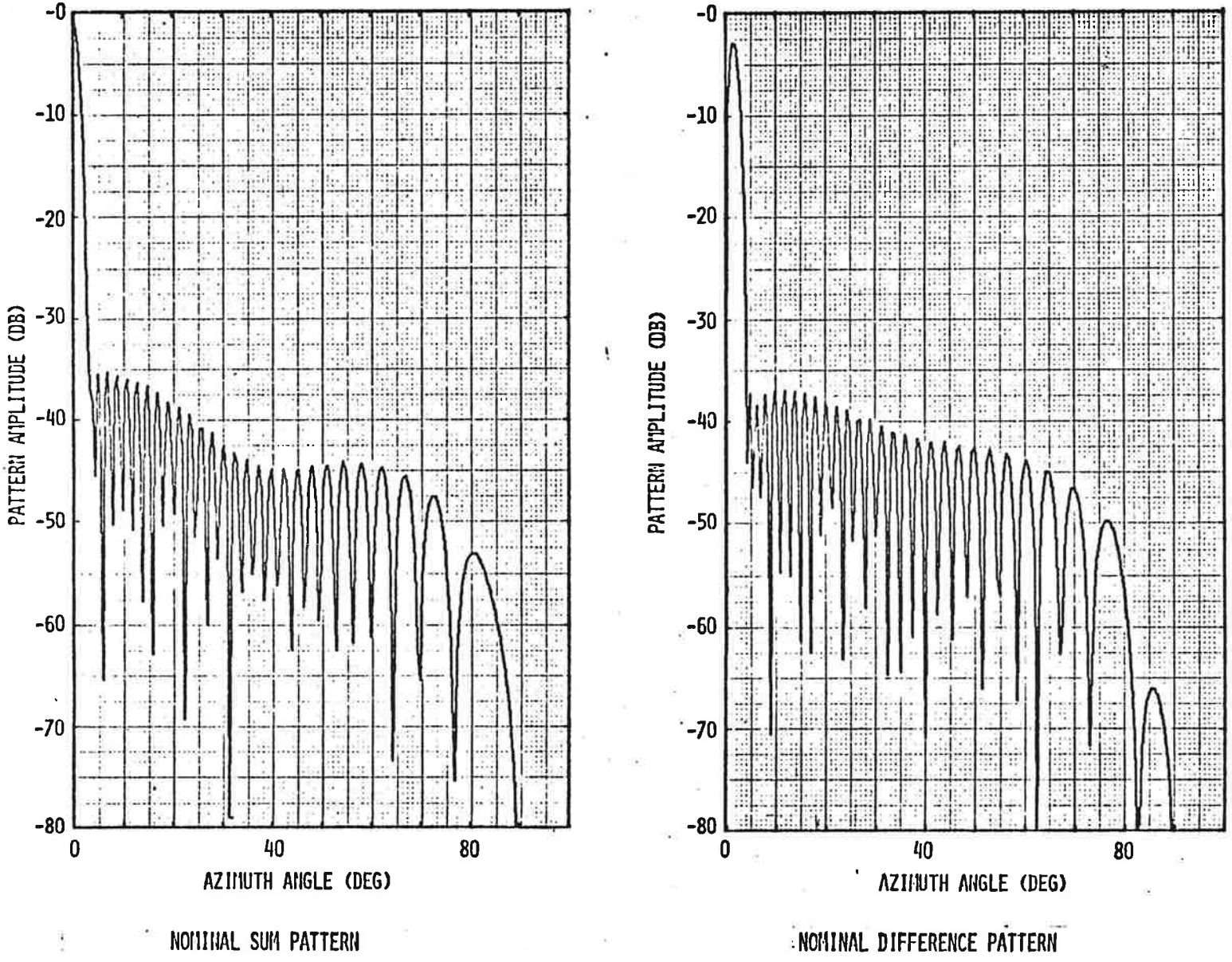

Figure 3-3. Nominal Azimuth Patterns

an aperture efficiency within 0.1 dB of the maximum possible for a -35 dB sidelobe level, and the difference pattern slope is within 0.1 dB of the maximum possible for the same sidelobe level. The calculated half power beamwidth of the sum pattern is 2.35 degrees at 1030 MHz and 2.2 degrees at 1090 MHz.

Elevation Pattern. The nominal elevation pattern is shown in figure 3-4. The pattern has a sidelobe level below the horizon of -24 dB and a pattern slope at the horizon of approximately 1.3 dB per degree. Above the horizon, the pattern is nearly flat up to 35 degrees, then drops off to a level of -20 dB at 55 degrees.

The aperture illumination associated with the elevation pattern has a low amplitude at the edge dipoles in each column. This characteristic reduces backlobes caused by diffraction around the edge of the array, and also minimizes the effect of tapering the ends of the rectangular aperture. The consequences of tapering the ends will be discussed later in this section.

Array Gain. The array power gain can be estimated from the directive gain of the array and the loss budget assigned to the components in the power division network.

If the array had a uniform illumination, the directive gain would be 31.5 dB at mid band. Because of the illumination taper, the aperture efficiency is -5.3 dB. Thus, the directive gain, exclusive of losses, is 26.2 dB.

The assumed component losses are tabulated in table 3-1. The values represent best estimates based on measured losses in similar array feed networks and will not necessarily agree with published cable loss figures, for example.

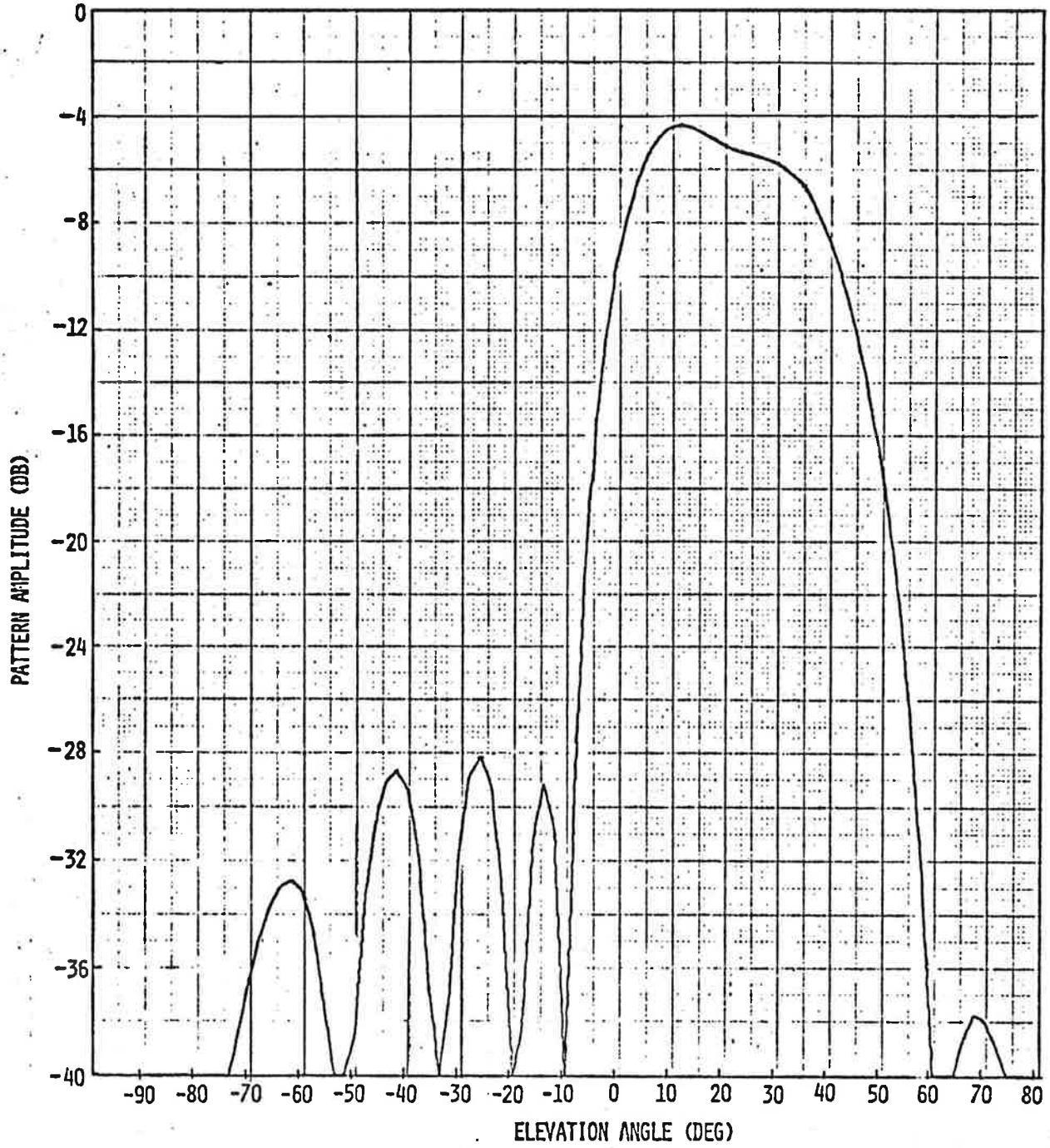

Figure 3-4. Nominal Elevation Pattern

Table 3-1

Directive Gain		26.2 dB
Loss:	Filter	-1.0 dB
	Azimuth network	-1.0 dB
	Azimuth cables	-0.9 dB
	Elevation network	-0.5 dB
	Elevation cables	-0.8 dB
	Reflection loss	-0.3 dB
Array Power Gain		21.7 dB

Error Budget. A tolerance budget for all components must be established in order to ensure acceptable array performance, especially in the sidelobe region. The errors in the elevation network and associated cables will be considered first.

Errors which influence the elevation performance can be divided into two classes: systematic errors, whose effect on the pattern can be directly calculated, and random errors, which must be treated on a statistical basis.

The only systematic error of concern in the elevation pattern is a beam tilt caused either by tolerances in the dielectric constant of the elevation network or by a mechanical tilt of an entire column. Mechanical tolerances on the columns and normal tolerances on the stripline board dielectric constant will keep the elevation pattern from each column aligned within approximately 0.2° of nominal. If necessary, a slight mechanical adjustment can be made to exactly align the elevation pattern with the horizon.

Of more concern are random errors, which will raise the sidelobe level and increase pattern ripple. Table 3-2 lists the source of error and the error magnitude for each. Each source of error

is assumed to have a uniform probability distribution so that the 1 σ error is $1/\sqrt{3}$ of the maximum allowable error.

Table 3-2. Elevation Error Budget

Source	Phase Error Max	Phase Error 1σ	Amplitude Error Max.	Amplitude Error 1σ
dipole	2°	1.2°	.25 dB	.14 dB
cables	0.5°	0.3°	--	--
network	2°	1.2°	.25 dB	.14 dB
Total	--	1.7°	--	.20 dB

Note that although the cables have a nominal tolerance of ±3 electrical degrees, a maximum error of ±0.5 degrees is used. This is because the cable errors are assumed to be uncorrelated across the 36 columns in the array. The cable errors will tend to average out, and so their error contribution is reduced to $1/\sqrt{N}$ where N is the number of columns.

The RMS pattern error can be calculated from the following equation:

$$\text{RMS pattern error} = \frac{\sqrt{\alpha^2 + \beta^2}}{\sqrt{N\eta}}$$

where:

α = RMS phase error

β = RMS amplitude error

N = number of independent elements

η = total aperture efficiency

The calculation results in an RMS error level of -30 dB. Using modified Rayleigh statistics, it can be determined that the sidelobe level will be below -21 dB, 90% of the time. Because only five elevation sidelobes exist, this error level will provide satisfactory performance.

Azimuth errors can also be divided into systematic and random errors. Figure 3-5 shows some of the possible systematic errors, the assigned tolerances and their effect on the azimuth pattern. Random errors are analyzed the same as for the elevation pattern.

Table 3-3

	Amplitude Error		Phase Error	
Source	Max.	1σ	Max.	1σ
Element	.2 dB	.12 dB		
AZ cable	--	--	7^{o}	4^{o}
Elevation network	.2 dB	.12 dB		
AZ Network	.5 dB	.3 dB		
TOTAL (RSS)	--	.35 dB	7^{o}	4^{o}

Note that only one phase tolerance has been assigned to all components. This is because, unlike the elevation networks, the phase from the input of the azimuth network to the output of each elevation network will be measured and trimmed in order to remove any accumulation of tolerance errors.

The RMS pattern error voltage can be calculated in the same manner as previously described, except the number of elements used in the calculation is 36. Using the above RMS amplitude and phase error results in an RMS pattern error level of -32 dB. With a -35 dB nominal sidelobe level and a -32 dB RMS error level, two percent of the sidelobes will exceed -25 dB and virtually no sidelobes will exceed -21 dB.

Simplification of Azimuth Network. A slight change in the azimuth illuminations will be used to achieve a 25% reduction in the size of the azimuth stripline board.

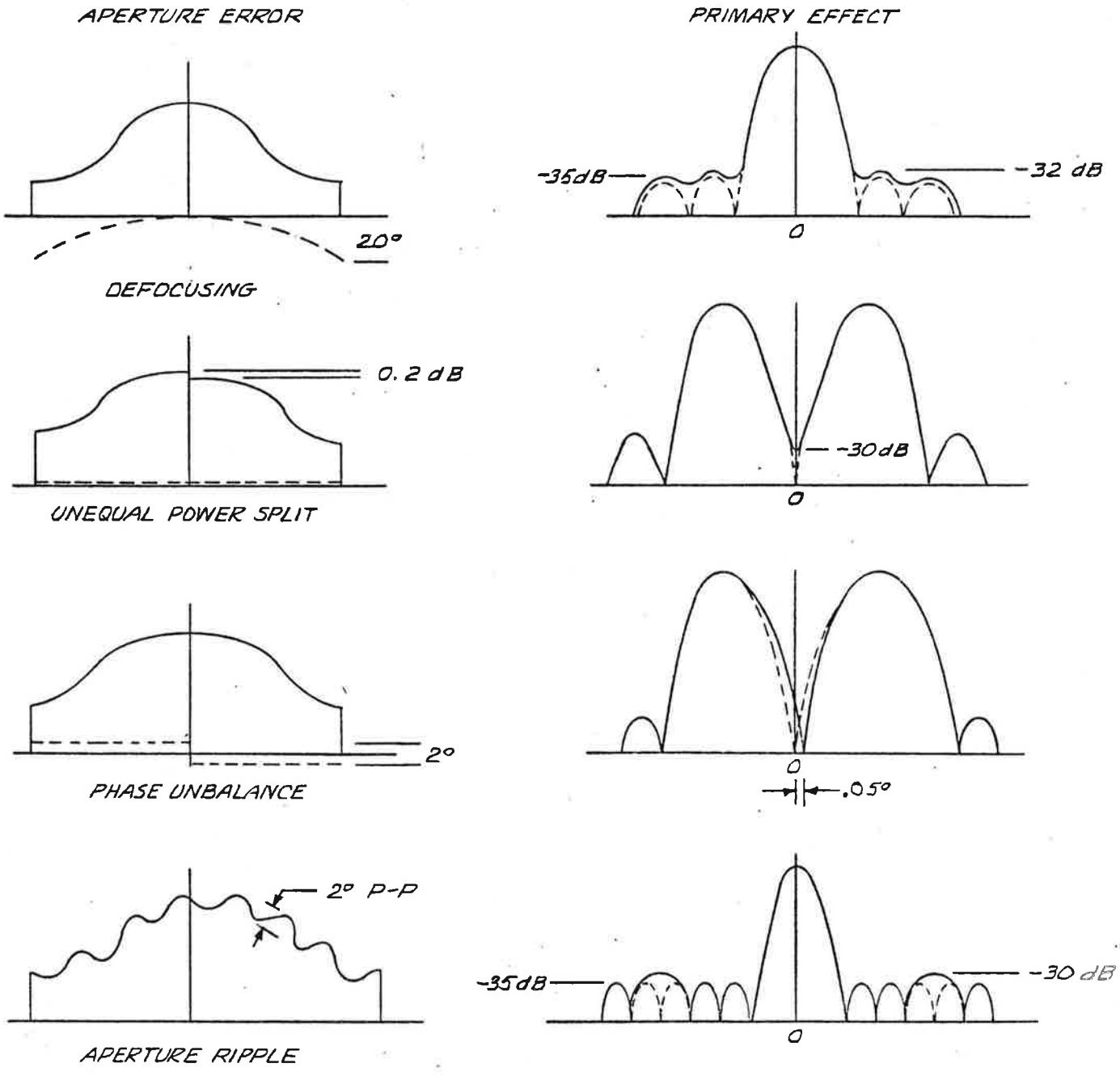

Figure 3-5. Effect of Systematic Errors on Azimuth Patterns

As shown in figure 3-6, a complete two-line network is needed to achieve two completely independent sum and difference illuminations. However, when low sidelobe sum and difference patterns are desired, it is possible to modify the illuminations so that the edge portion of both illuminations is the same. This permits the elimination of a number of couplers in the secondary line of couplers. For the illuminations presented previously, it is possible to eliminate 7 couplers. Figure 3-7 shows the calculated azimuth patterns with the modified illuminations. As can be seen, the sidelobes of the patterns are increased 1 dB for the sum pattern and 4 dB for the difference pattern.

Effect of Tapering Structure. A further modification to the azimuth and elevation illuminations may be required because of the taper required at each end of the array structure. The primary effect of the taper is to make the azimuth pattern vary with elevation angle. A loss in gain also results. However, the strength of illumination is very weak in the area removed, and so the additional loss is insignificant (.02 dB).

Of more concern is the effect on patterns, where even a small change in the illumination can seriously degrade the sidelobe performance. In order to accurately evaluate the patterns, it is necessary to sum the radiation from all of the 252 dipoles in the array at each pattern point. Rather than perform this laborious calculation on the computer, an approximate evaluation of the array performance was made. To calculate the azimuth patterns, the voltage on the dipoles in each column were added, with the dipole voltages as determined by the elevation illumination. The nominal azimuth illumination for each column was then multiplied by the appropriate voltage sum, and a new azimuth pattern was calculated. Basically this procedure is equivalent to exactly calculating the azimuth pattern at some

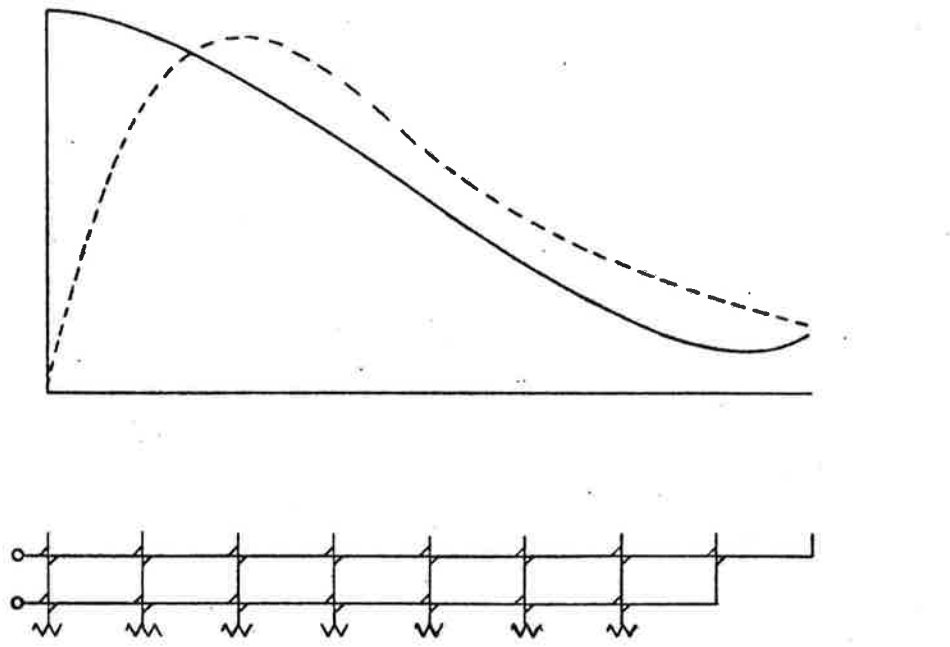

Figure 3-6. Simplification of Azimuth Network

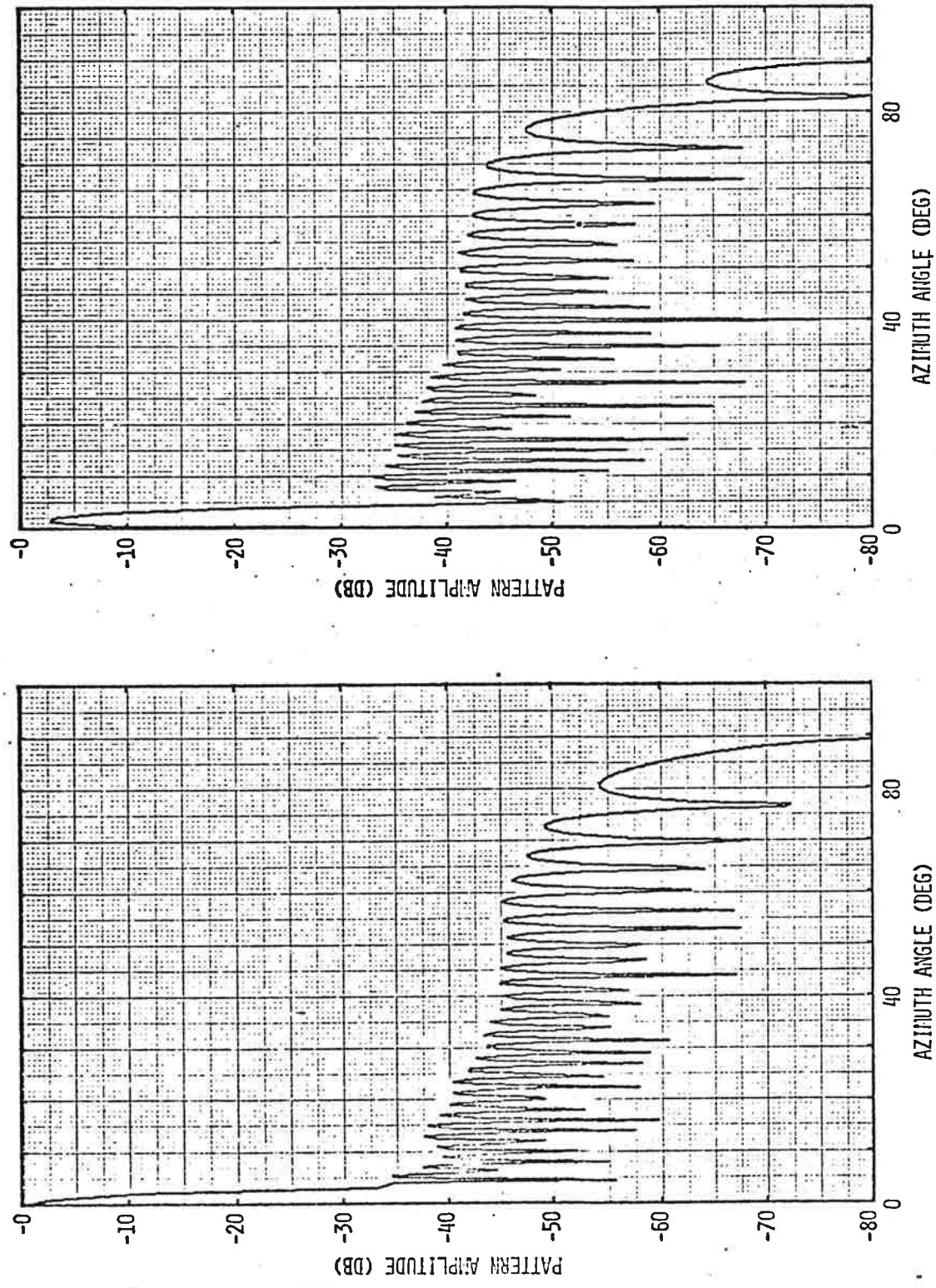

Figure 3-7. Calculated Azimuth Patterns with Modified Illuminations

elevation angle (appoximately 22 degrees) where the radiation from all dipoles in a column is in phase. Figure 3-8 shows the sum and difference patterns obtained from the above calculation.

A slight increase (2 dB) in sidelobe level resulted, and so it is expected that some modification to the azimuth illumination will be required. The more exact calculation of azimuth pattern performance will be made before a final illumination is selected.

A similar calculation was performed for the elevation pattern. In this case, the result is that the elevation pattern will be slightly different for the sum and difference patterns. As shown in figure 3-9, the change in the elevation pattern is primarily a slight decrease in the cutoff slope and a significant decrease in the sidelobe level. Again, some modification of the elevation illumination is anticipated after a more thorough evaluation.

Omni Antenna. The omni antenna configuration is similar to the design Hazeltine used for the DABS experimental facility antenna, and a sketch of the antenna is shown in figure 3-10. The vertical aperture of the open array is matched by the omni array by using 8 printed circuit dipole cards, each card containing two printed dipoles fed in parallel. As in the array column, each dipole will be connected to an elevation beam forming network with semi-rigid cables. it is expected that the same cables and network as the main array can be used. The printed dipoles will be covered with a cylindrical radome to protect them from the weather. As shown, the elevation network will be mounted below the array. It is anticipated that the omni antenna will be mounted on a mast, and suitable mounting hardware will be provided.

The elevation patterns of the omni should be virtually identical to those of the open array. The different dipole environment may result in some minor pattern variations. The azimuth pattern is

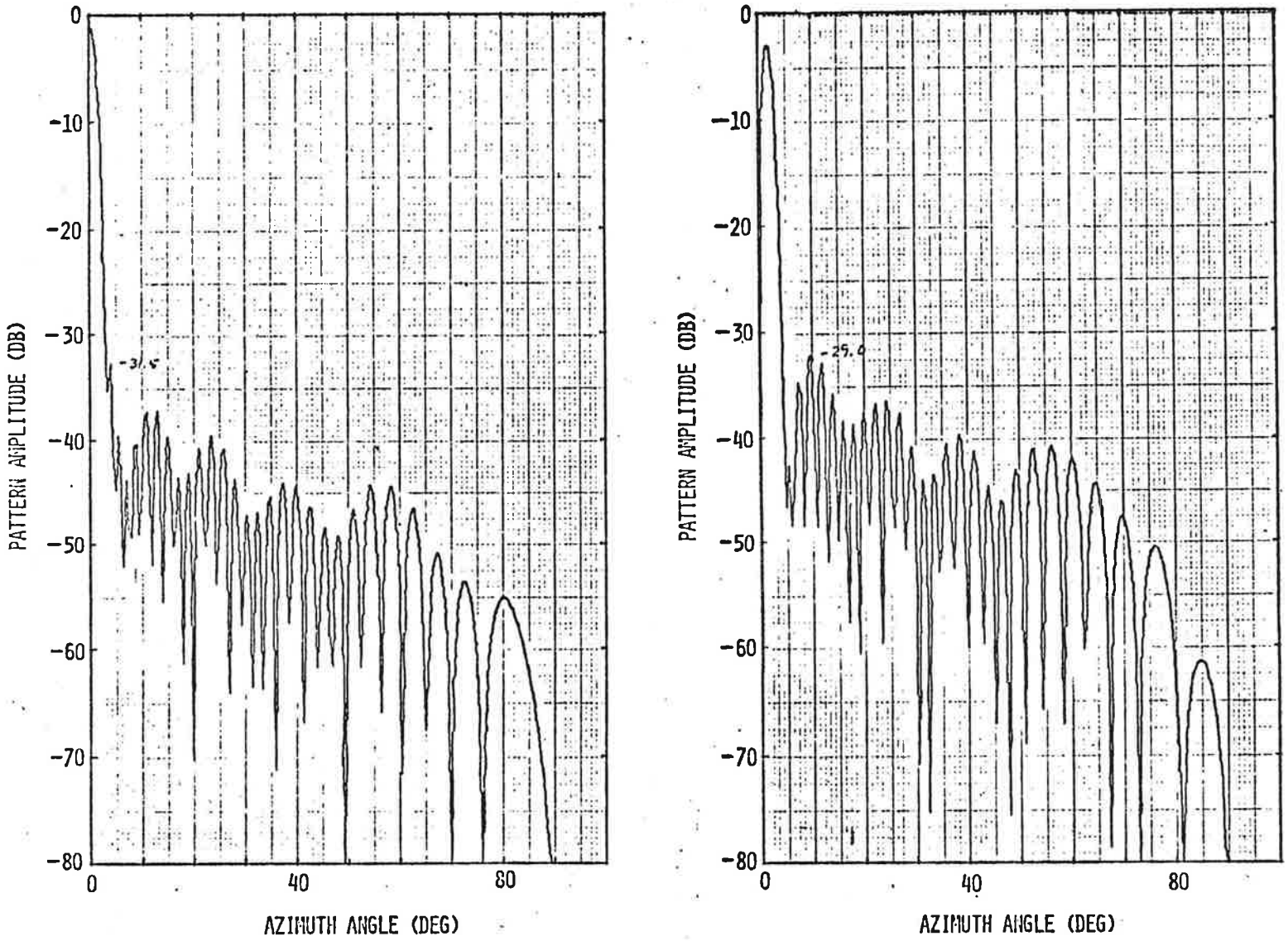

Figure 3-8. Tapered Aperture Pattern

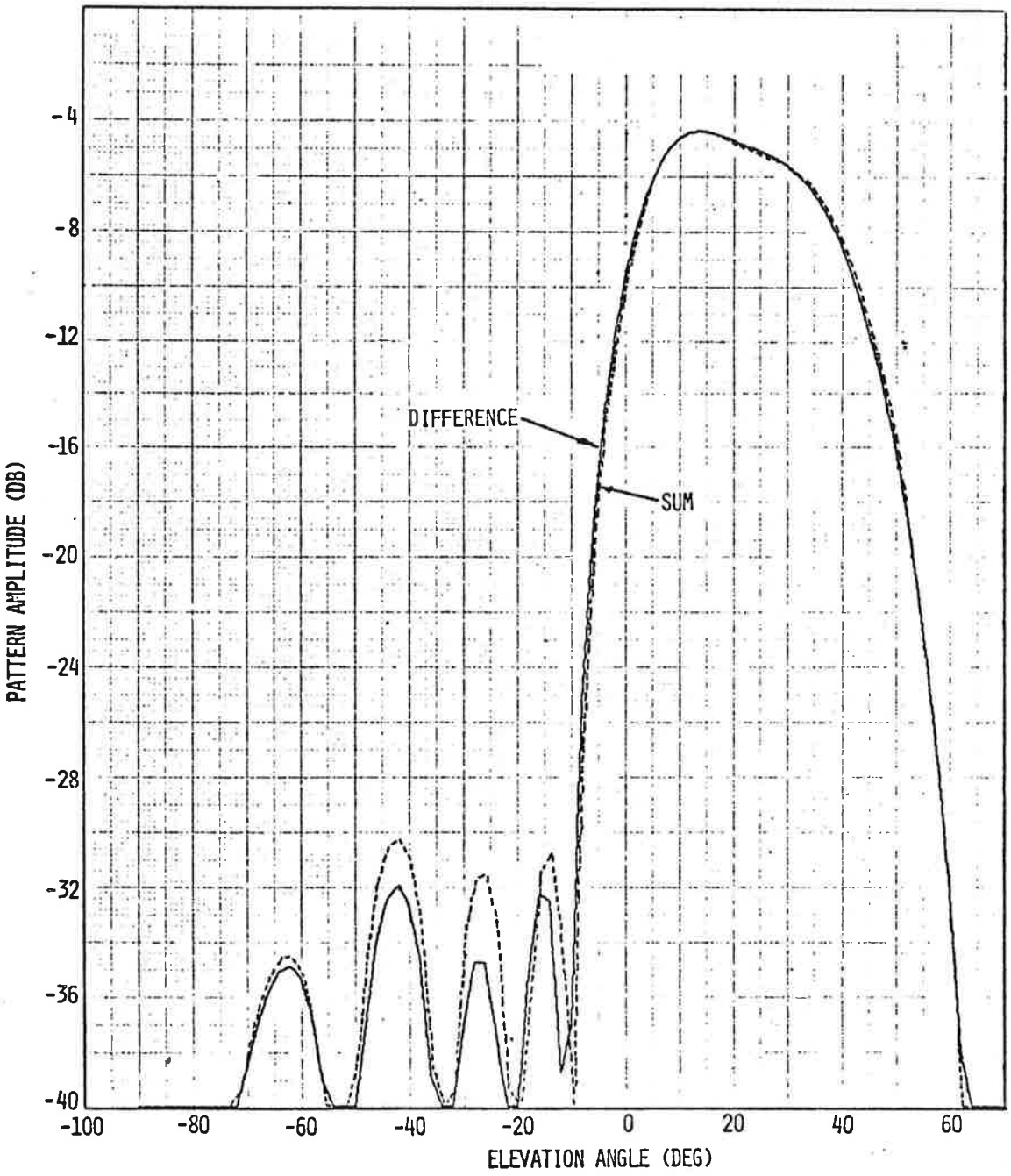

Figure 3-9. Effect of Edge Taper on Elevation Pattern

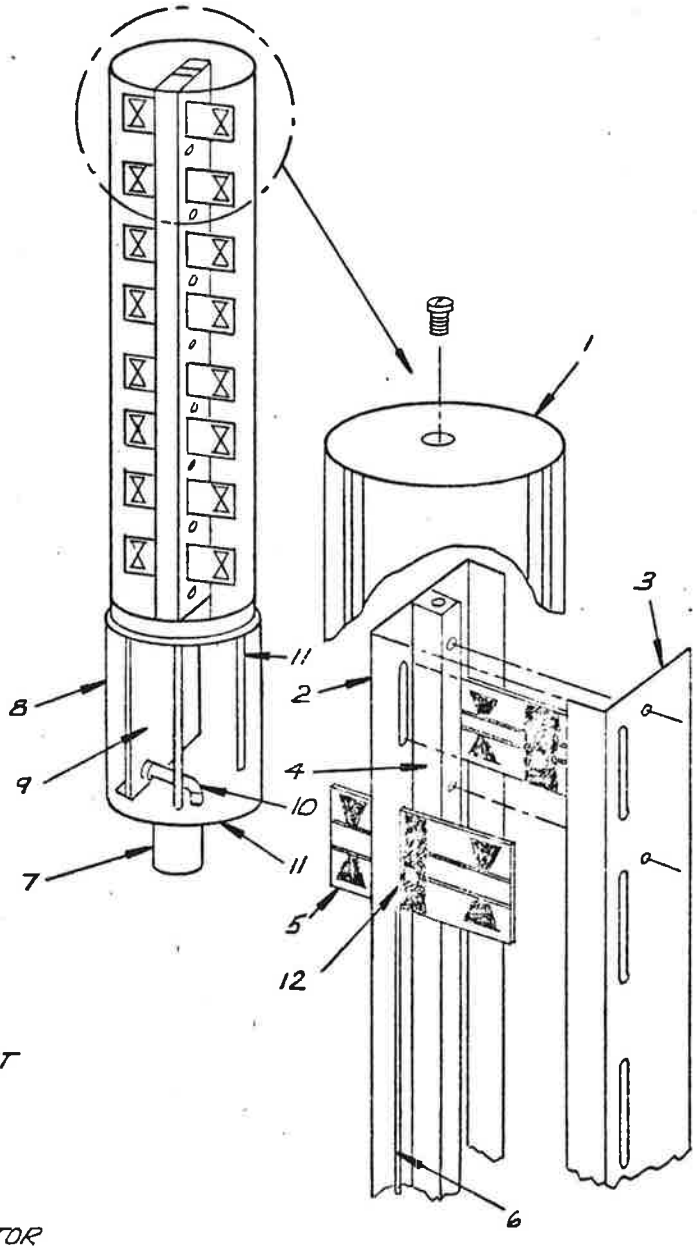

1. RADOME
2. GROUND PLANE
3. GROUND PLANE
4. MAIN DIPOLE SUPPORT MAST
5. DIPOLE RADIATOR (8)
6. .141 SEMI-RIGID CABLE
7. MAST
8. REMOVABLE COVER
9. ELEVATION FEED NETWORK
10. CABLE & BULKHEAD CONNECTOR
11. SUPPORT STRUCTURE FOR NETWORK
12. SMA CONNECTOR

Figure 3-10. Sketch of Omni Antenna

controlled by the dipole and ground plane configuration, and the pattern should duplicate the results of the DABS omni, which had a 3.5 dB peak-to-peak ripple on the omni-directional pattern.

RF Components

Elevation Network. The elevation network consists of seven printed circuit couplers on a board 9.25 inches long by 3 inches wide. The purpose of the network is to couple off the required power to each dipole element in a column. The desired phase is obtained by selecting the correct cable lengths.

A preliminary layout of the elevation network circuitry is shown in figure 3-11. As described in the proposal, the network is a three-layer design, with the photo etched circuit on the center board. The two outer boards will be .128 inches thick and the center board will be .027 inches thick, for a total network thickness of .283 inches, excluding hardware and connectors.

The seven printed couplers are quarter-wave long backward wave designs, and the coupled line spacing is used to vary the coupling. Because the couplers are spaced nearly one-quarter wave apart, it is expected that the network will be well matched. Measured VSWR values of 1.1 are typical on networks of this type.

Mechanical tolerances must be assigned to the network in order to adhere to the tolerance budget established previously for the feed network. The two significant mechanical tolerances are the thickness of the center board, which controls the coupling value of strong couplers, and the line-to-line spacing, which determines the coupling of weak couplers. It has been established in previous work that a tolerance of ±.001 inch is attainable on the thickness, and a tolerance of ±.002 inch on the spacing. Both of these tolerances result in coupler variations of ±0.25 dB and, because the two effects are almost mutually exclusive, it can be concluded that network amplitude errors will be approximately ±0.25 dB.

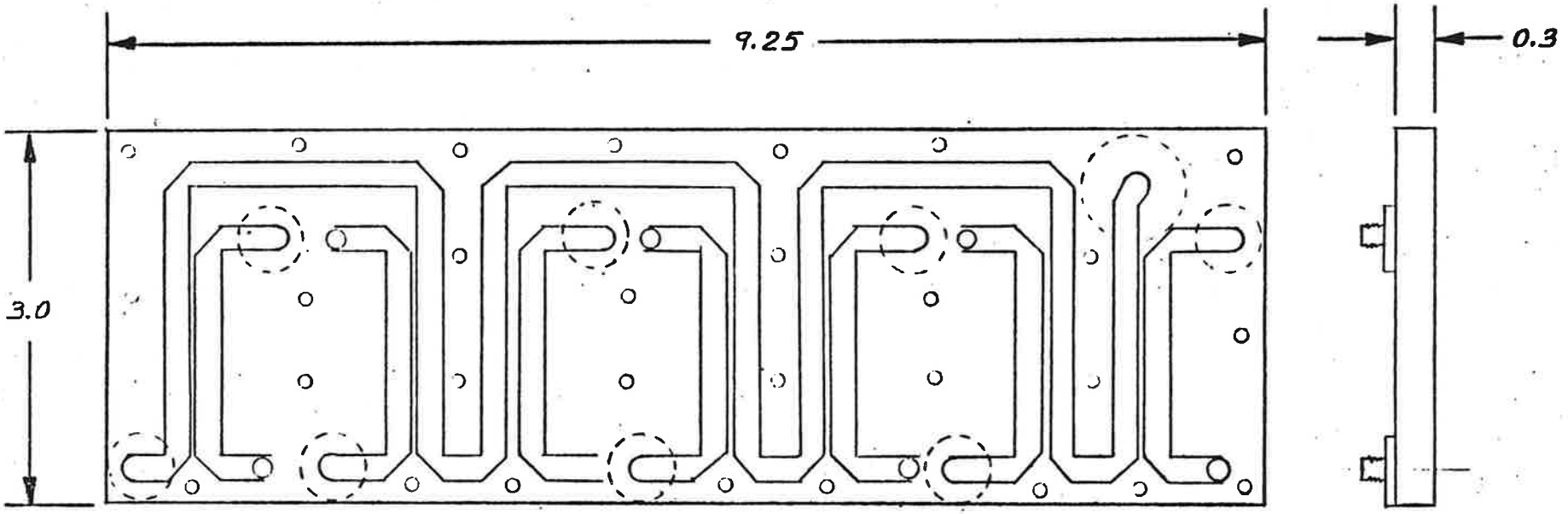

Figure 3-11. Layout of Elevation Network

Azimuth Network. The azimuth network, as described previously, consists of two stripline double-line networks, two coaxial hybrids, and one coaxial coupler. The two stripline networks are identical, and a layout of one is shown in figure 3-12. Because of the reduction in the number of couplers, it is possible to fabricate the network on a single 3-inch by 35-inch board.

The network has two inputs, a front line input and a rear line input. The front line is a series line with 17 couplers and 18 outputs. The front line couplers form one-half of the azimuth sum illumination. When the two networks are fed from the in-phase output of the coaxial hybrid, the entire sum illumination is generated. For the difference illumination, both the front line and the rear line must be excited. To accomplish this, the two hybrids and the coupler are used, as shown in figure 3-2. The combination of the front and rear lines on each stripline board generate one-half of the difference illumination. The anti-phase outputs of thw two coaxial hybrids feed the two stripline networks, thus forming the difference illumination.

The front and rear stripline couplers are interconnected with printed lines. The rear line of couplers are terminated with inexpensive stripline terminations. The same board thickness will be used on the azimuth stripline networks as on the elevation network, and the same mechanical tolerances will apply. The hybrids and coupler will be purchased. Figure 3-13 tabulates the performance of the hybrid.

Dipole Design. The dipole used in the array must combine good electrical performance with mechanical strength, weather resistance, and ease of manufacture. Figure 3-14 contains a cut-away drawing of the preliminary dipole design.

Experimental measurements have shown that dipole unbalance and dipole stem radiation could increase the backlobes of the open

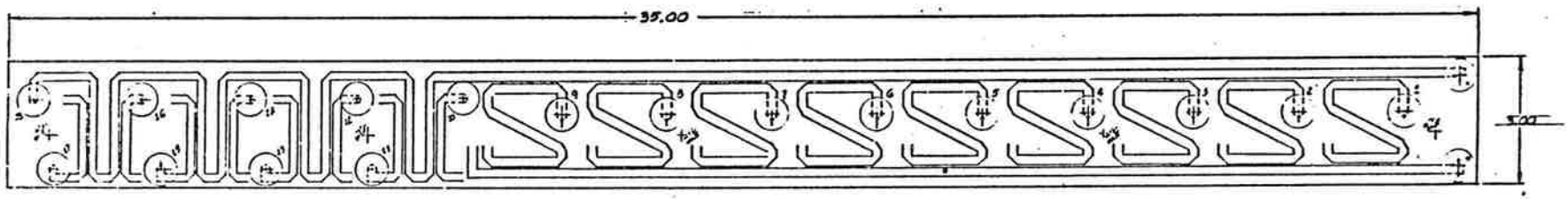

Figure 3-12. Azimuth Network

73158

Frequenty range:	950-1150 MHz
Isolation:	30 dB
Amplitude balance:	±0.2 dB
Phase balance:	±1 degree
Insertion Loss:	0.3 dB

VSWR

H arm: 1.35:1
H arm: 1.25:1

Power capacity: 175 watts

Figure 3-13. Tabulation of Hybrid Performance

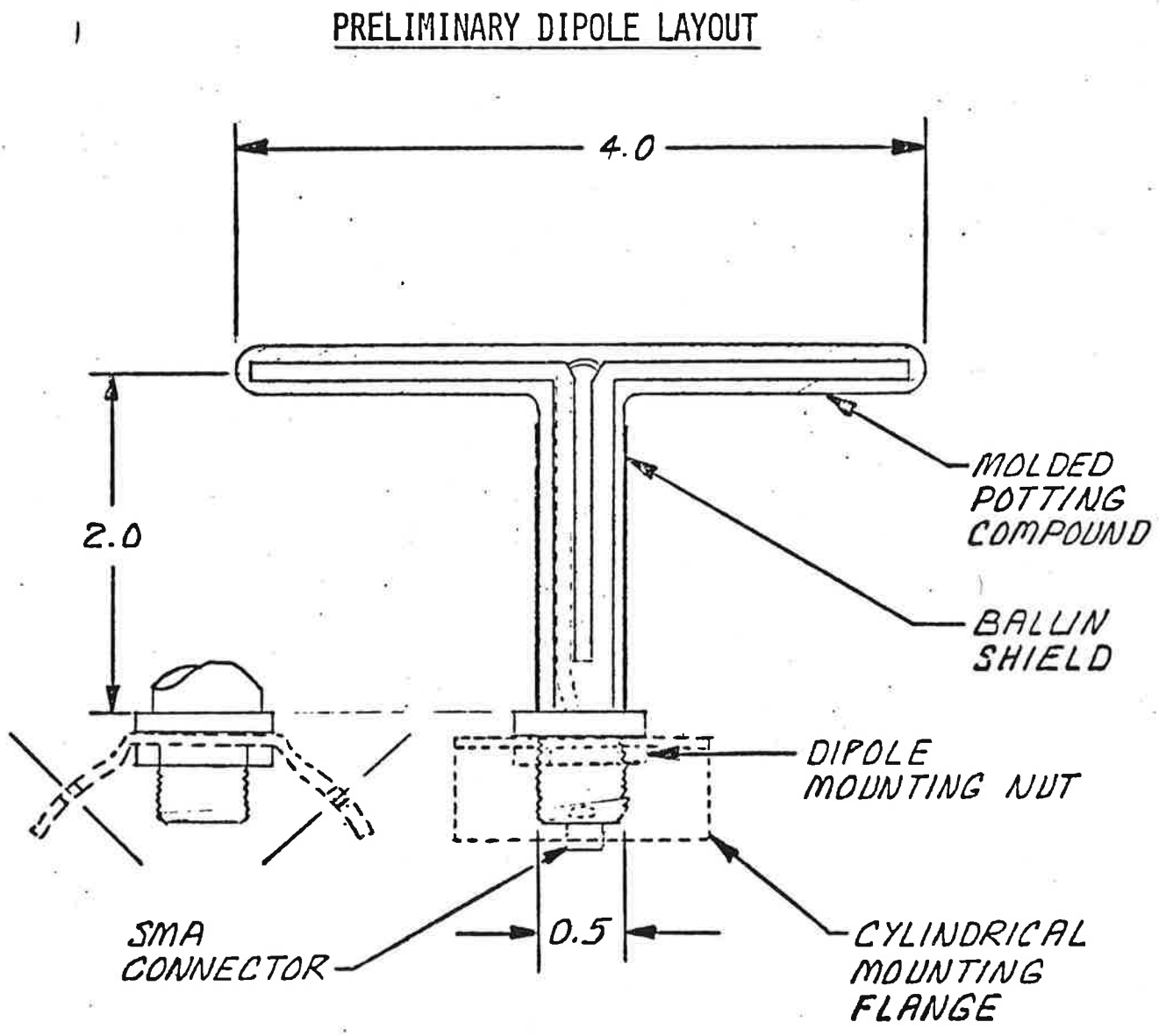

Figure 3-14. Dipole Design

array. To minimize this problem, the length of the dipole is considerabily less than the dipole-to-dipole spacing. Although the dipole is not self resonant, the balanced stem can be used to achieve excellent bandwidth. Figure 3-15 shows a schematic of the dipole equivalent circuit, with the series resonant circuit of the dipole connected to the parallel resonant circuit of the balun stem. By selecting the correct circuit values, (e.g. by adjusting the dipole length, the balun stem impedance, and the short circuit point) it is possible to double tune the dipole impedance and obtain a satisfactory match over the entire band. The DABS experimental array operated satisfactorily over the 970 to 1150 MHz band using a printed dipole one-quarter wave long.

The experimental work also established the need for a shield around the balun, despite the excellent balance of the single dipole design. A shield is routinely added to Hazeltine's IFF dipoles by painting a conductive sheath on the molded dipole, and so no problem is anticipated in implementing the shield.

The major difficulty in the dipole design comes from the requirement that the element be matched in an array enviornment. Ordinarily, a simple waveguide simulator is used, with some final correction made for the non-uniform aperture illuminations. Because of the open structure, two alternatives are available for matching the dipole: first, the dipole can be matched as an isolated element, then the mutual impedance between elements as a function of distance must be measured, and the effect of the surrounding elements on the dipole impedance can be calculated and compensated for. Alternatively, a more sophisticated simulator can be designed and fabricated. The simulator approach appears more attractive because it eliminates the errors inherent in calculating performance, and probably will be used if a suitably simple design can be achieved.

The molded potting compound shown in figure 3-14 serves two purposes. First, it serves to isolate the dipole tuning from

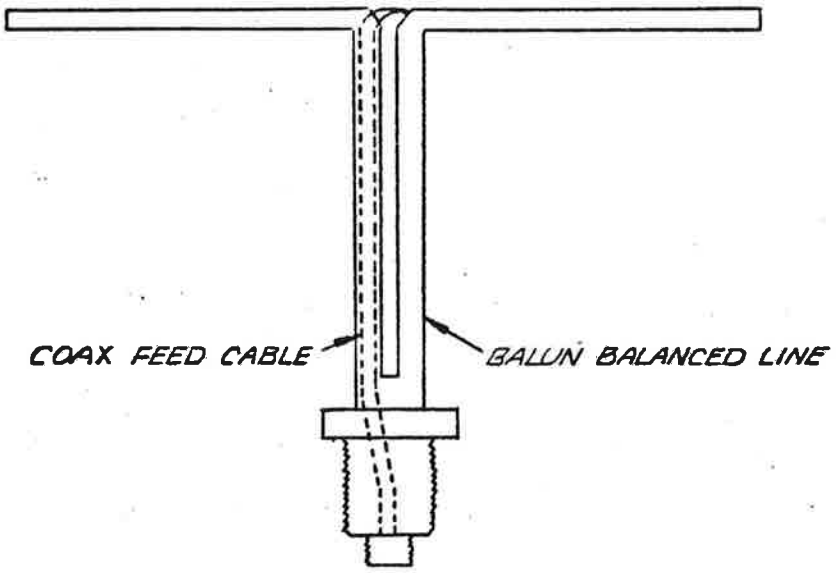

a. DIPOLE

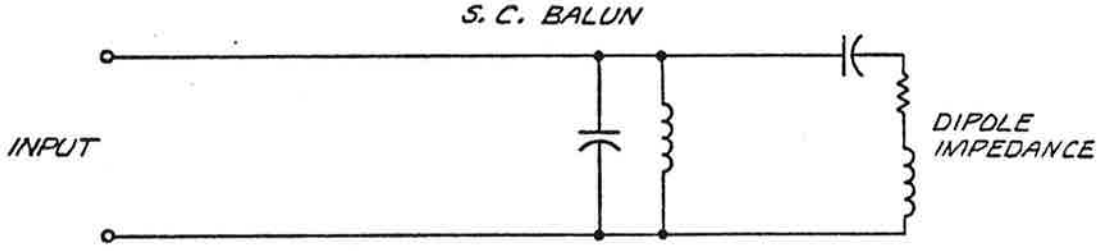

b. EQUIVALENT CIRCUIT

Figure 3-15. Dipole Element Equivalent Circuit

ice and snow and second, it provides a mechanically strong coating which will not degrade with exposure to weather.

The manufacturing cost of the dipole has been minimized by using as simple a design as possible. The dipole assembly might consist of a single metal piece forming the arms and balun, a threaded base, and a short piece of semi-rigid cable to connect the SMA connector to the feed point of the dipole. The entire assembly would then be potted using an injection molding machine. The final mechanical configuration will be designed in close cooperation with manufacturing, so that the final costs will be minimized.

Cables. There are two major sets of cables used in the array. One set connects the elevation network to the dipoles while the other set connects the azimuth network to the elevation network.

The elevation cables will be purchased electrically measured and trimmed by the cable manufacturer. These cables will be .141 copper jacketed semi-rigid cable, which provides acceptable loss, adequate flexibility and good phase stability. The connectors will be SMA, which provide weather sealing and also good electrical performance.

To minimize loss and weight, the azimuth cables will be .250 inch diameter aluminum jacketed foamflex. The cable is a semi-rigid design with a foamed dielectric which reduces the loss to less than one-half of the .141 diameter cable. Because the quantity is not large, the cables may be fabricated during assembly of the array. The azimuth cables will be phase trimmed after assembly of the array in order to minimize the azimuth phase errors. The connectors to be used are TNC, a design similar in performance to the SMA connectors but compatible with the aluminum jacketed cable.

Recommended Performance Specification

The following table lists the performance goals for the open array antenna. These estimates have been derived from consideration of the experimental and theoretical results obtained during Phase I. For comparison, the table also lists both the TSC specification and the Hazeltine calculated or measured value. The monopulse performance is compared to the recommendations of Lincoln Laboratory for their DABS design.

Design of Tuned-Reflector Ground Plane

A key component of the open-array antenna that is being developed is the tuned reflector. During Phase I of the program, significant effort was applied to optimizing the design of the tuned reflector and verifying its performance in the open-array configuration.

Two versions of the tuned reflector were employed. In the first, a simplified construction was used for ease in making experimental adjustments. Figure 3-16 shows this experimental tuned reflector consisting of a 1/2-inch diameter rexolite rod on which aluminum tape is wound to form hollow metal cylinders with gaps between the cylinders. With this construction, the gap could easily be changed during optimization of the design. The optimization was performed with a 4-foot by 8-foot ground plane as will be discussed subsequently.

In the second version of the tuned reflector, a construction was used that, although less easy to change, provides shielding against ice and rain; this version will be used in the antenna that is developed in Phase II of the program. Figure 3-17 shows this tuned reflector consisting of 1/4-inch diameter aluminum rods separated by rexolite disks, supported in a thin-walled dielectric sleeve. Surrounding this assembly and separated from it by an air space is a 5/8-inch O.D. fiberglass tube. This tube prevents ice and rain from coming very close to the tuned reflector, and permits the optimum tuning of the tuned reflector to be retained in the presence of ice and rain. The air space between

RECOMMENDED PERFORMANCE SPECIFICATION

Parameter	Ref. Para.	TSC Spec	H/C Calculated	H/C Design Goal
Directional Pattern Gain	1.4.1	21 dB	21.7 dB	>21 dB
Azimuth Beam-width 1030 MHz				
horizon (3dB)	1.4.2	2.1° to 2.6°	2.3°	2.1° to 2.6°
horizon (10dB)	1.4.2	<4.5°	4.1°	<4.5°
from -2° to +25°	1.4.2	horizon ±15%	-	horizon ±15%
Azimuth Sidelobes 1030 MHz				
-2° to 0° elev.	1.4.2	-15 dB	-33dB (error free)	-15 dB
0° to 5° elev.	1.4.2	-20 dB	"	-21 dB
+5° to 25° elev.	1.4.2	-15 dB	"	-25 dB
Azimuth backlobes	1.4.2	-21 dB	-25 dB	-21 dB
Azimuth beamwidth 1090 MHz	1.4.6	same as 1030	-	same as 1030
Azimuth sidelobes 1090 MHz	1.4.6	same as 1030	-	same as 1030
Elevation Pattern 1030 MHz				
Beam nose	1.4.4 (Rev)*	<+10°	+13°	≤13°
Min power +1° to +5° elev.	1.4.4	-5 dB	-5 dB	-5 dB
Max power -1° elev.	1.4.4	-7.5 dB	-7.6 dB	-7.5 dB
Max power <-9° elev.	1.4.4	-21 dB	-24 dB	-20 dB
Ripple +5° to +30° elev.	-	-	2.2 dB	3.0 dB
Elevation Pattern 1090 MHz	1.4.6	same as 1030	-	same as 1030
Directional beam skew lower 3dB point to +25°	1.4.5	±0.3°	-	±0.3°
Directional beam squint 1030/1090 lower 3dB point to +25°	1.4.8	±0.2°	-	±0.2°
Cross polarized radiation				
1030 MHz -2° to +25°	1.4.3	<-15 dB	-20 dB	<-15 dB
1090 MHz	1.4.7	<-15 dB	-20 dB	<-15 dB
VSWR	-	-	-	1.5:1
E.M.I. Filter				
Insertion loss	1.6			
1015 to 1105 MHz	1.6	<1.0 dB	-	<1.0 dB
Attenuation	1.6			
1250 to 11,000 MHz	1.6	>50 dB	-	>50 dB
VSWR	-	-	-	1.25:1
Omni Pattern				
Uniformity	-	-	±1.5 dB	±1.75 dB
Elev. Pattern Relative to directional	1.4.9	matched		matched ±2 dB
VSWR	-	-	-	1.5:1
Cross Polarization	-	-	-	<-15 dB

*1.4.4. As revised in contract DOT-TSC-598, page 3, dated April 25, 1973.

RECOMMENDED PERFORMANCE SPECIFICATION (Cont)

Parameter	Lincoln Laboratory Recommendation	H/C Calculation	H/C Performance Estimate
Sum Gain	20 dB	21.7 dB	21.0 dB
Peak Az. Sidelobes (0^o to 35^o elev.)	21 dB	33 dB(error free)	
Volt. Av. Sidelobes (20º Az sector) (0^o to 35^o elev.)	-30 dB	-30 dB	-28 dB
Slope	3 dB/deg.	1.3 dB/deg	1.25 dB/deg.
nominal Σ/Δ crossover	3 dB	3 dB	3 dB
Δ/Σ linearity (best lin. fit)	±2%	±6%*	±8%
Δ/Σ slope variation			
0^o to 10^o elev.	±2%	-	±4%
10^o to 35^o elev.	±20%	-	±25%
Σ-Δ phase	$\pm 10^o$	-	$\pm 10^o$
Δ Null depth (0^o to 35^o	$\geq$30 dB	-	$\geq$30 dB
Null position	$\pm 0.02^o$	-	$\pm 0.2^o$
(0^o - 10^o elev.)	$\pm 0.02^o$	-	
Rotating Joint Δchannel	Yes	-	Yes
Amplitude unbalance	0.2 dB	-	0.2 dB
Phase unbalance	5^o	-	5^o

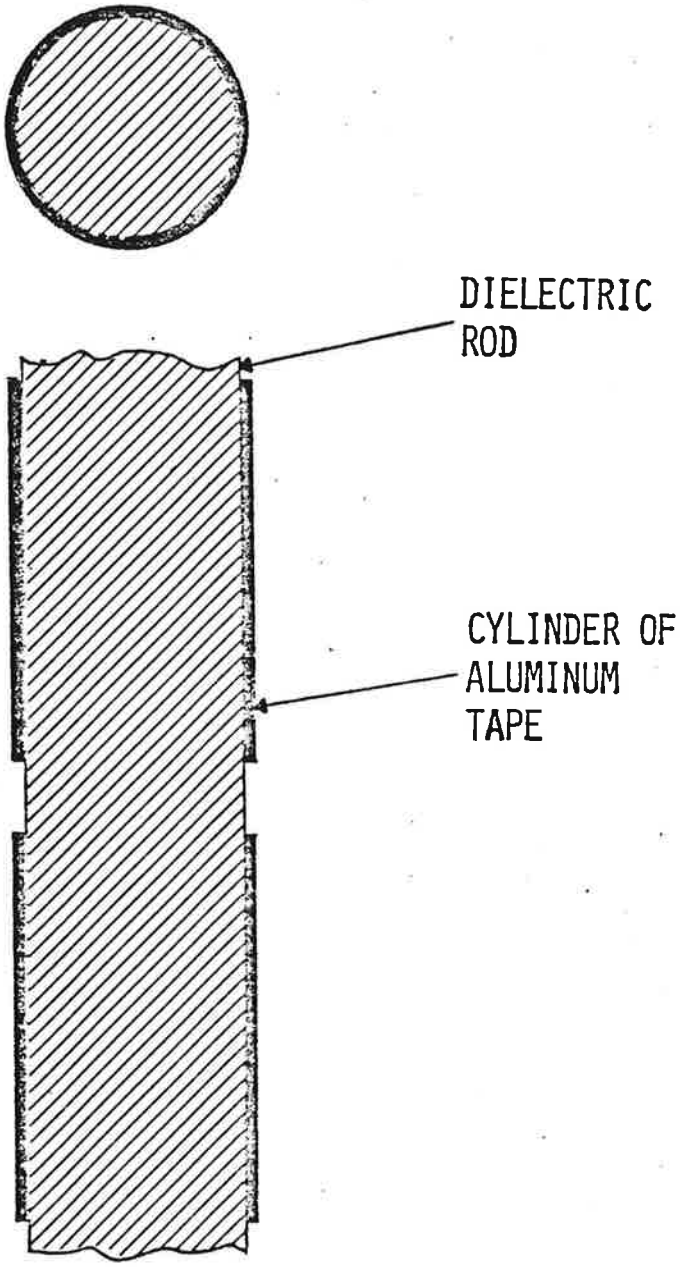

Figure 3-16. Experimental Tuned Reflector

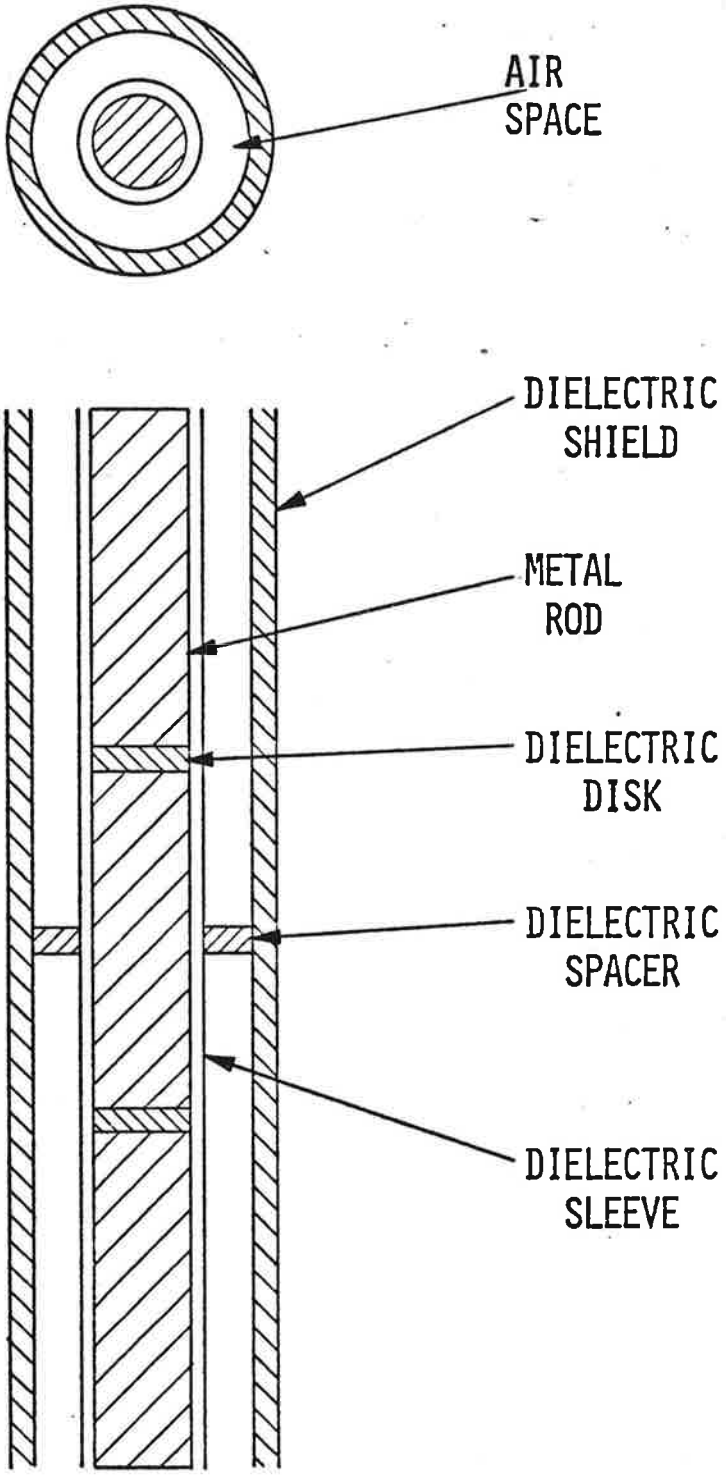

Figure 3-17. Final Tuned Reflector

the tuned reflector and the outer tube enhances the shielding action of the outer tube.

The shielded tuned reflector was designed to be equivalent in reflecting properties to the optimum experimental tuned reflector. This equivalence was obtained by measurements inside a waveguide where only a small sample of the tuned reflectors was needed and changes to the shielded design were feasible. A measurement of simulated ice was also made inside the waveguide and showed that the shielded design was unaffected by ice outside the shield. Then a shielded design was incorporated in the 4 x 8 foot ground plane and tests under simulated heavy rain showed little effect of the rain. These tests, which confirmed the expected immunity of the shielded design to ice and rain, are described later.

Radiation Pattern Test

Objectives. The experimental program described in this section served a three-fold purpose. First, and most important, the program has demonstrated the feasibility of the open array comcept using tuned reflectors. This has been accomplished by measuring the pattern performance of a single dipole element in a test environment which electrically duplicates the environment of the actual array. By extrapolating array performance from the measured element patterns, it has been concluded that the open ground plane will perform satisfactorily. Because the remainder of the array design is well within the state of the art, the successful measurements of the element indicate that the array design and fabrication should present no problems.

Second, the measurements have served to reduce the risk associated with a new design such as the open array. To minimize the risk, potential trouble areas were defined and these areas of concern were thoroughly investigated during the measurement

program. For example, one area of concern at the inception of the program was dipole unbalance, and subsequent investigation demonstrated that a particular dipole design was required in order to minimize the effects of unbalance.

Finally, the experimental program has provided design information, expecially in the area of tuned reflectors, which will expedite the final design of the array in Phase II. A number of possible tuned reflector configurations have been evaluated using the waveguide test fixture which will be described later.

Experimental Hardware. The purpose of the experimental program, as described above, was to measure the characteristics of a single dipole in an environment similar to that in the actual array. To accomplish that, the test ground plane shown in figure 3-18 was fabricated. The overall width of the ground plane is eight feet and the height is four feet, the same height as the actual array. Each of the columns is a 2 inch diameter tube, and the spacing of the tubes is 9 inches, as in the open array. One tuned reflector is mounted between each 2 inch column. As described previously, the reflector consists of aluminum tape wound on a rexolite rod, with periodic gaps cut in the tape. The horizontal black lines in the photograph are cords which hold the dielectric rods straight.

As can be seen, nine experimental dipoles were mounted on the three center tubes. The dipoles are spaced vertically by 6 inches. Only the center element was fed; the surrounding eight dipoles were terminated in 50 ohm loads. The feed cable for the center element was brought down the tube and connected to a mixer mounted inside the center of the upper azimuth table.

The test ground plane was mounted on an azimuth over elevation mount approximately 20 feet above the upper roof of the Smithtown facility, and was illuminated by a source antenna at the same height and approximately 30 feet away.

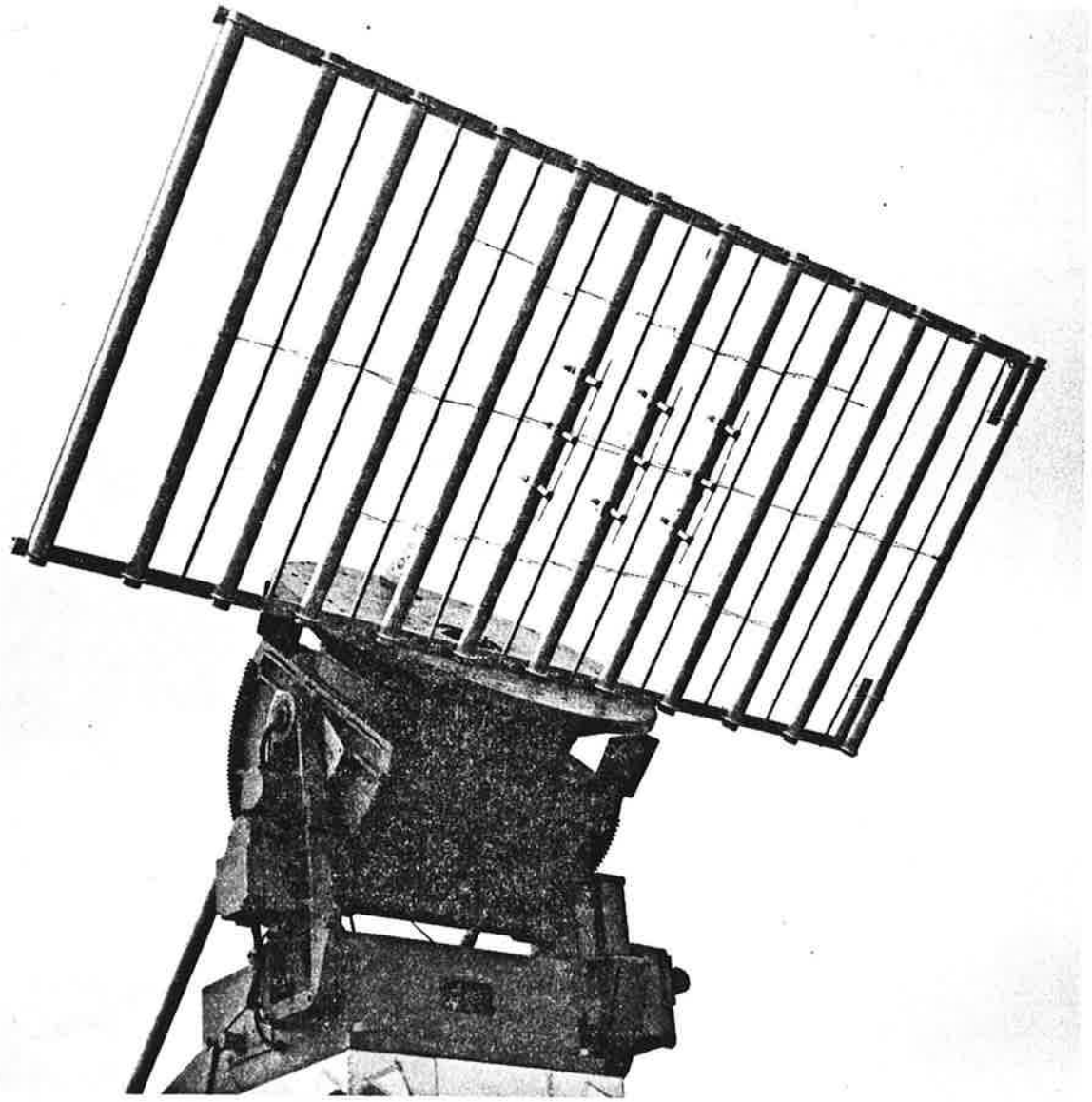

73270

Figure 3-18. Photograph of Experimental Open Ground Plane

Pattern cuts were taken in the principal planes (E and H), and in a number of conical cuts. The various pattern cuts are illustrated in figure 3-19.

Experimental Results. The experimental work proceeded in the following manner. First, a single dipole was mounted and an investigation made of the ground plane performance with the tuned reflectors, with solid half inch rods in place of the reflectors, and with a solid aluminum sheet covering the entire open array.

Figure 3-20 shows the measured H plane pattern for each configuration. The solid ground plane has the best backlobe performance at this elevation angle; better than -40 dB. It should be noted that, because of diffraction around the edges of the ground plane, the backlobe structure is a function of elevation angle. However, at any elevation angle the solid ground plane backlobe is less than -30 dB. The open array with solid rods in place of the tuned reflectors illustrates the improvement in performance achievable with the tuned reflectors. The backlobe at the horizon is only -14 dB. The tuned reflector pattern shows a general backlobe level of -20 dB, with a notch in the critical 180° direction of -30 dB.

Upon completion of the tuned reflector measurements, the remaining 8 dipoles were added and a complete survey of the upper hemisphere was performed. The results of these measurements are summarized in figures 3-21. Three H-plane conical cuts are shown; at 0 degrees, 10 degrees, and 30 degrees. A contour plot of the entire backlobe region resulted in a backlobe as high as -16 dB.

The high backlobes above the horizon were thought to be caused by radiation from the stems of the dipoles. This unbalanced stem current, nonexistant in the original dipole design, was

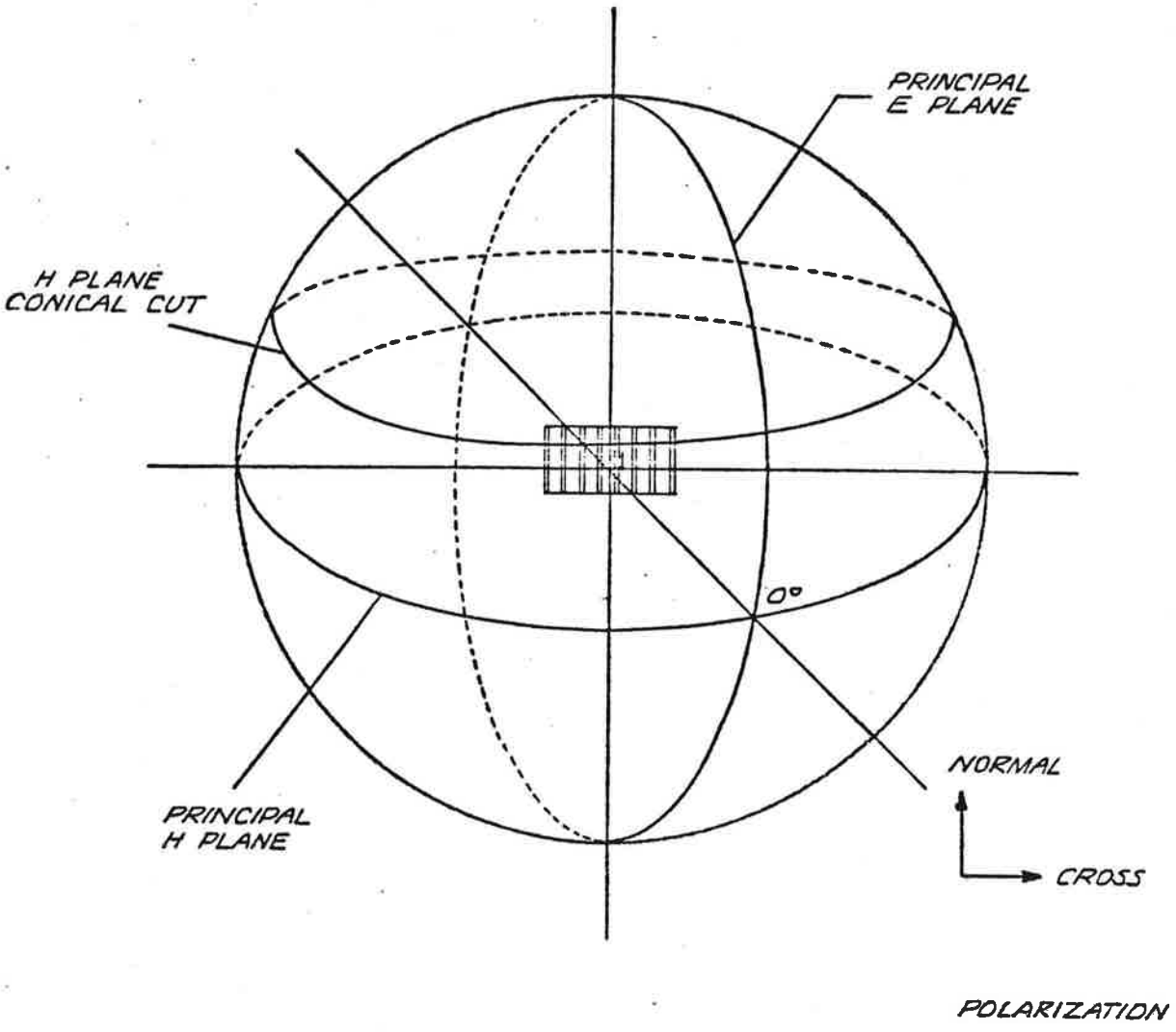

Figure 3-19. Definition of Pattern Cuts

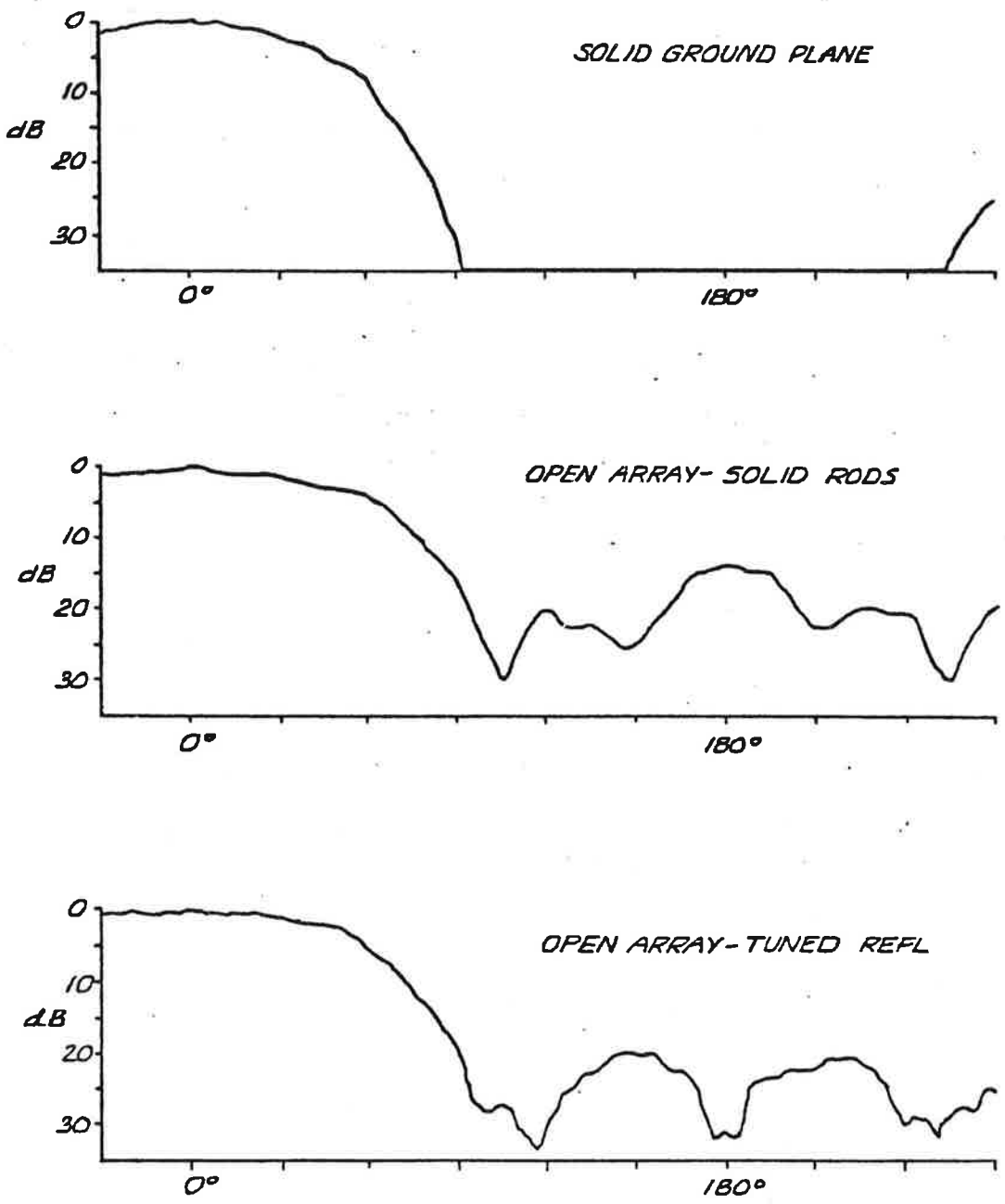

Figure 3-20. Comparison of Reflector Performance

caused by coupling between the adjacent dipoles. To verify this theory, a shield was designed for the dipole balun, and experiments showed that this shield effectively suppressed radiation from the stem, even when the dipole was purposefully unbalanced.

A new set of conical cut patterns was measured with each of the 9 balun stems shielded. H-plane patterns were measured every 5 degrees in elevation from 0 degrees to +70 degrees, for both desired and cross polarization. Complete sets of patterns were measured at 1030 and 1090 MHz, and principal plane patterns were also measured at 1000 and 1120 MHz. The results were entirely satisfactory, indicating a maximum backlobe level of -25 dB. Typical H plane patterns at 1000, 1030, 1190 and 1120 MHz are shown in figures 3-22 through 3-25, respectively. These patterns are all measured at 0 degrees elevation.

As can be seen from the figures, the patterns show a well defined element pattern, with an average backlobe level down approximately 25 dB. In the critical angular region about 180 degrees, the backlobe level is down between 25 and 35 dB.

The dotted pattern is the cross-polarized measurement, and is usually down 25 dB in the forward sector and an average of 30 dB down in the rear sector.

Because of concern about the frequency bandwidth of the tuned reflector technique, patterns were measured at twice the operating bandwidth of the array. As can be seen, no serious degradation of the patterns occurs.

Additional patterns are included in the appendix.

Extrapolated Array Performance. To arrive at an estimate of final array performance, the following procedure was used. The measured element pattern, which had been measured in as realistic an environment as possible, was multiplied by the theoretical array

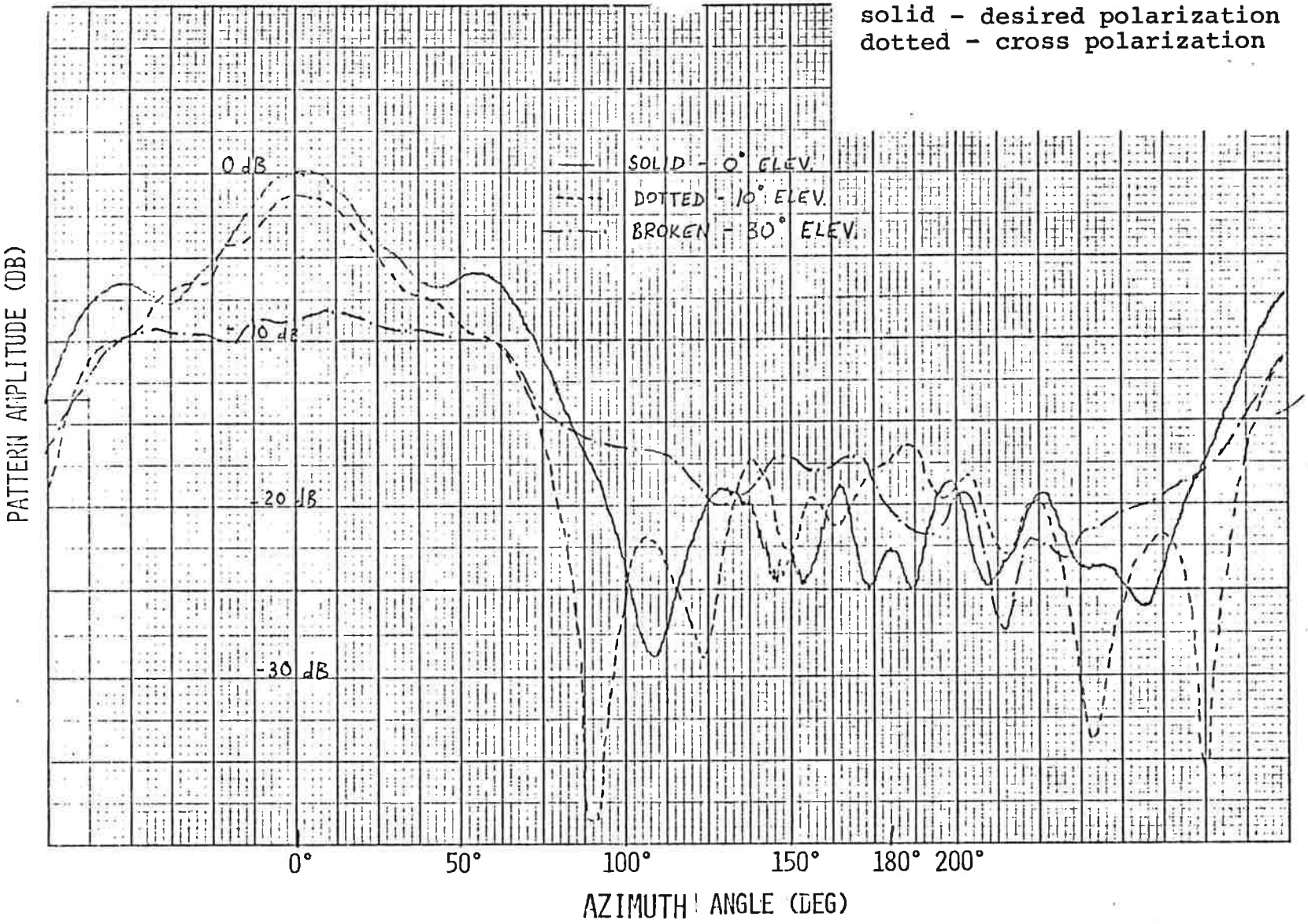

Figure 3-21. Azimuth Element Pattern, 9 EL, Preliminary Measurement with Unshielded Dipole Stems

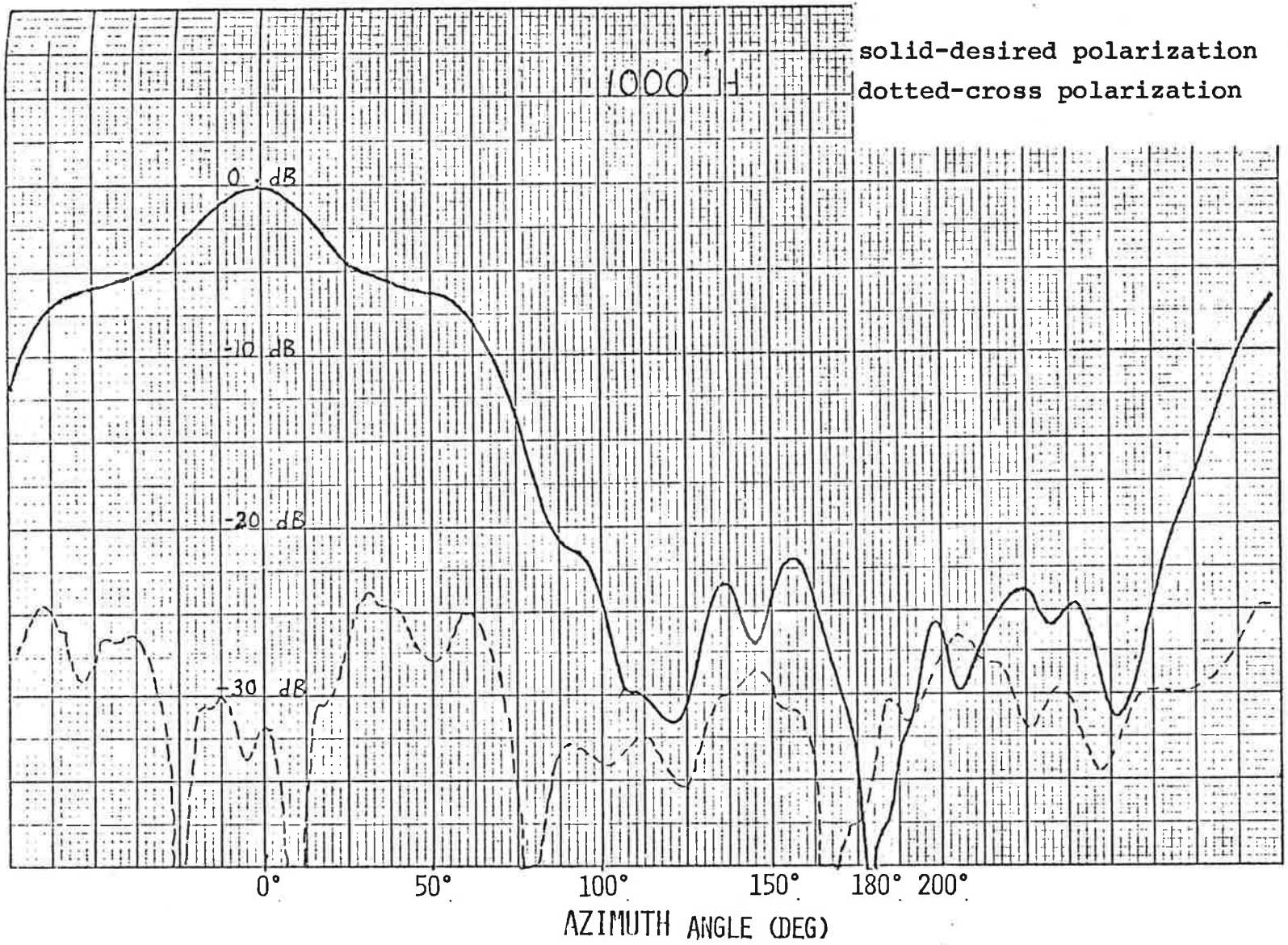

Figure 3-22. Azimuth Element Pattern, 1000 MHz

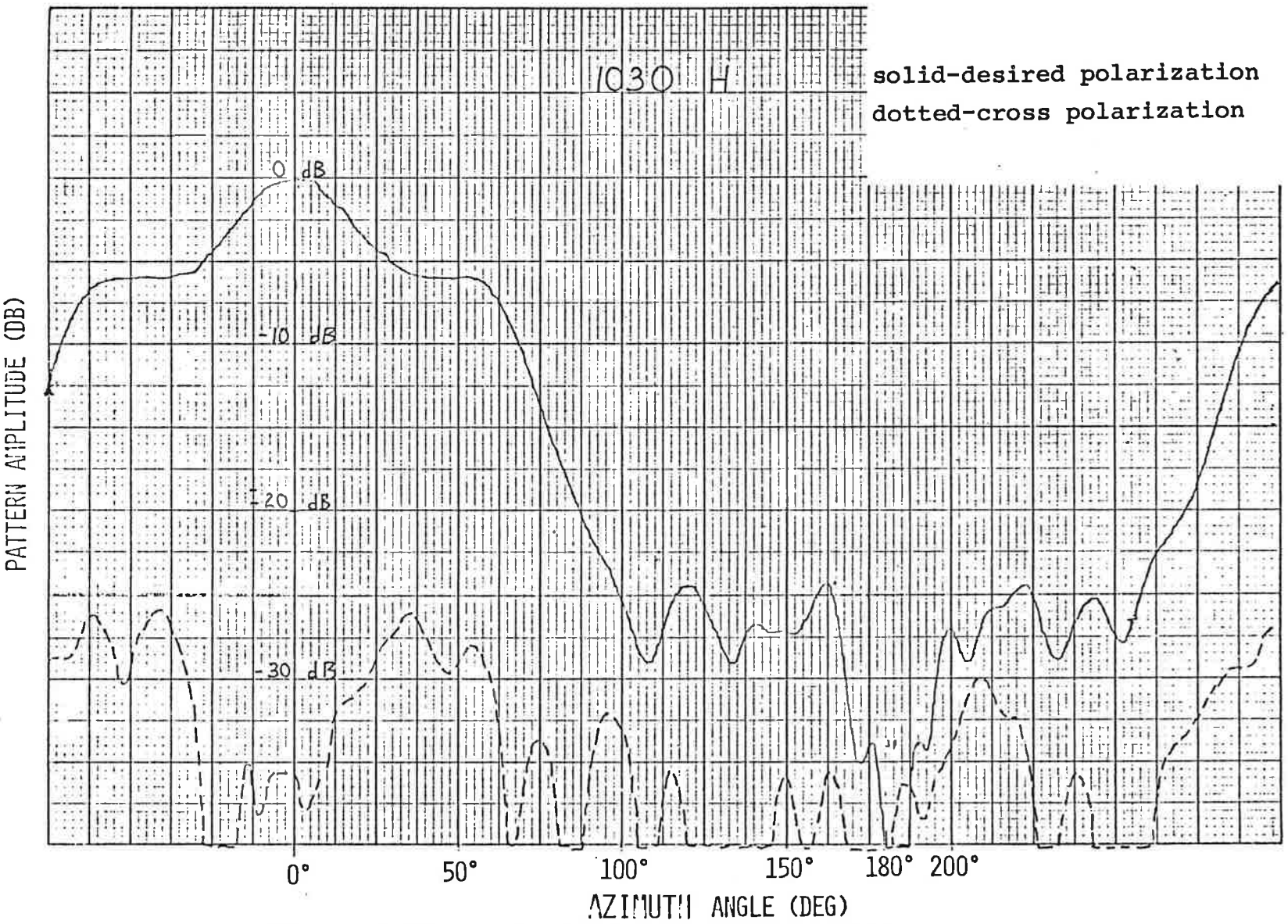

Figure 3-23. Azimuth Element Pattern, 1030 MHz

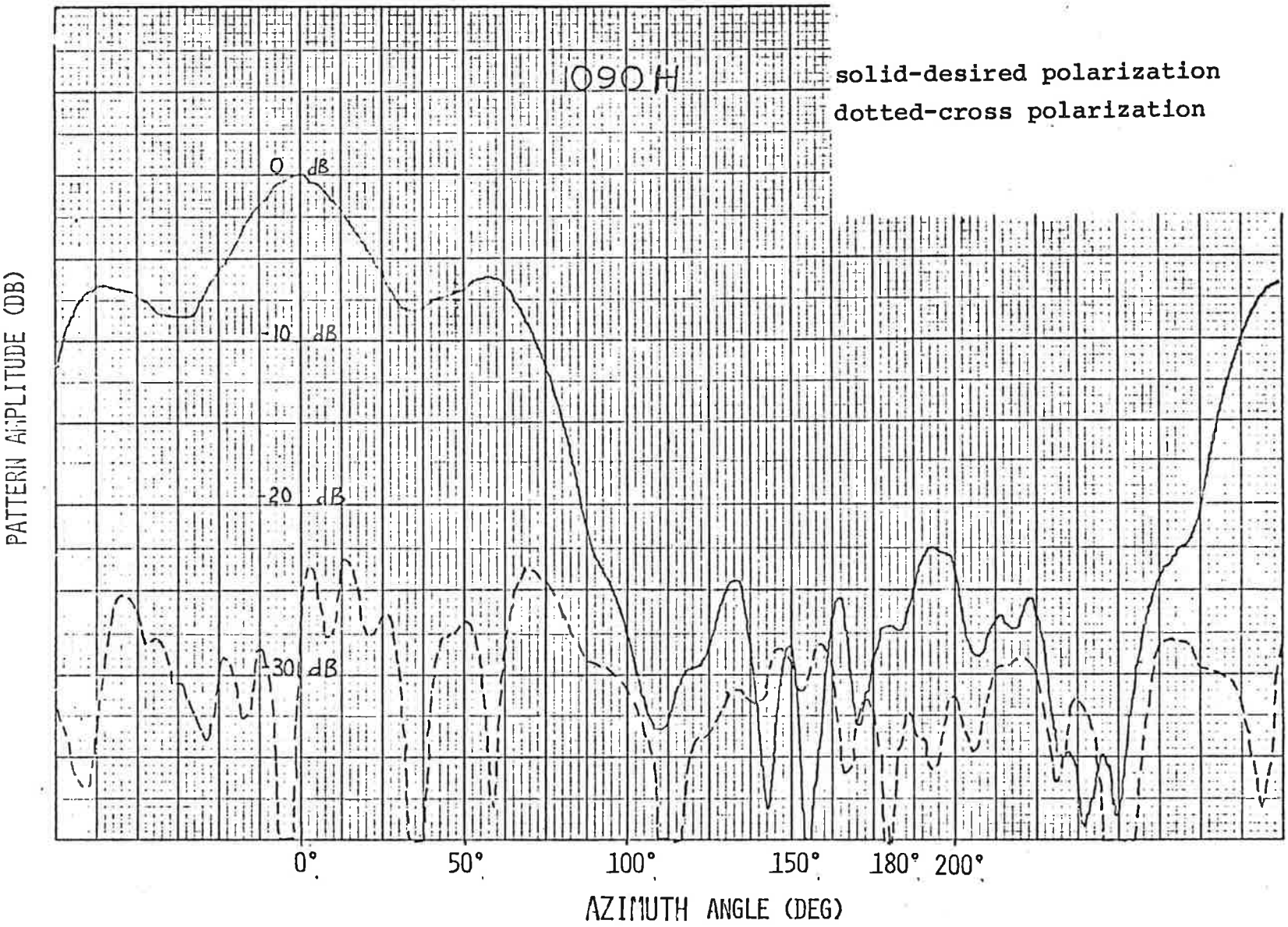

Figure 3-24. Azimuth Element Pattern, 1090 MHz

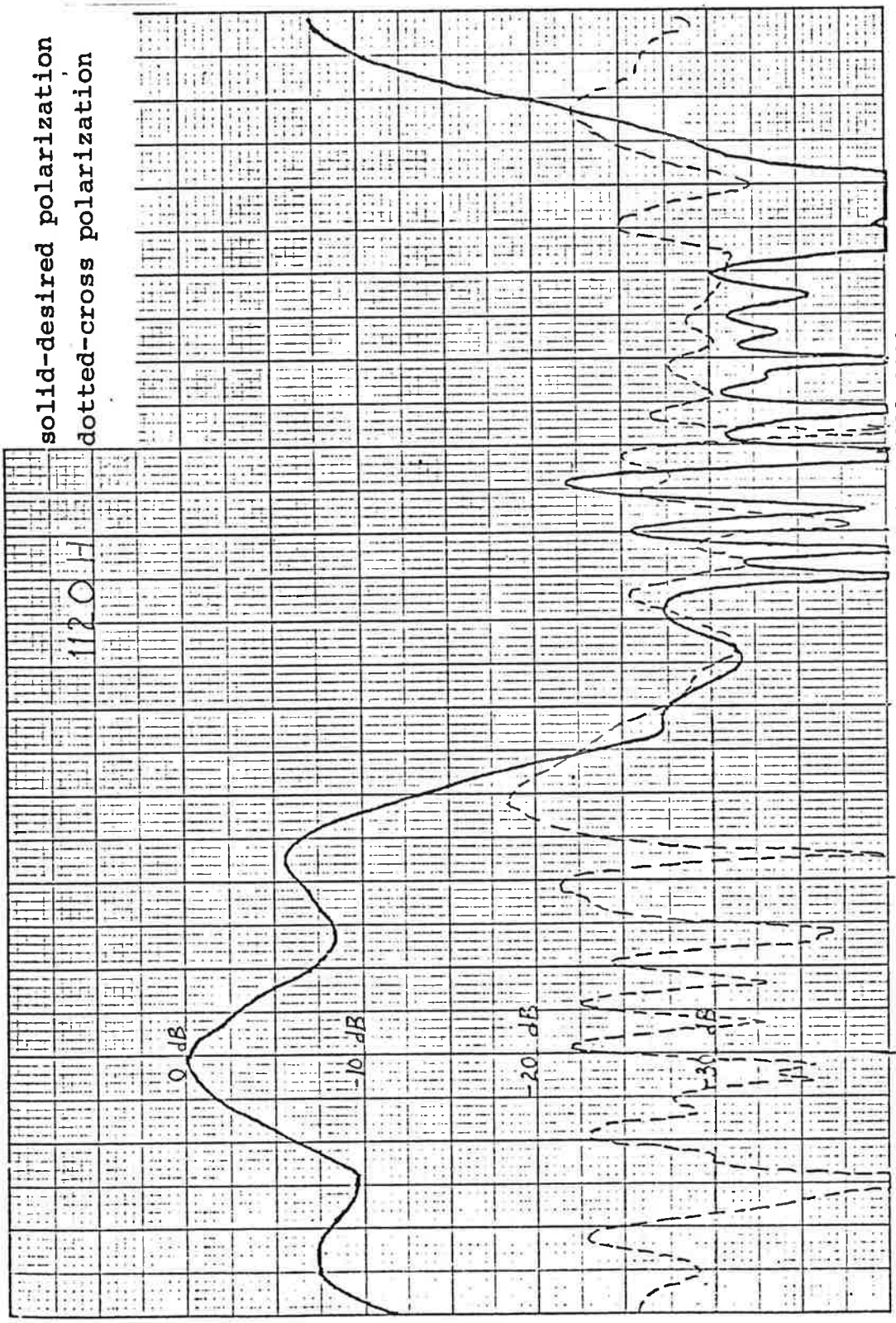

Figure 3-25. Azimuth Element Pattern, 1120 MHz

factor which the array is designed for. The product of the array factor and the measured element pattern predicts, to a good approximation, the final performance of the array. The procedure neglects diffraction around the edges of the array, changes in the element pattern of dipoles at the edge of the array, and the effect of tolerance errors. All these effects usually have little influence on the performance of a large array, except perhaps in the sidelobe region, which is of little concern in this particular calculation.

To best illustrate the estimated array performance, contour plots have been made of the front and rear hemisphere of the array for four conditions: sum pattern, 1030 MHz; sum pattern 1090 MHz; difference pattern 1030 MHz; difference pattern 1090 MHz. It should be noted that only contours which convey significant information have been plotted, and contours have been omitted in the sidelobe region, especially in the rear hemisphere, where signal levels will be controlled primarily by diffraction around the edge of the array.

Figures 3-26 thru 3-33 show the resulting contour plots. The front hemisphere performance is primarily controlled by the assumed array factors. The sum pattern generates a fan beam coverage which has a 3 dB beamwidth of 2.3 degrees in azimuth and 3 dB points of $+3^{o}$ and $+35^{o}$ in elevation. Because of the elevation feed network design, the lower 3 dB point in elevation does not change with frequency, while the upper 3 dB point moves down about 2 degrees from 1030 to 1090 MHz. The difference pattern has the same elevation performance as the sum, but of course has the characteristic two lobe azimuth pattern.

In the backlobe region, the significant angular sector is the small region at 180 degrees azimuth, and extends from 0 degrees to 50 degrees in elevation.

In this region, the maximum points are shown on the contours, no point exceeding 25 dB below the peak of the beam in the forward direction.

Effect of Rain and Ice. Because the tuned reflectors must operate during exposure to all weather conditions, and because the resonance of the reflector could be influenced by ice or rain on the surface of the reflector, it was considered desirable to perform some experimental measurement of ice and rain effects.

Ice, with a dielectric constant of approximately 3.5, was thought to be less of a problem than the accumulation of rain water, with a dielectric constant of approximately 80. To evaluate the effect of ice accumulation on the tuned reflector, measurements were made of a tuned reflector in a waveguide with dielectric simulating the ice.

The waveguide, used for preliminary evaluation of tuned reflector designs, consists of a 3 foot long waveguide, 3.5 inches high by 8 inches wide. The height is equal to the periodicity of the tuned reflector, thus imaging a single section of reflector into an infinite line. One end of the guide was terminated, and the impedance looking into the opposite end was measured. A tuned reflector design which had been verified on the Smithtown antenna range was used as a reference. All other reflector designs are tuned to match the measured impedance of the reference design. This procedure eliminates the problem of interpreting the waveguide impedance measurement in terms of backlobe performance.

To evaluate the effect of ice, a shielded tuned reflector was first adjusted in the waveguide to match the reference impedance. The shielded reflector consisted of a 5/8 inch diameter fiberglass tube, with a 1/4 inch diameter aluminum rod and rexolite disc tuned reflector inside. Then, a square piece of nylon with a dielectric constant of 4.0 was drilled and placed around

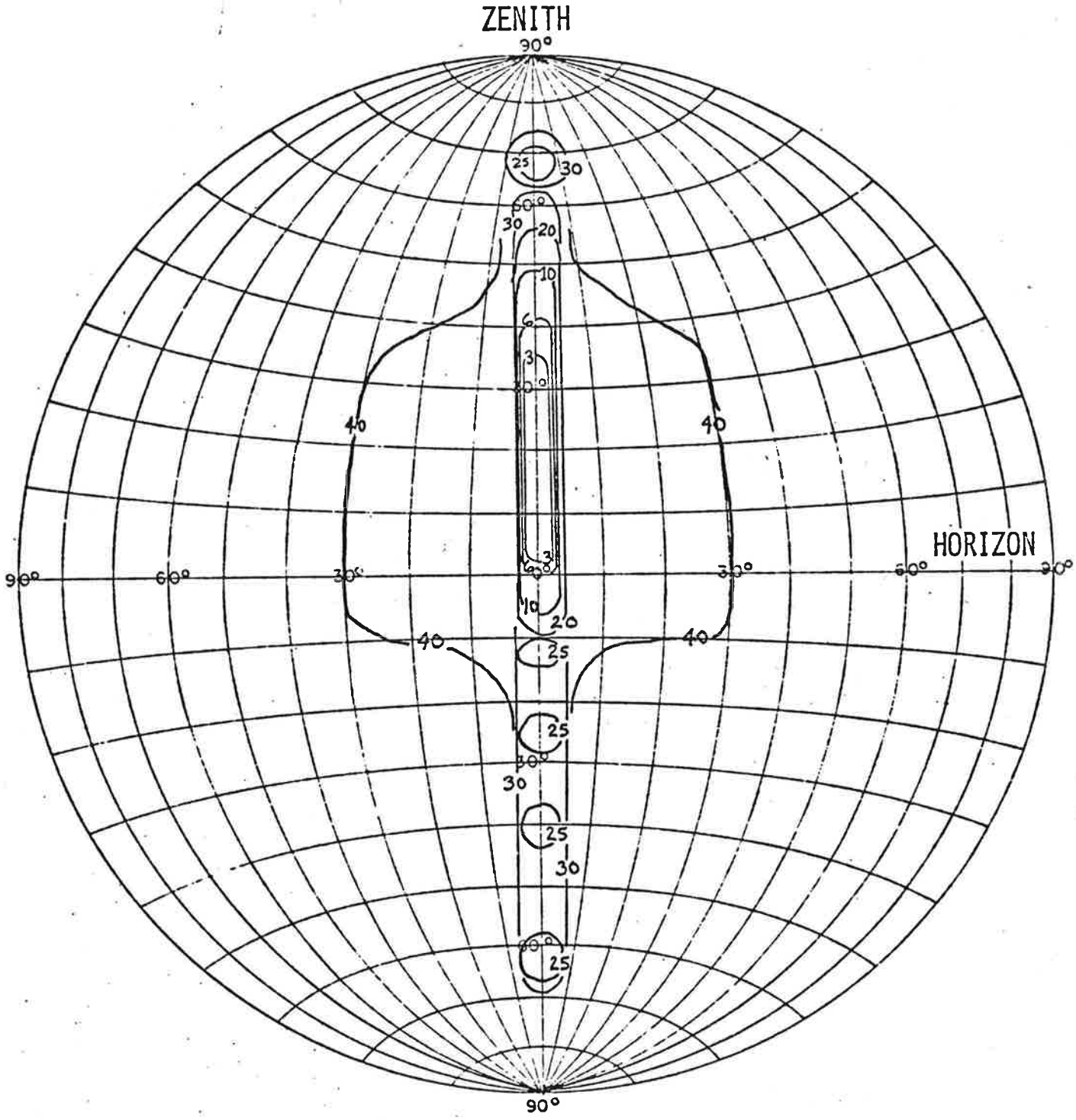

FRONT HEMISPHERE

SUM
PATTERN AMPLITUDE IN DB
RELATIVE TO PEAK OF BEAM

1030 MHz

Figure 3-26. Estimated Array Performance

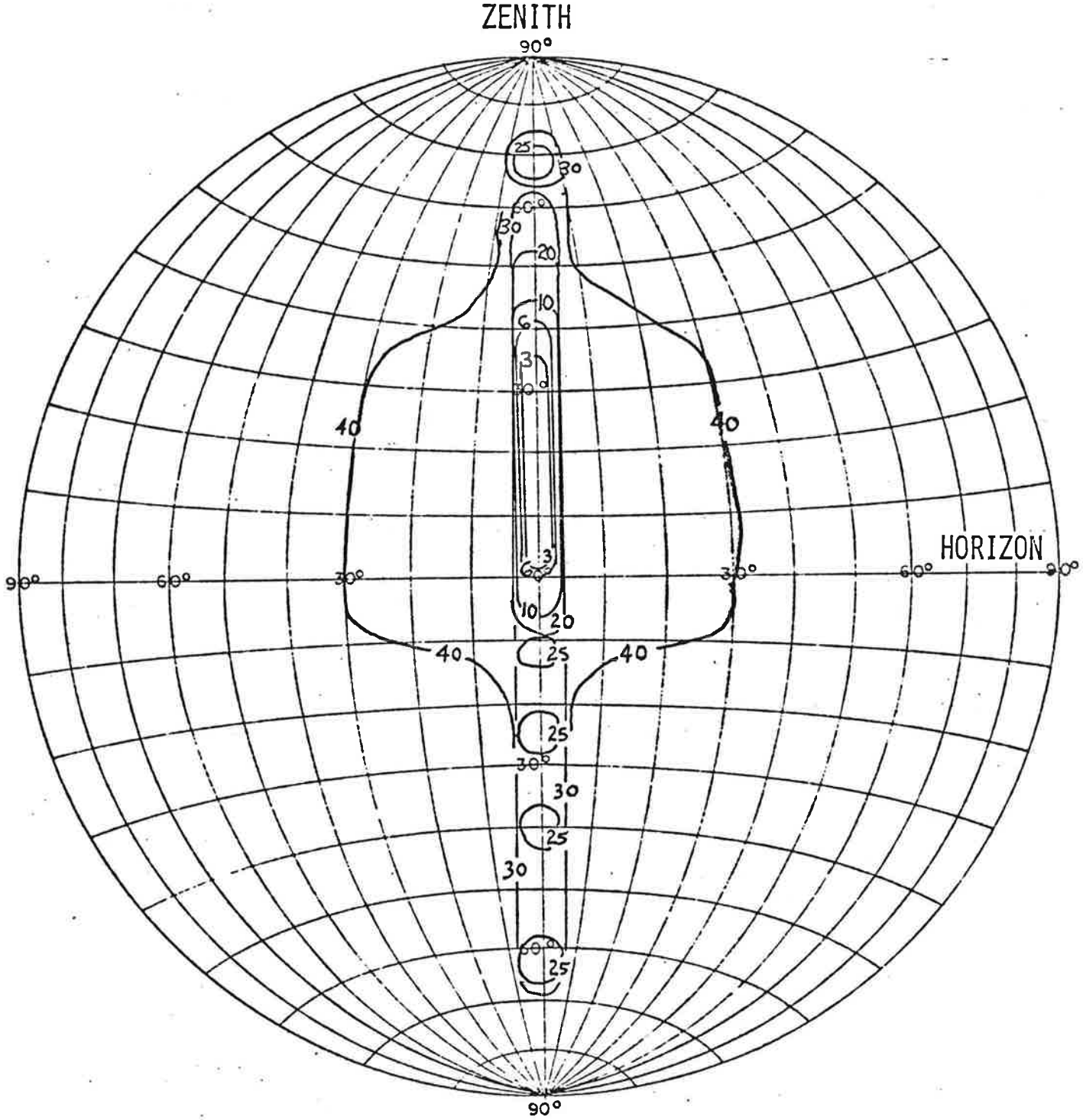

Figure 3-27. Estimated Array Performance

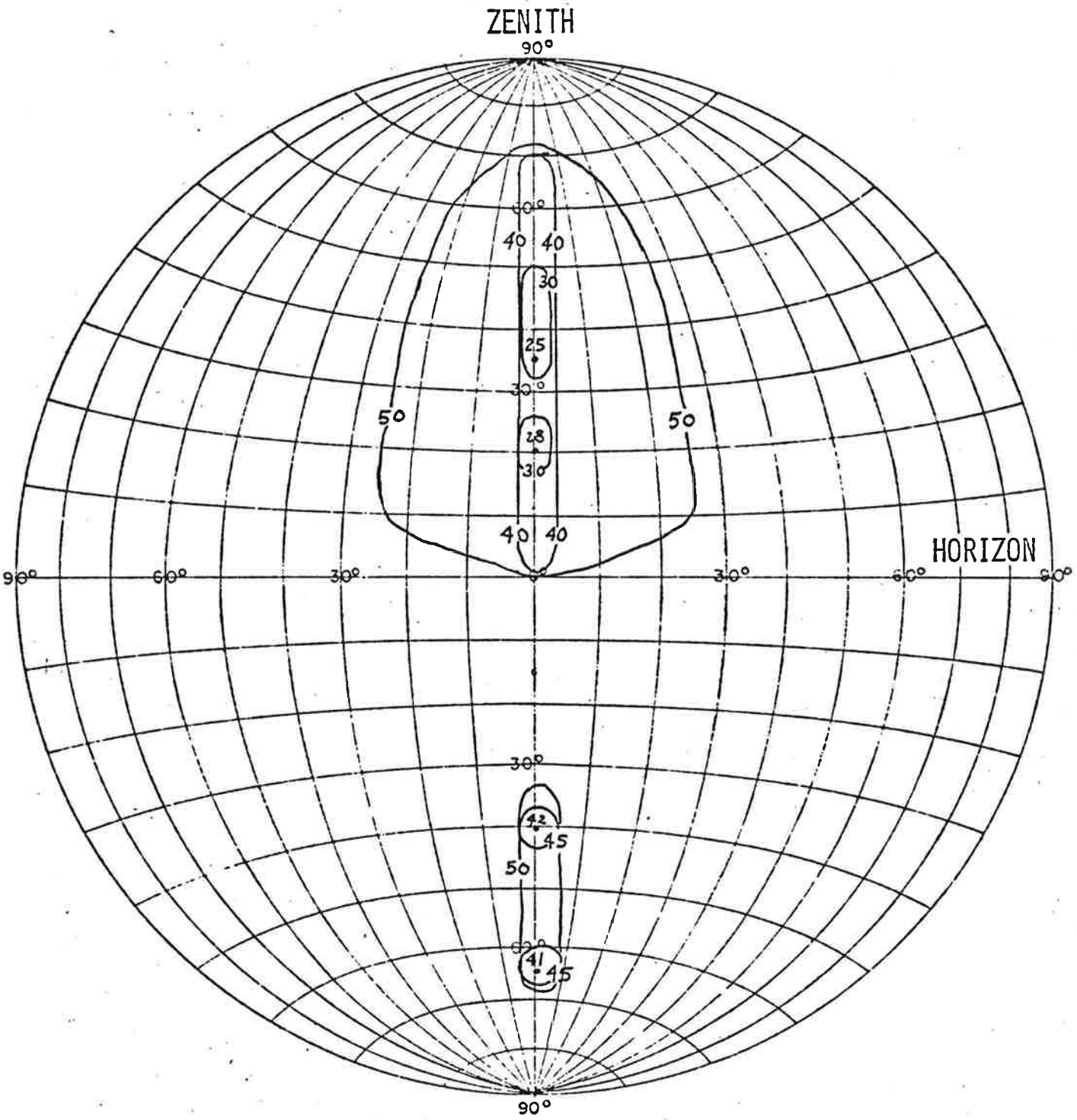

REAR HEMISPHERE

SUM
PATTERN AMPLITUDE IN DB
RELATIVE TO PEAK OF BEAM

1030 MHz

Figure 3-28. Estimated Array Performance

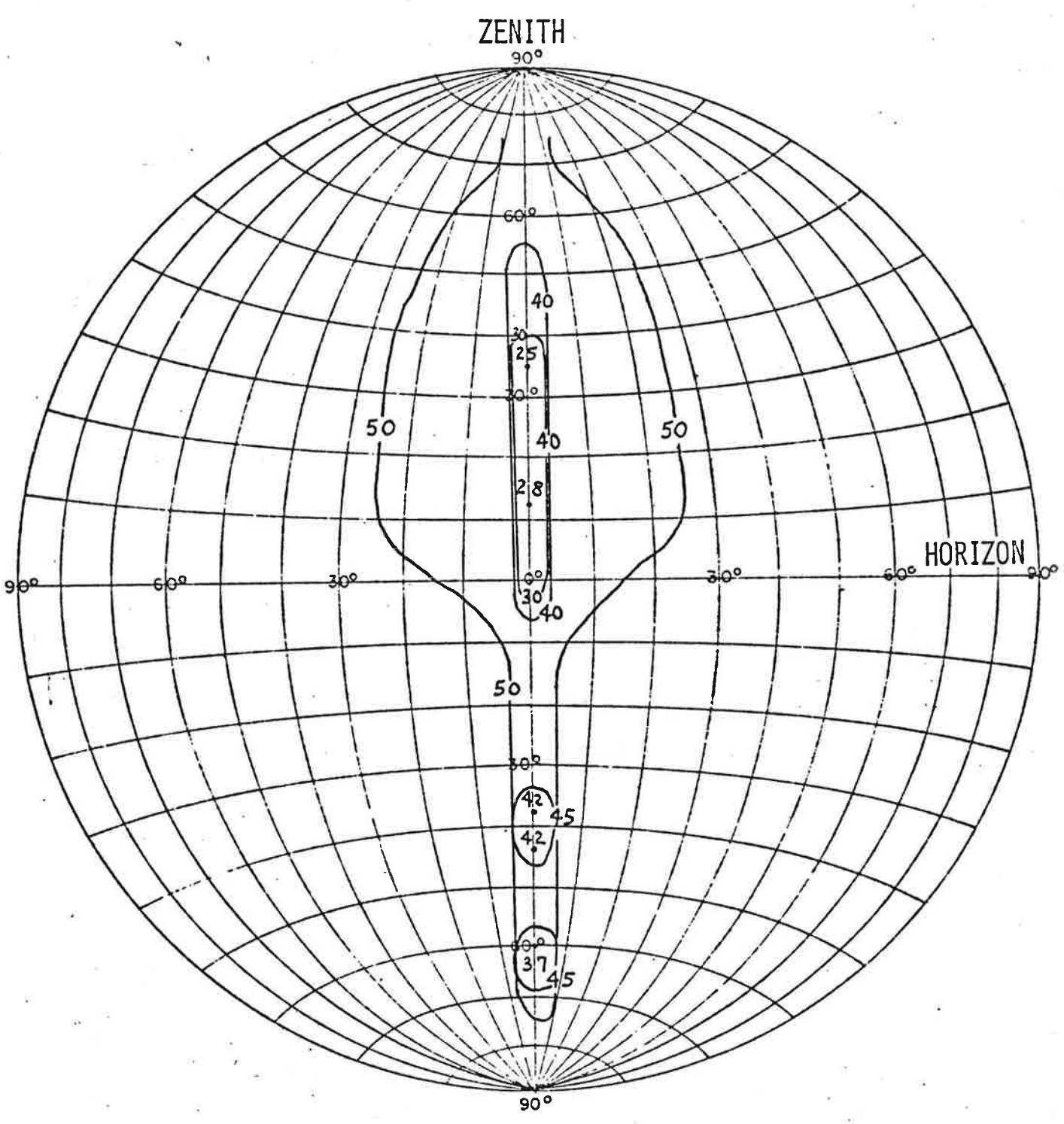

REAR HEMISPHERE

SUM
PATTERN AMPLITUDE IN DB
RELATIVE TO PEAK OF BEAM

1090 MHz

Figure 3-29. Estimated Array Performance

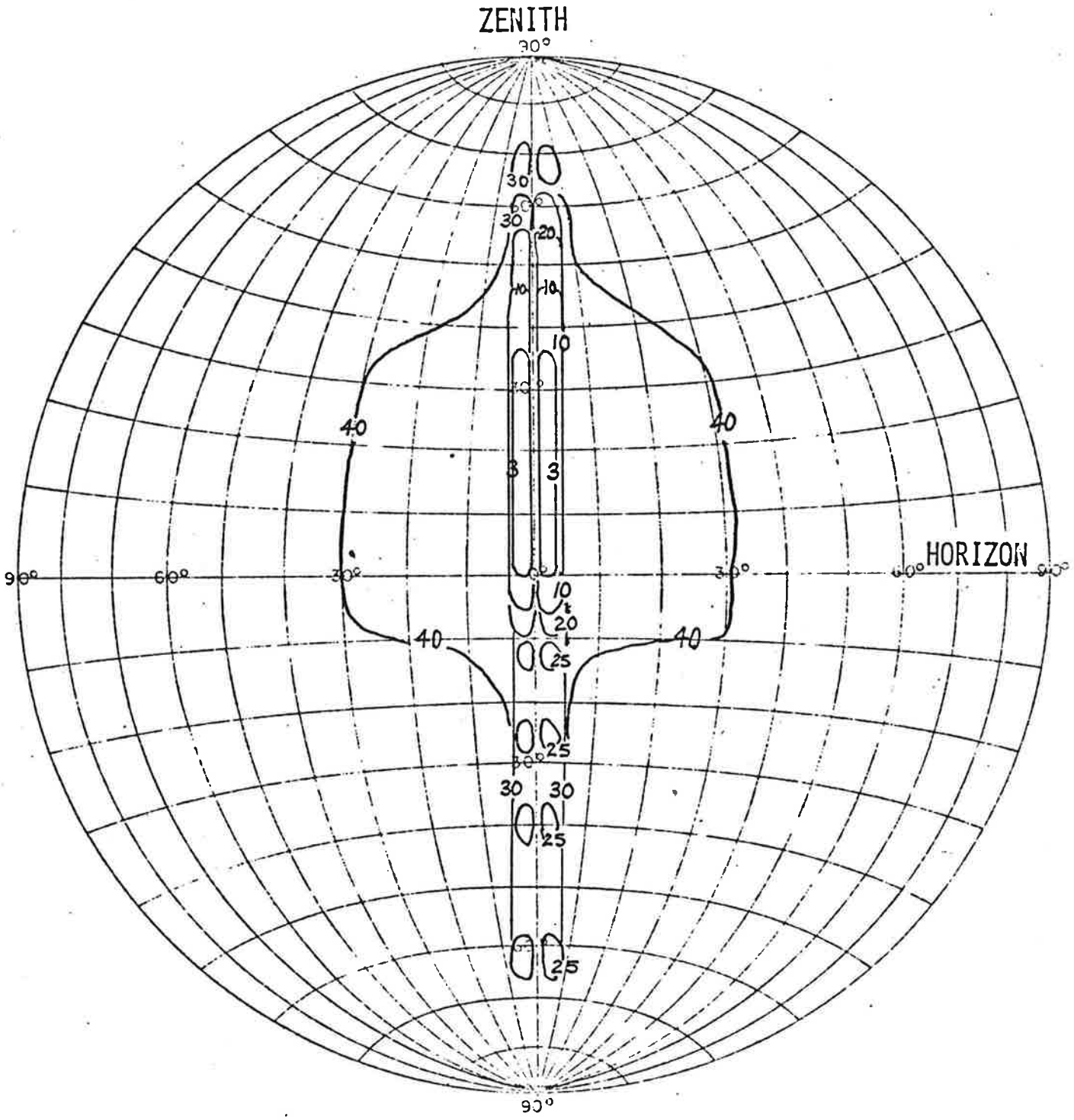

FORWARD HEMISPHERE
DIFFERENCE
PATTERN AMPLITUDE IN DB
RELATIVE TO PEAK OF BEAM

1030 MHz

Figure 3-30. Estimated Array Performance

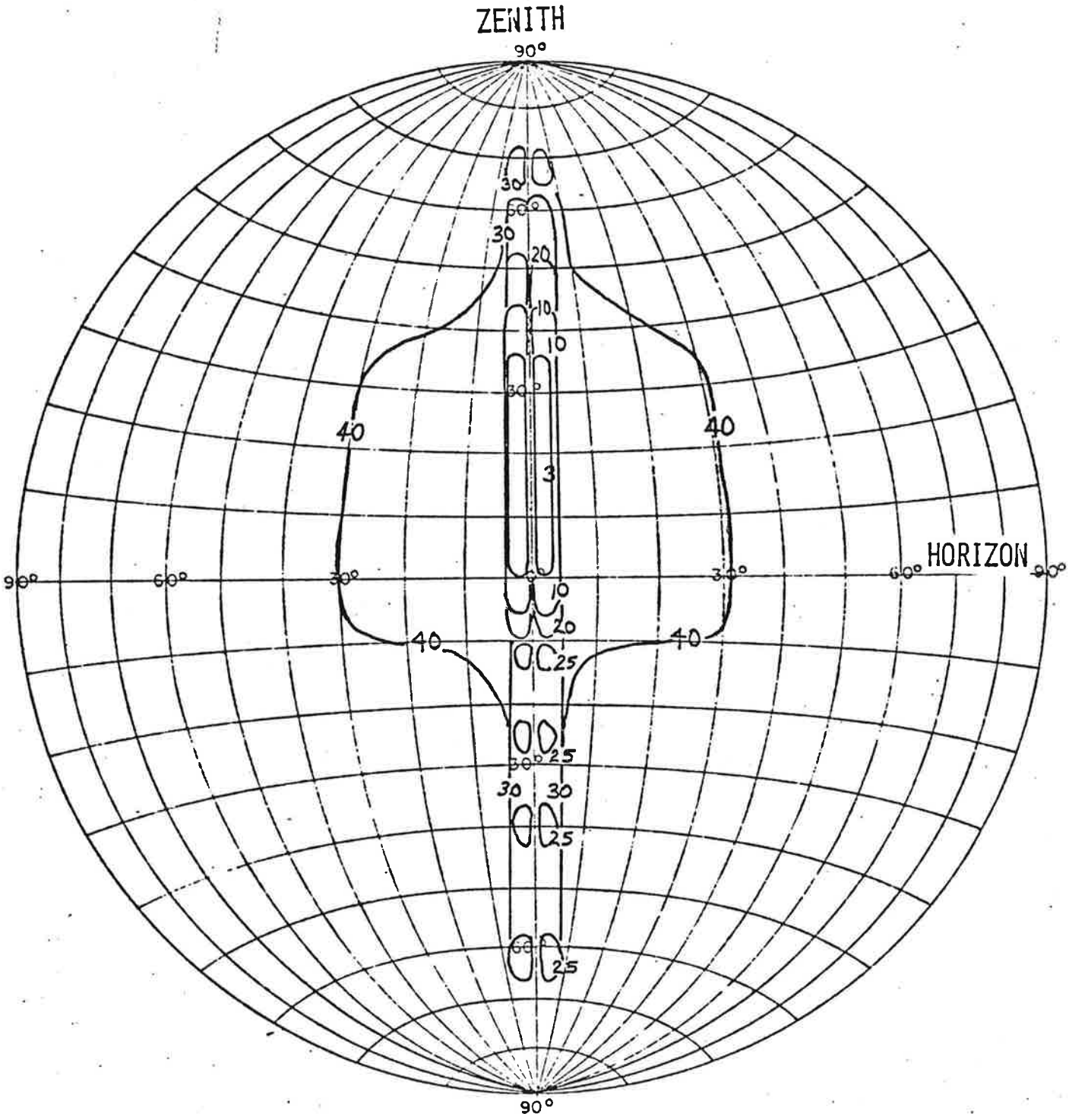

FORWARD HEMISPHERE
DIFFERENCE
PATTERN AMPLITUDE IN DB
RELATIVE TO PEAK OF BEAM

1090 MHz

Figure 3-31. Estimated Array Performance

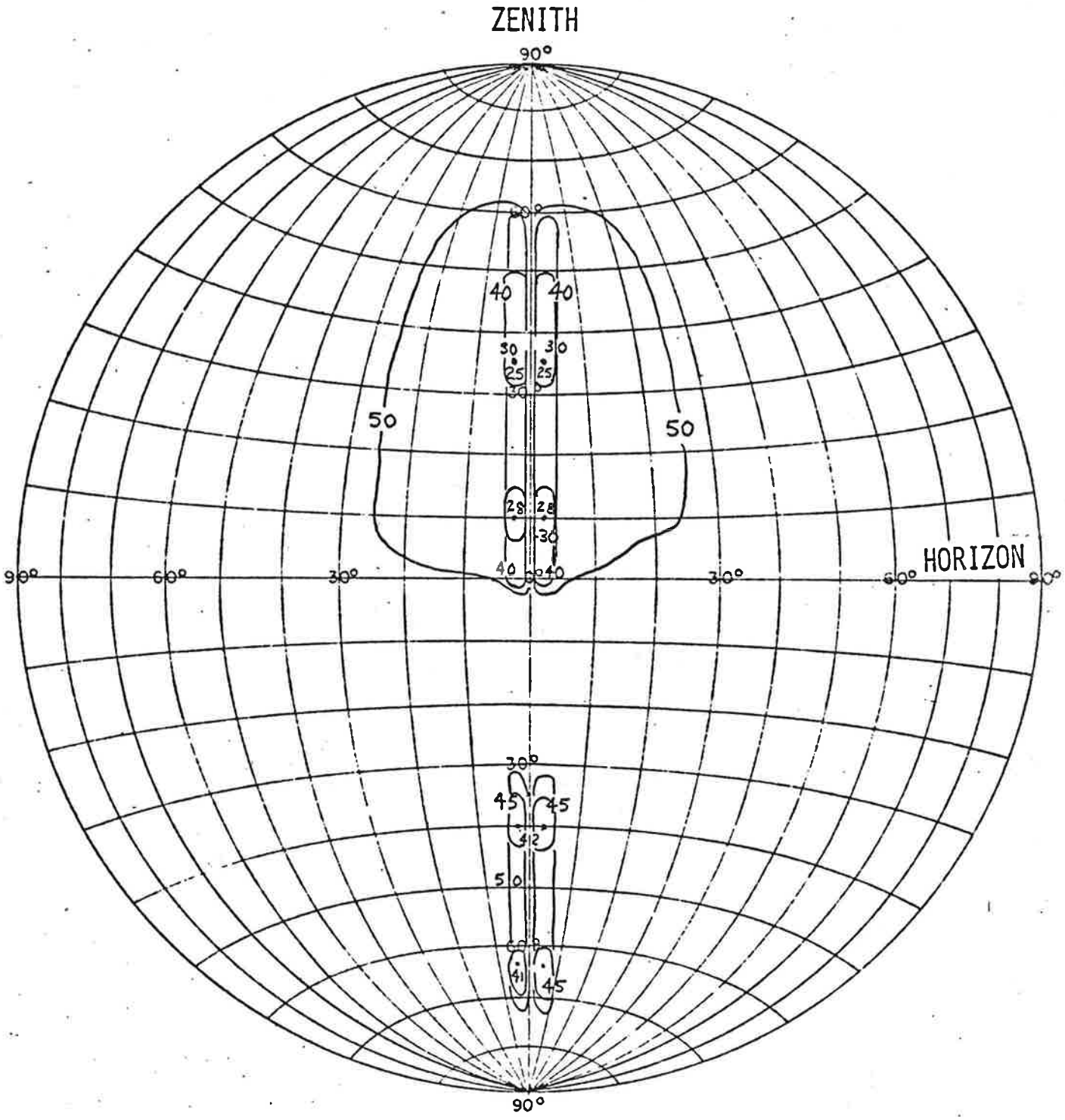

REAR HEMISPHERE
DIFFERENCE
PATTERN AMPLITUDE IN DB
RELATIVE TO PEAK OF BEAM

1030 MHz

Figure 3-32. Estimated Array Performance

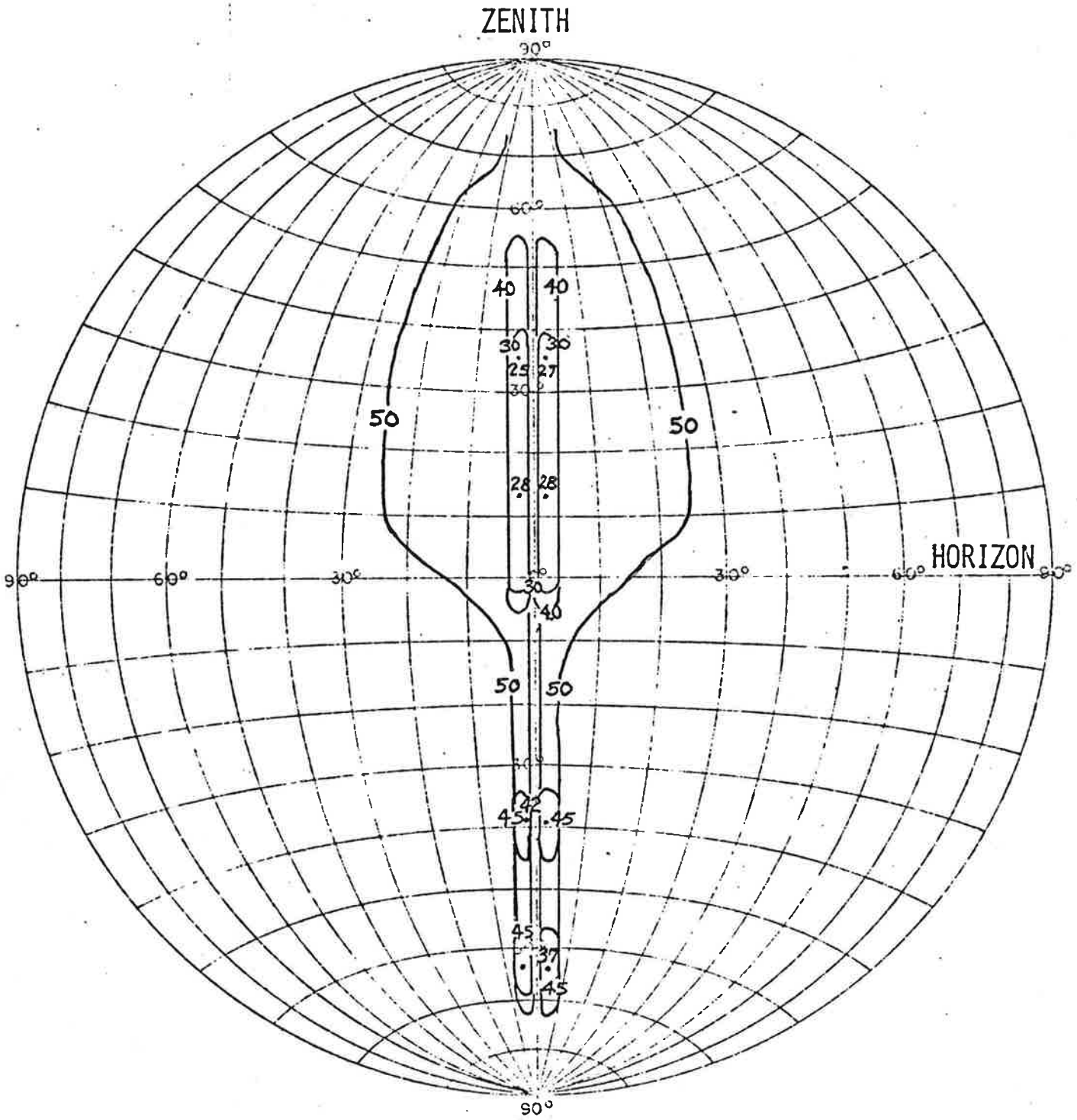

REAR HEMISPHERE
DIFFERENCE
PATTERN AMPLITUDE IN DB
RELATIVE TO PEAK OF BEAM

1090 MHz

Figure 3-33. Estimated Array Performance

the reflector. The average radial thickness of nylon was approximately 1/2 inch. Figure 3-34 shows the close correspondence between the measurements with and without the nylon. The insignificant change in tuning indicated that no significant change in backlobe performance should occur with 1/2 inch of radial ice on the rods. Further, because the fringing fields in the vicinity of the tuned reflector gap do not extend very far from the rod, there is little possibility that a greater ice thickness will cause more detuning.

Water presented a greater problem in trying to simulate. The actual distribution of water on the tuned reflector was unknown, and any measurements would be influenced more by the assumed distribution than by the shield design.

Also, any detuning caused by simulated rain could not be readily interpreted in terms of actual array performance. Thus, it was concluded that the experimental ground plane should be measured in a rain environment, using shielded reflectors.

Six shielded reflectors were made up for the test, this time using 5/8 inch diameter polycarbonate tubes because fiberglass was unavailable. The tuned reflectors were fabricated from aluminum tape and 1/4 inch diameter rexolite rod. The new reflectors were adjusted for a satisfactory backlobe level at 1060 MHz. Because the experimental dipoles were not encapsulated, as the final dipoles will be, all dipoles were covered with watertight plastic bags.

The measurement procedure consisted of taking a reference pattern, and then measuring another pattern while simulating rain. A small plastic container mounted at the base of the array was used to estimate the effective rain rate.

The first measurement consisted of mounting a sprinkler hose on top of the experimental ground plane and taking reference and rain measurements. This set-up is shown in figure 3-35. The

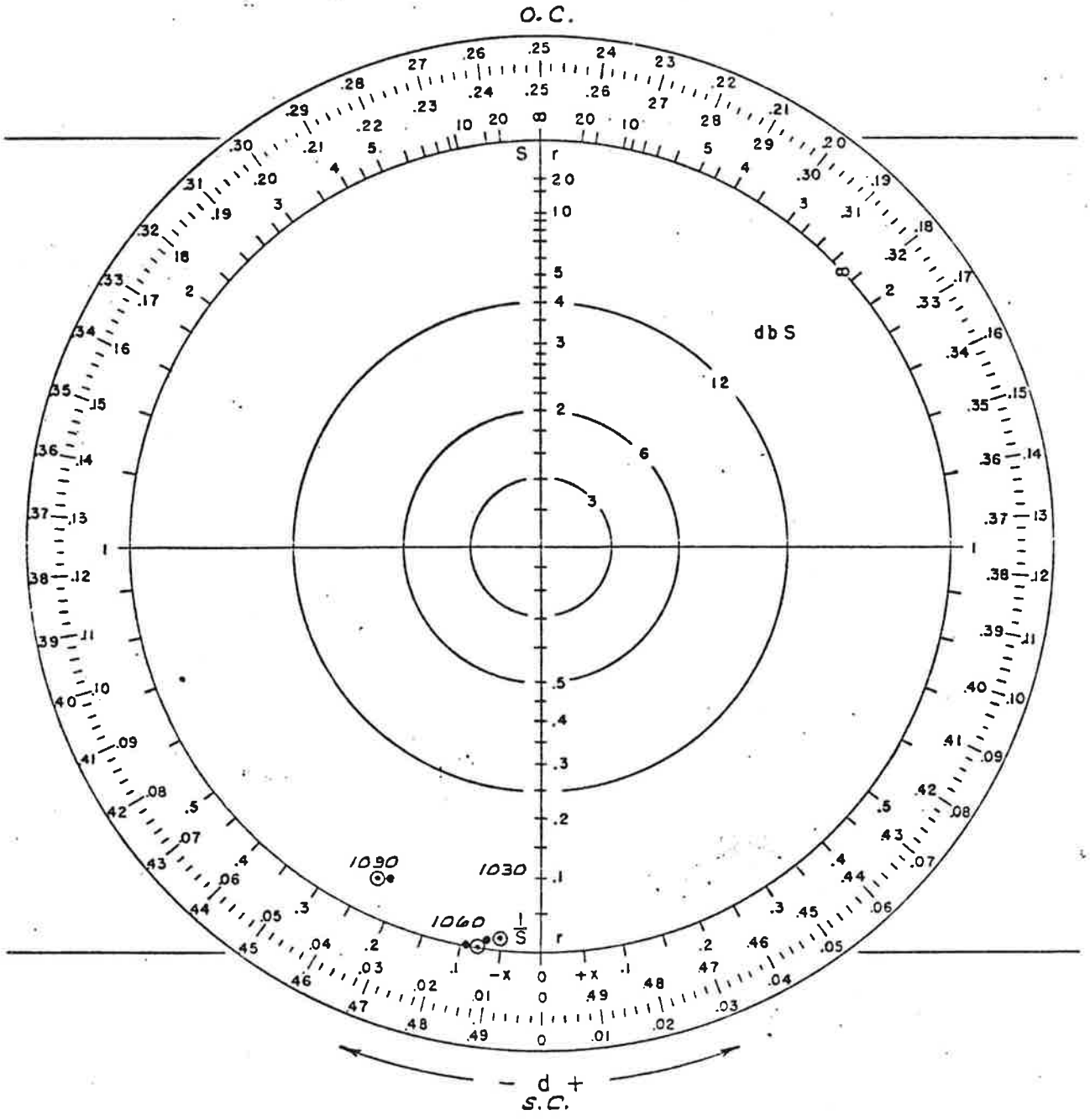

Figure 3-34. Effect of Simulated Ice on Impedance of Reflector in Waveguide Simulator

measured rain rate was 4.5 inches per hour, and the measurements were made in a 10-15 MPH breeze. The resultant measurements are shown in figure 3-36. The backlobe performance has not changed substantially, increasing only 3 dB at 180 degrees.

Because of concern that high wind velocities could still degrade the array performance by blowing large amounts of rain against the array, another measurement was made while a technician directed a hose at the front of the array. In this case, the equivalent rain rate was 12 inches per hour, and again no serious degradation in the pattern occurred. Figure 3-37 shows the measured results.

In summary, our best efforts to simulate weather conditions which may degrade array performance have failed to disclose any substantial problems.

Mechanical Design

Component Design and Layout. The mechanical design of the replacement beacon and omni antennas along with the packaging of their associated R.F. equipment is consistent with the design concept presented in the proposal. The antenna mechanical designs are the same for both the ASR and ARSR mounted configurations. However, due to the difference in ASR and ARSR mounted configurations, different interface structures are necessary for attachment of the 4 foot by 28 foot open array to the ASR or ARSR antennas. A general description of both the replacement beacon and OMNI antennas are presented below, followed by the mechanical design features of the major components and mounting.

The 4 foot by 26 foot replacement beacon antenna, illustrated in figure 3-38 is of the open array configuration. It is rectangular with truncated ends beginning 8 feet from the vertical centerline, sloping from both top and bottom, to measure 1.25 feet at the tips.

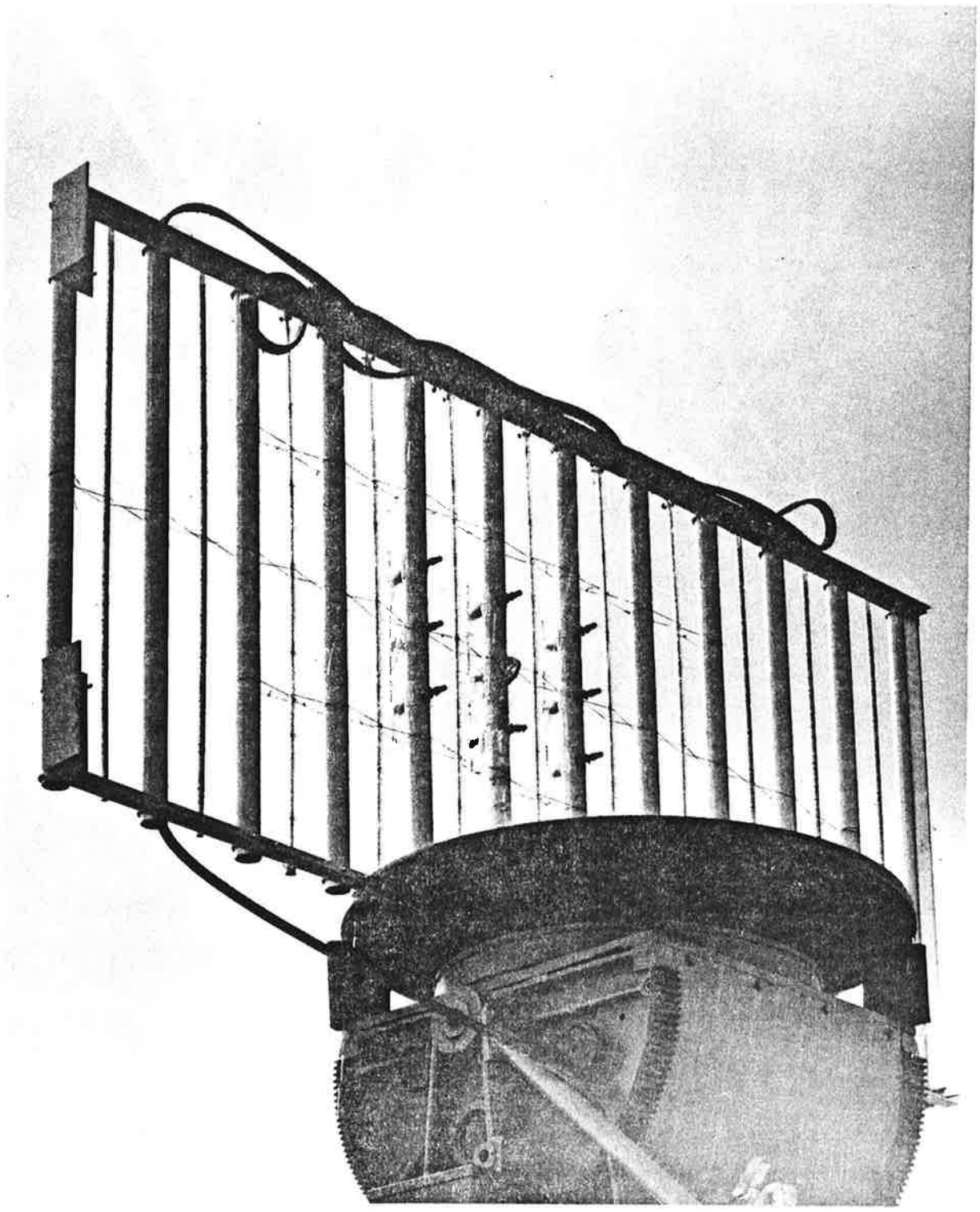

73271

Figure 3-35. Experimental Open Array in Simulated Rain

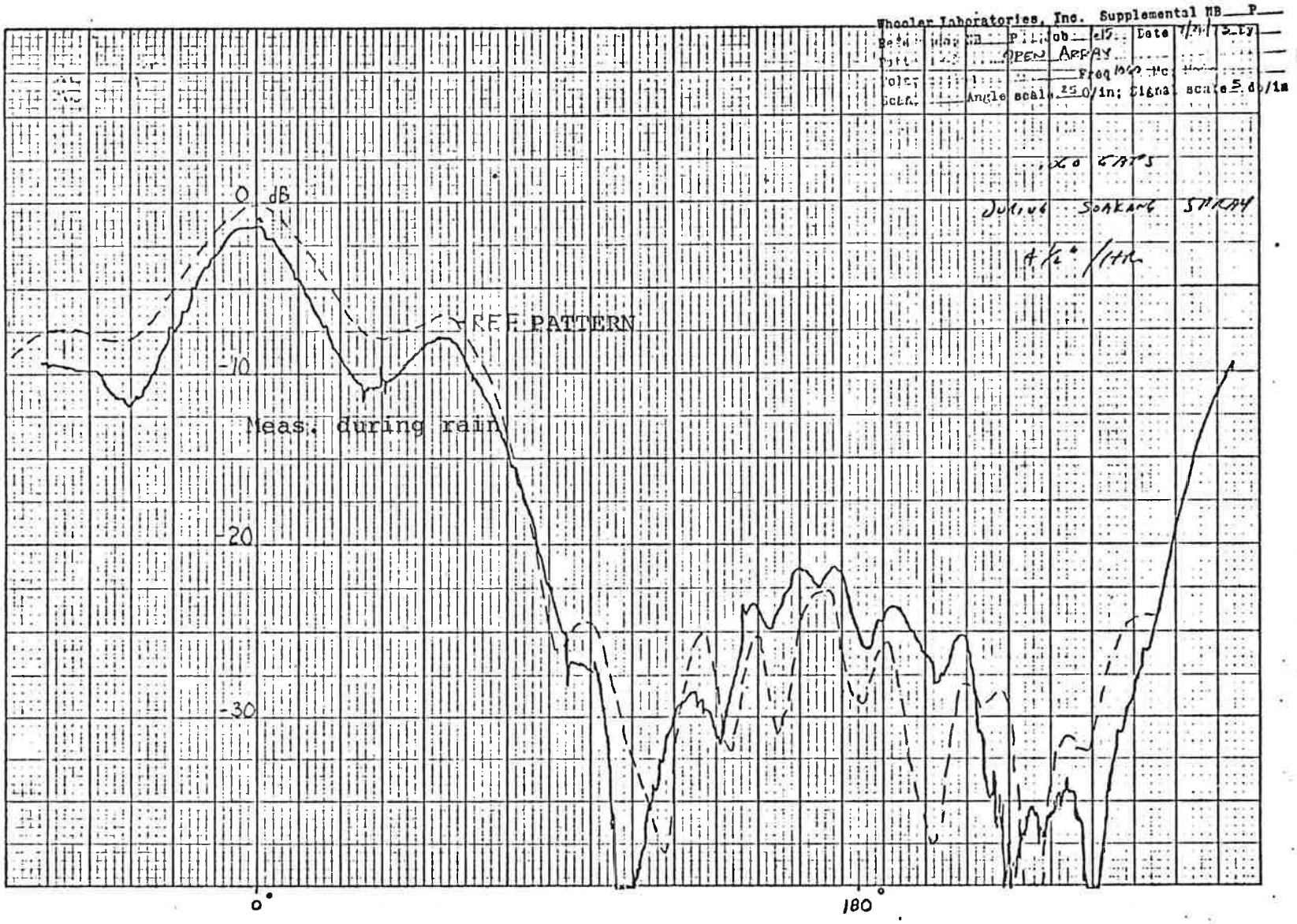

Figure 3-36. Azimuth Patterns - 4-1/2 inches rain/hr.

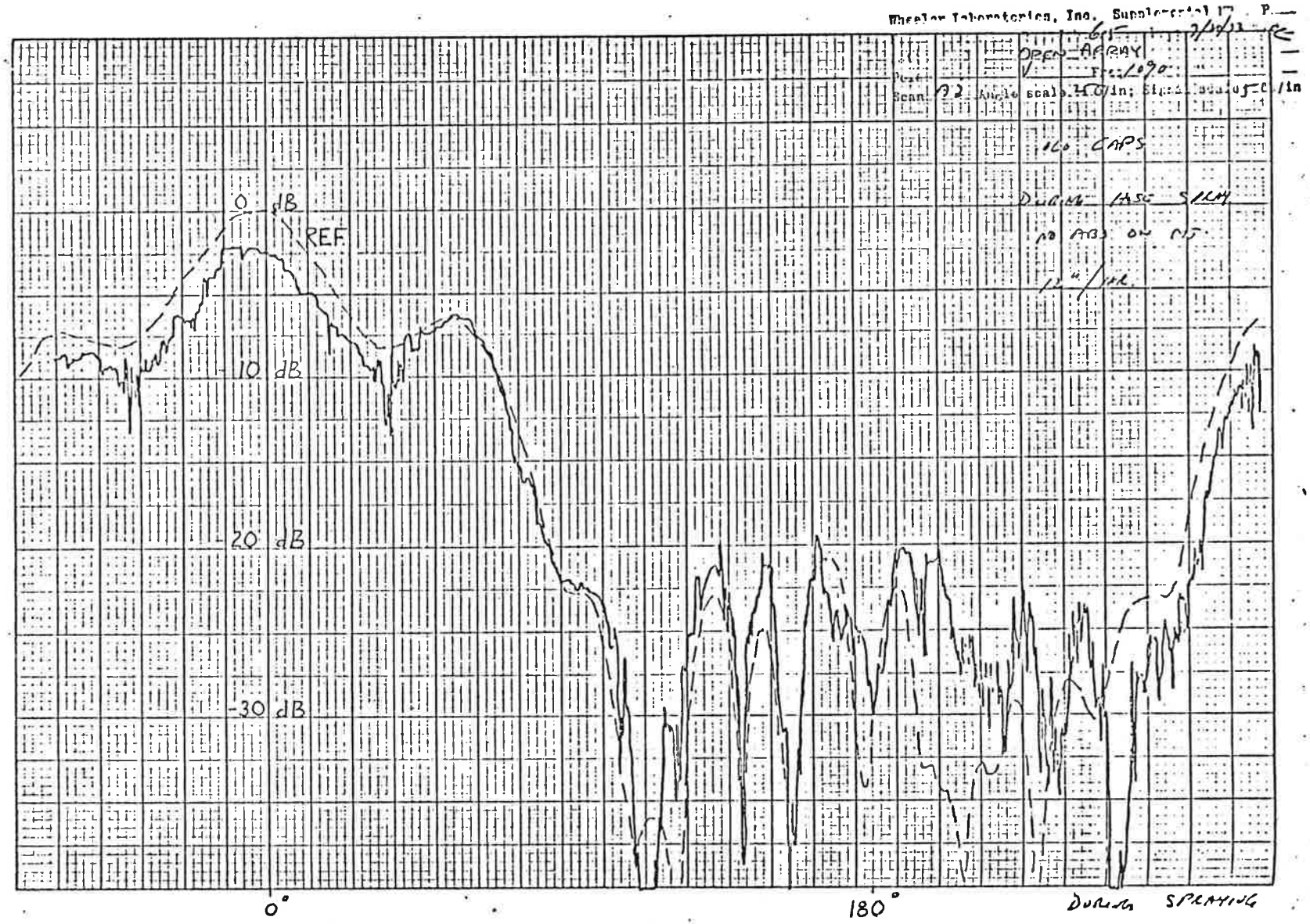

Figure 3-37. Azimuth Patterns - 12 in. rain/hr.

The antenna structure itself consists of a series of 36 vertical 2-inch diameter aluminum tubes on 9-inch centers forming the load supporting members between the main horizontal supports. The main supports are 3-inch diameter thin-walled aluminum tubes on the top and 4-inch by 1.72-inch by .32-inch structural channels on the bottom. The 36 vertical aluminum tubes serve for both mounting of the individual dipoles, as well as part of the electrical ground plane. Located on each side of the vertical columns at 4.5-inch centers are a total of 37, 5/8-inch diameter tuned reflector rods. These fiberglass-enclosed assemblies are fastened to the main top and bottom antenna structural members. Antenna mounting flanges are welded directly to the 3-inch diameter tube and bottom channel in the areas designated in figure 3-38. These flanges attach the interface structure to the ASR/ARSR structures. The 4-foot by 26-foot open structure is designed to be separable into two sections of approximately 14 feet each. This facilitates fabrication, as well as mounting and transportation of the antenna.

An aluminum sheetmetal enclosure housing the rf components is fastened to the lower channel. Access panels for maintainability are located along the bottom of the enclosure to allow for the installation and servicing of the rf components housed inside. The rf cables interconnecting the dipoles to their associated elevation networks (located in the enclosure along the bottom of the antenna) are routed through the 2-inch diameter aluminum tubes (see figure 3-39). The dipole feed cables are coiled in the web area of the lower channel before connecting to the elevation networks, resulting in efficient space utilization and an organized packaging arrangement if repair or replacement should be necessary.

The dipole design consists of an element and RF connector encapsulated in an epoxy resin. The dipole arms are reinforced with a fiber glass tube before encapuslating with Emerson Cummings Stycast 2651MM. This procedure has been used successfully in the past under similar service conditions in Hazeltine

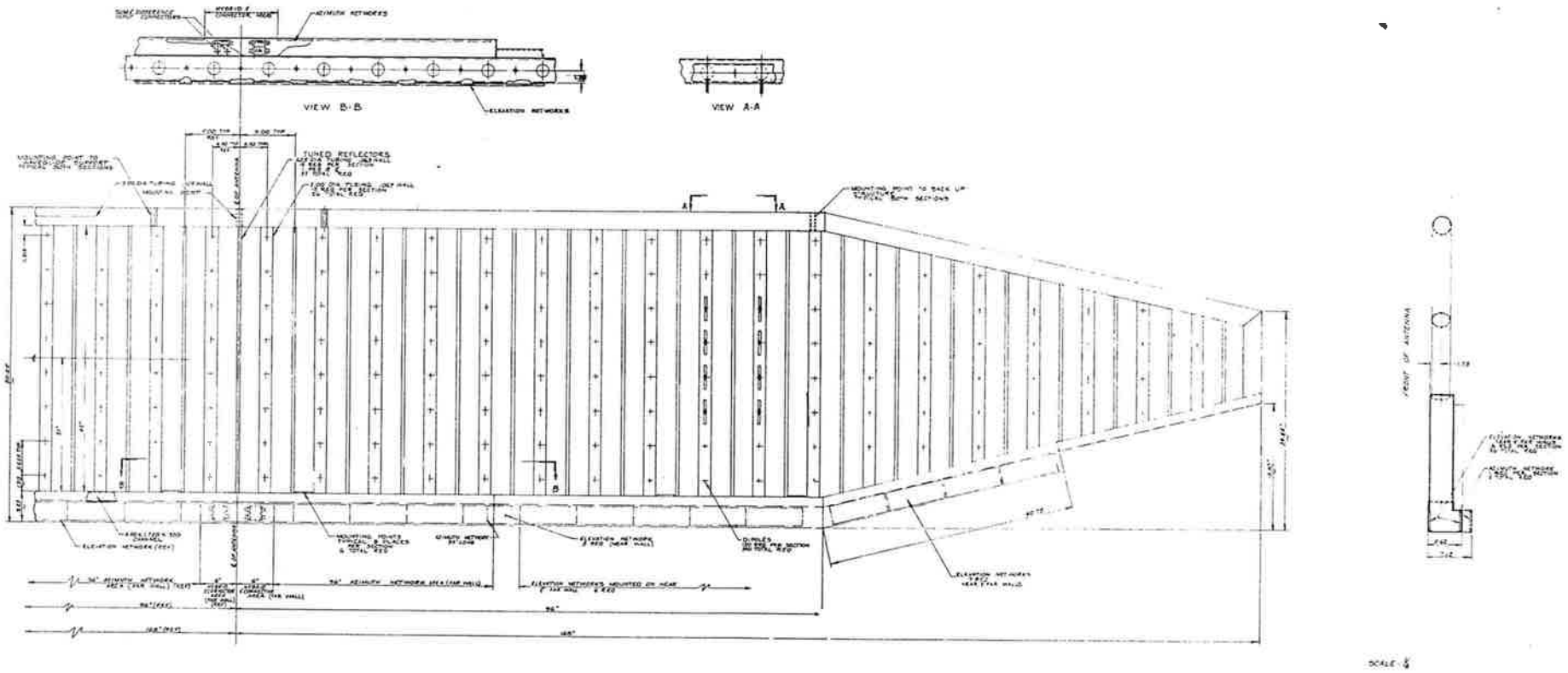

Figure 3-38. Replacement Beacon Antenna, 4' x 28'

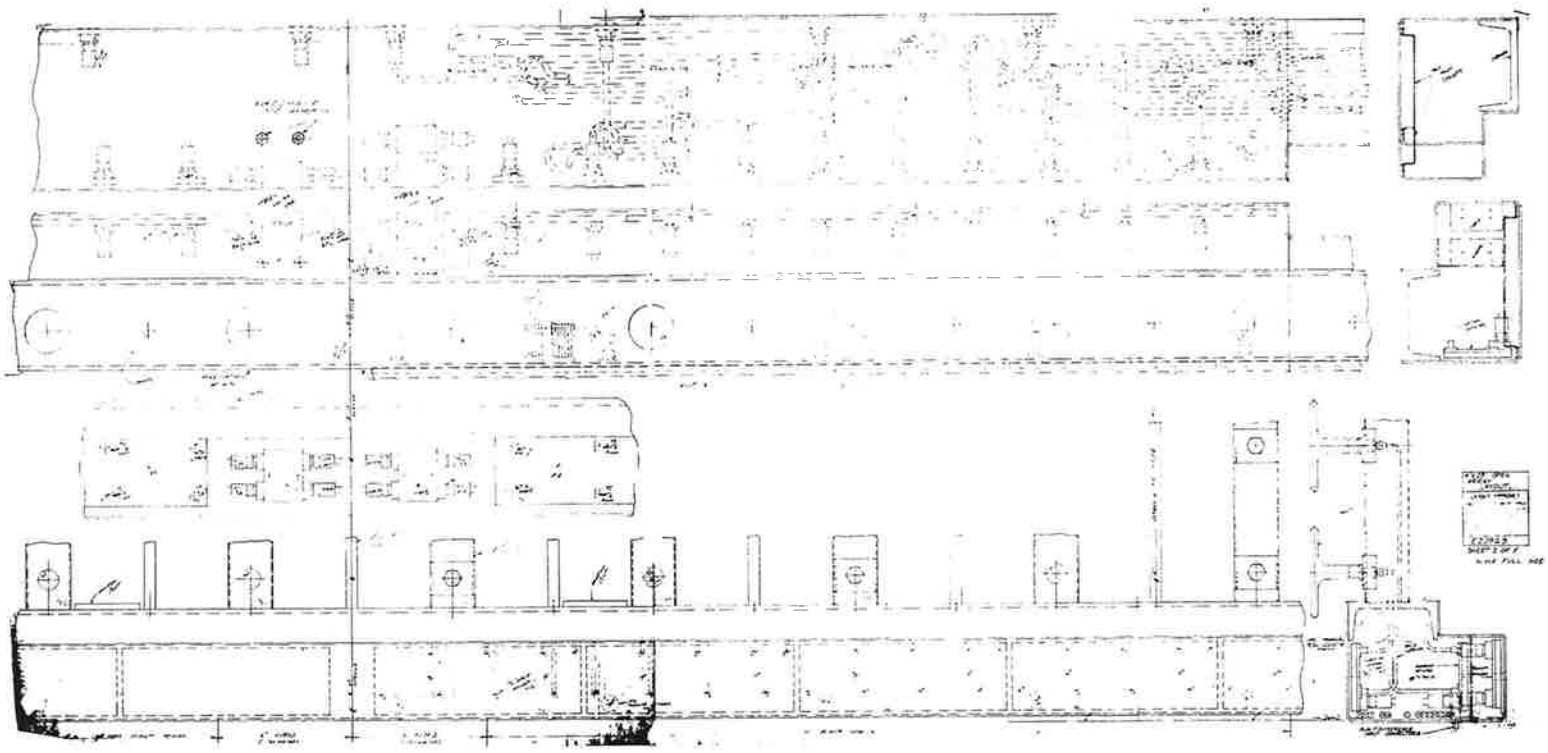

Figure 3-39. RF Cables, Interconnection (Sheet 1 of 3)

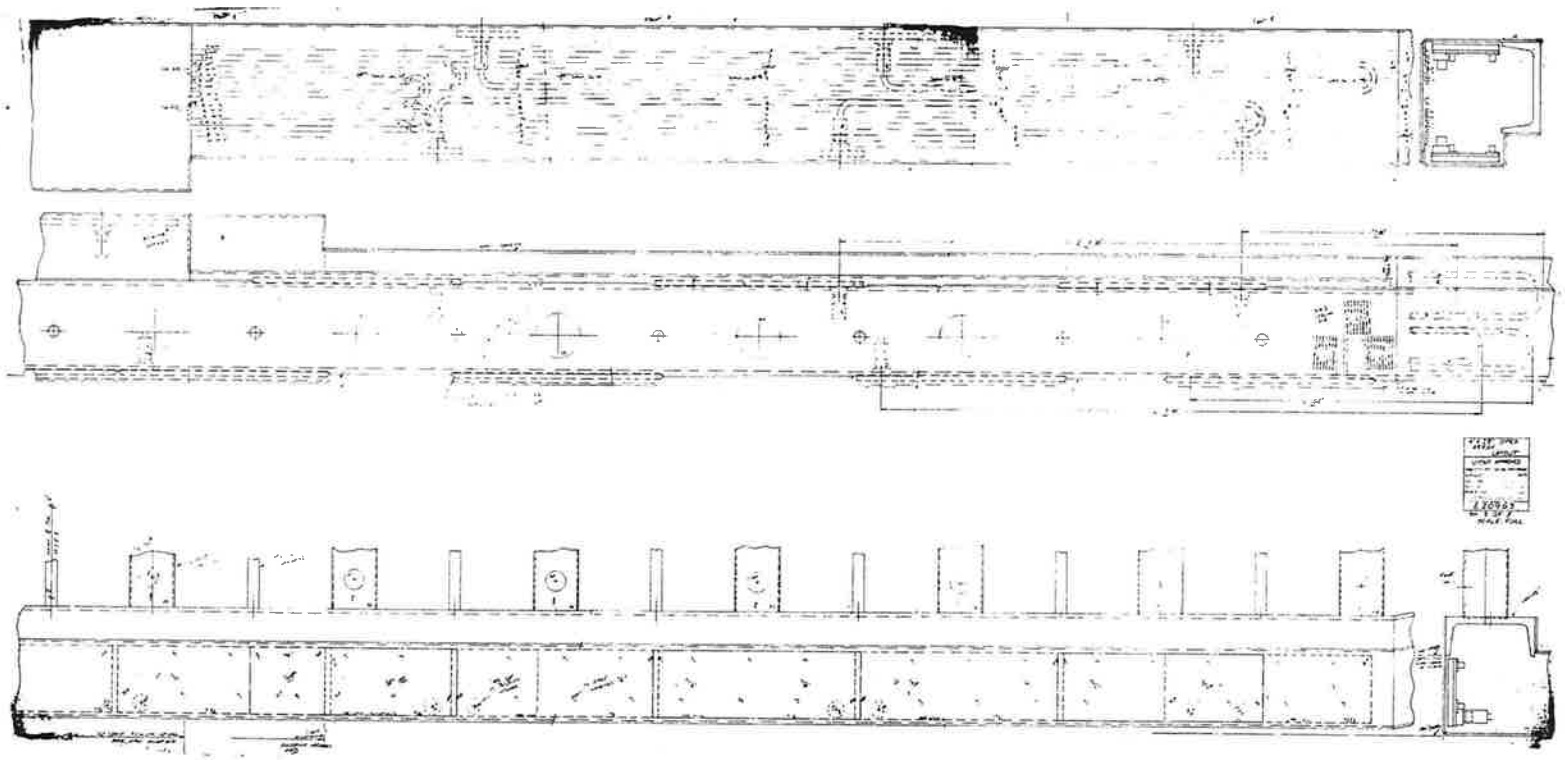

Figure 3-39. RF Cables, Interconnection (Sheet 2 of 3)

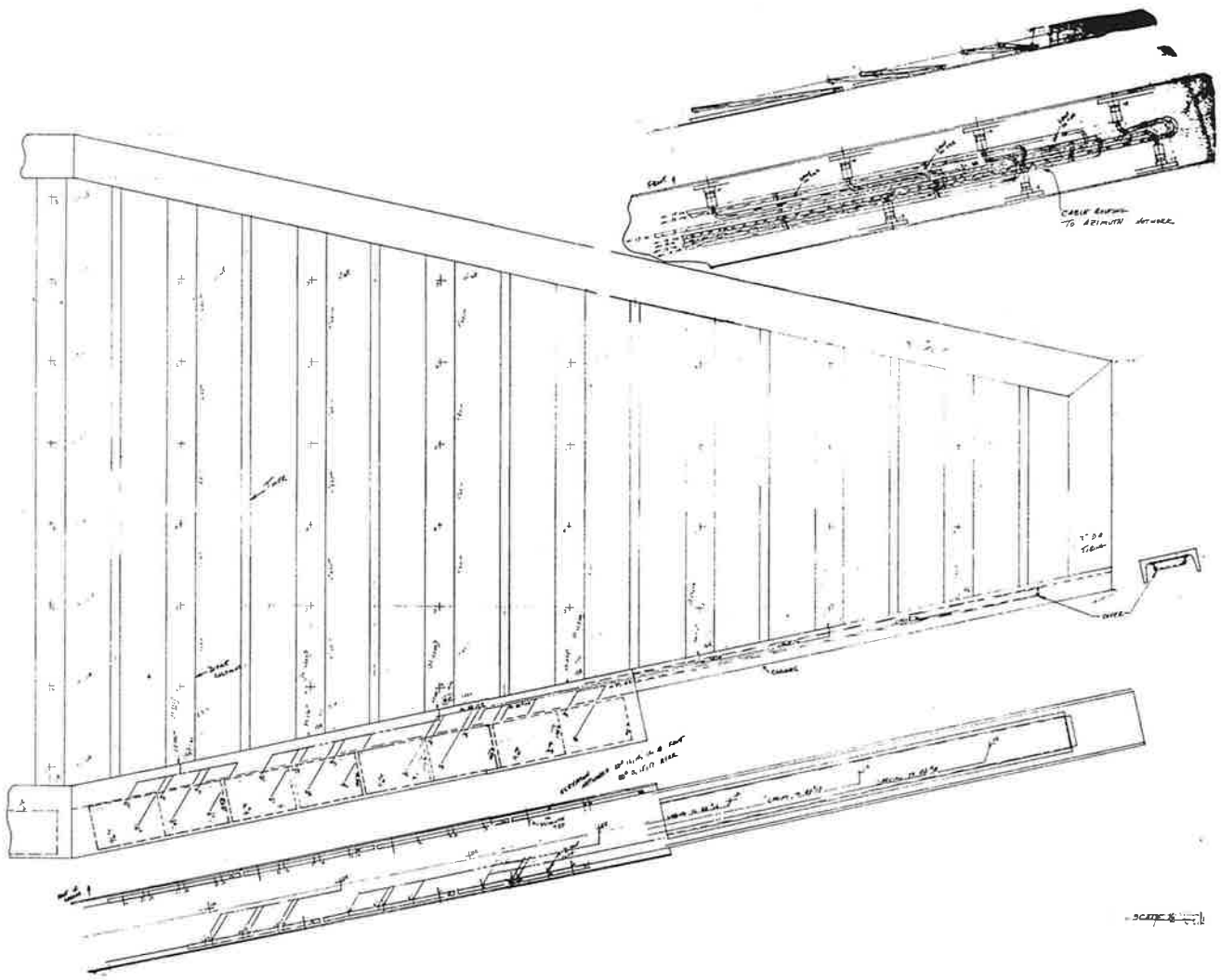

Figure 3-39. RF Cables, Interconnection (Sheet 3 of 3)

IFF applications such as the AN/TPX-46 Interrogator System. The dipole is mounted at its connector surface to a stamped mounting flange which is gasketed for environmental protection and screwed to the vertical mounting tubes (see 3-40). Threaded inserts pressed into the 2-inch diameter columns allow for this mounting arrangement.

The 37 tuned reflector assemblies along with the 2-inch diameter columns complete the electrical ground plane requirements. These reflectors are constructed of 1/4-inch diameter aluminum rods 3-1/2-inches long stacked within a thin wall dielectric tube separated by .030 dielectric spacers (see figure 3-40). The entire assembly is then epoxied at each end inside a 5/8-inch diameter (1/16-inch wall thickness) fiberglass tube with spacers located midway along each 3-1/2 rod section to maintain the desired air gap. The mounting of the tuned reflector is accomplished with screwed flanges to the 3-inch diameter top support and the 4-inch structural channel at the bottom.

The elevation networks are enclosed in the aluminum housing located along the bottom of the antenna structure. Each network is mounted to the side of the enclosure below the dipole column which it feeds (see figure 3-39, pages 1-3). The elevation networks themselves are stripline devices measuring 9 inches long, 3 inches wide and 3/8 inches thick (see figure 3-40. They consist of a chemically cross-linked styrene copolymer, reinforced with glass fiber. An aluminum plate is fixed to one side for added rigidity and secure mounting. The networks are coated with a black epoxy paint for environmental resistance.

The central area of the lower housing has a protrusion on the back, extending for 42 inches on each side of the antenna center-line (see figure 3-39). This area houses the azimuth horizontal distribution network, and associated hybrids and couplers. The two antenna Type HN connectors (sum and difference) protrude out the bottom of the housing 4 inches from the antenna center line. The 1/4-inch diameter aluminum shielded foam-flex cables, which connect the elevation networks to the azimuth network, are routed

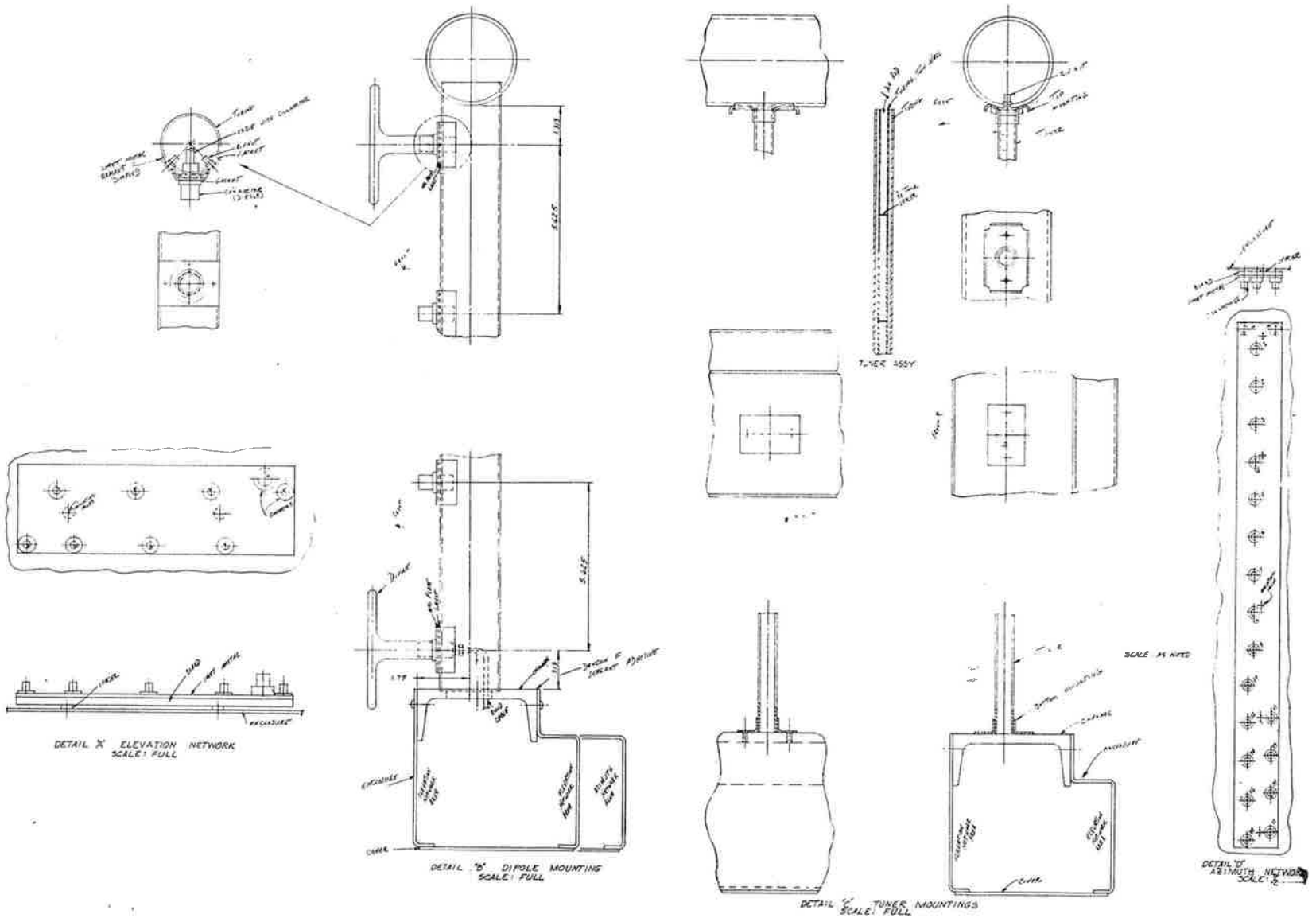

Figure 3-40. Elevation Network Mounting

through the lower-most portion of the enclosure. This configuration eases the installation problem presented by the large amount of cabling required for antenna interconnections.

The azimuth horizontal distribution networks are stripline devices similar in their method of construction to the elevation networks. They are 35 inches long, 3 inches wide and 3/8 inches thick (see figure 3-40). Twenty TNC type rf connectors are located on one side for power input and distribution to the elevation networks.

The hybrids and couplers are located in the lower enclosure in the area surrounding the antenna vertical centerline 6 inches on each side. All rf components are designed to operate within the service environment of the final installation.

Omni Antenna. The mechanical configuration of the antenna is illustrated in figure 3-41. It consists basically of a 4-foot high by 7.5-inch diameter radome covering a column of 8 dipoles. The dipoles are mounted to a support mast/reflector which is approximately 4-inch wide and 1-inch thick. The entire radome and support mast assembly are bolted to a main mounting plate. The elevation network is enclosed in a 10-inch diameter by 3-3/4 inch deep circular housing below the main mounting plate.

The mounting arrangement of the OMNI Antenna permits direct replacement of the existing OMNI.

The mounting of the dipoles to the support mast/reflector enables the feed cables to be routed through the support mast to the elevation network, resulting in an efficient packaging arrangement. Coiling of the excess cable is accomplished in the elevation network enclosure. The antenna input connector will project out the bottom of the network enclosure.

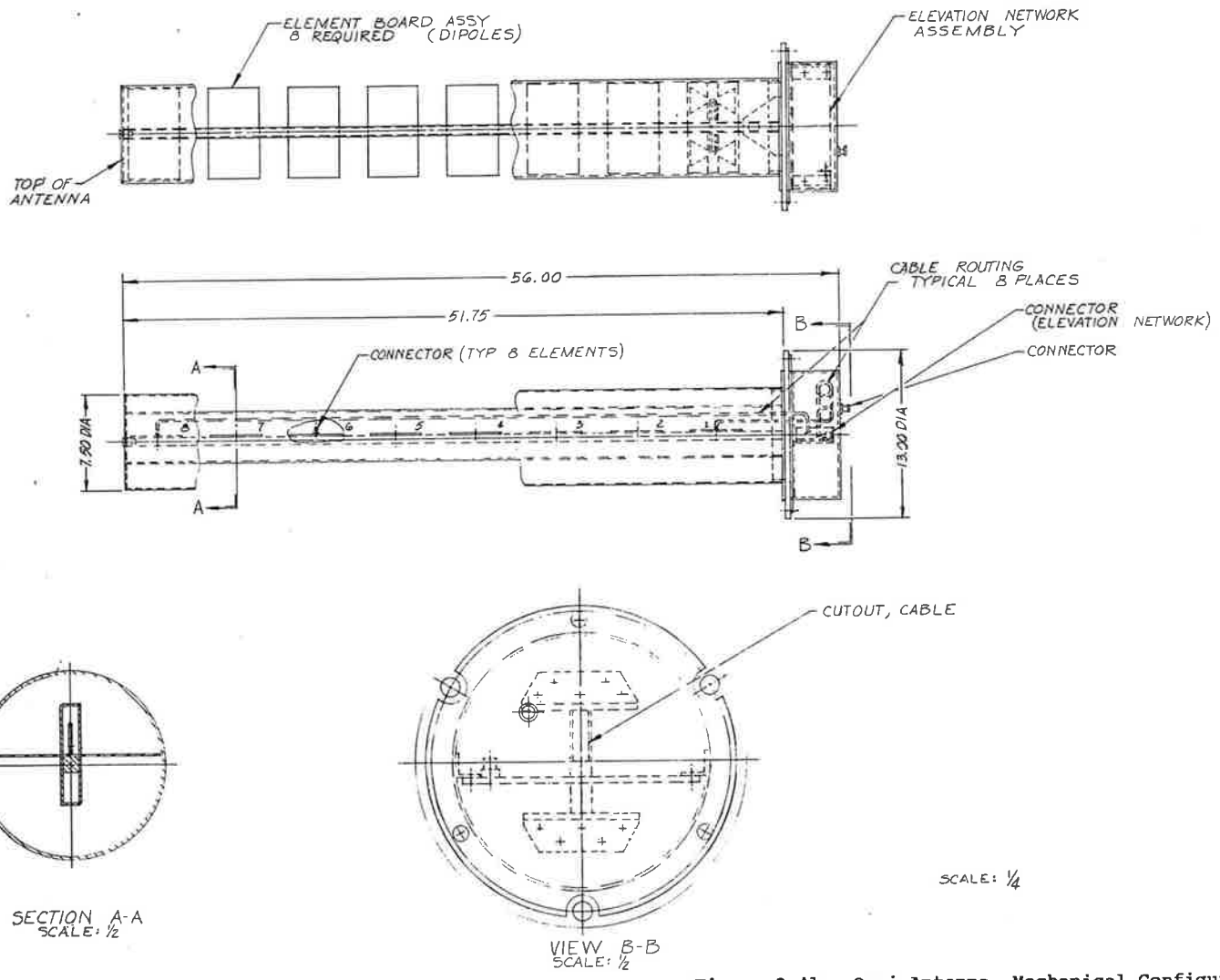

Figure 3-41. Omni Antenna, Mechanical Configuration

The opposing dipoles employed in the antenna will be printed on a single stripline board with a "T" junction at the central feed point. The stripline material is copper-clad chemically cross-linked styrene copolymer, reinforced with glass fibers. This design has been successfully employed by Hazeltine in the past on similar antenna installations such as the DABS antenna for Lincoln Labs.

The elevation network design is similar to that used in the 4-foot by 26-foot Open Array, therefore all design details previously presented apply.

Weight Analysis. The mechanical design of the 4-foot by 26-foot Open Array and OMNI Antenna has as a major objective the achievement of the maximum strength to weight ratio necessary to meet both the operating and non-operating structural requirements. Lightweight materials are employed throughout the antennas. Aluminum Alloy 6061-T6 is used exclusively for structural members. This alloy exhibits especially good strength to weight ratios and can be easily welded. The networks are designed with lightweight styrene plastic with an aluminum support plate for rigidity. The tuned reflectors use lightweight fiberglass tubes and aluminum rod segments inside.

A weight breakdown of the basic antenna structures and components is presented below. The mounting support structures for the ASR and ARSR configurations are shown also.

Table 3-4. WEIGHT BREAKDOWN

a. 4-Foot by 26-Foot Antenna Weight Estimate

Dipoles	22
Cables	50
Elevation & Azimuth networks	45
Tuned reflectors	15
Structure & Enclosure	210
	342 lbs

b. ASR Configuration

4' x 26' Antenna Assembly	342
Support Structure	44
	386 lb.

c. ARSR Configuration

4' x 26' Antenna Assembly	342
Support Structure	20
	362 lb.

d. 4' OMNI Antenna Weight Breakdown

Dipoles	1.5
Cables & Elevation network	2
Radome	8.5
Support Structure	20
	32 lbs.

Environmental Protection. The ASR installation which consists of the 4' x 26' Open Array mounted on top of the ASR and the Omni antenna attached to its mast, represents the most stringent design conditions since the antenna is exposed to all combinations of environments. The ARSR boom mounted configuration is enclosed in a radome. The protective treatments and corrosion resistant materials used, and described below, are common to both antennas and apply to all configurations.

The 4' x 26' antenna is structurally designed to operate at 15 RPM in wind velocities up to 85 knots in all manner of precipitation, including encasement in 1-1/2-inch thick radial ice. The antenna is also designed to survive 130 knot winds in all types of precipitation, including encasement in 1-1/2-inch thick radial ice. The structural analysis of the Open Array presented in Appendix C verifies meeting these conditions. It should be noted that though the 4' x 26' antenna meets these conditions

when it is mounted to the ASR, the combination of the extreme operating conditions of 100 mph and 1-1/2-inch radial ice on both antennas (ASR reflector and open-array) may produce deflections in the ASR reflector that are beyond its specification limit. There would also be loads on the antenna azimuth drive system and bearing which are beyond the loads imposed by the present beacon antenna under the same condition. This condition is discussed in more detail in the ATCRBS/ASR Interface Analysis, Section VI.

Other major environmental parameters that the antenna is designed to meet are operating temperatures ranging from -50°C to +70°C, relative humidity from 5% to 100%, including condensation due to temperature changes, altitudes to 12,000 feet above sea level and a maximum barometric pressure of 30.5 inches of mercury.

The major rf components and antenna structure's environmental protection for both the 4-foot x 26-foot Open Array and Omni antennas are presented below. The design philosophy to accomplish this protection is to prevent moisture accumulation in the antenna and enclosure. In addition, all components will be coated to seal against condensation of trapped moisture or possible leakage.

The 4-foot x 26-foot antenna structure is made exclusively of aluminum alloy 6061-T6 fusion welded together. Each seam is completely welded, thus assuring watertight integrity between the 3-inch diameter tubes, 2-inch diameter tubes, and the 4-inch structural channel. Aluminum Ally 6061 exhibits excellent corrosion resistance. The enclosure located at the bottom of the structure is also constructed of 6061 sheet with the interfaces between it and the channel sealed with Devcon F Adhesive Sealant in addition to the mounting screws. The removeable access panels at the bottom of the antenna are installed with silicon gaskets to prevent moisture seepage. Drain holes are provided in the access panels to allow for condensation escape. The entire exterior of the structure is primed with zinc chromate and painted with in accordance with FAA-STD-003 Paint System BE-9, Color No. 17875 White Gloss per FED-STD-595. The support structures

necessary for ASR and ARSR mounting, as well as all mounting flanges are also finished in accordance with the above spec.

The Omni antenna structure is fabricated of Aluminum Alloy 6061. The entire structure is finished in accordance with MIL-C-5541 Chem. Film CL3. This is a gold irridescent finish offering additional corrosion protection. All the exterior surfaces will be finished in accordance with FAA-STD-003 Paint System BE-9 Color No. 17875 White Gloss per FED-STD-595.

The dipoles are potted with an epoxy casting resin - Emerson Cumming's Stycast 2651 MM. They are also finished with white enamel. The mounting flange is sealed against the 2-inch diameter column mount with a silicon rubber gasket.

The dipoles employed in the OMNI antenna are of the printed stripline variety and will be effectively protected by coating with PT207. This is a polyvinyl fluoride compound often used to seal printed wiring boards against moisture and dirt. It offers adequate protection against moisture in the radome enclosed enviornment.

The networks are finished with Emerson Cumming's Eccocoat EC210 which is a black epoxy paint. This finish effectively seals against mositure and can easily be inspected for complete coating of the networks. All cable connections made to the networks and dipoles will be brush coated with MIL-V-173 varnish to insure sealing, as well as supplying a locking feature against vibration-induced loosening of connections.

The radomes used for the Omni antenna and tuned reflectors are both constructed of glass reinforced ployester resins. The exterior surfaces shall be primed and painted using white enamel. Color shall be lusterless white No. 37875 per FED-STD-595. The tuned reflectors shall also have an epoxy filler at each end of the radome to prevent moisture leakage inside.

ATCRBS STRUCTURAL DESIGN FOR ASR

Mounting Arrangement

A. MOUNTING ARRANGEMENT

The 4-foot x 26-foot Open Array was designed to be a direct replacement for the existing FAA Beacon Antenna, presently mounted to the top of the ASR Antenna. To minimize the structural impact on the ASR, the wind loads and weight of the beacon were to be duplicated as nearly as possible by the open array. This ideally would result in only a marginal increase in total load seen by the ASR antenna reflector, bearing and motor drive. Structurally, the critical enviornmenta; design specifications required for the 4-foot x 26-foot antenna consists of an operating level is 85 knot winds while rotating at 15 rpm with 1-1/2-inch radial ice over the entire structure. The survival condition is non-rotating, 130 knot winds, while encased in 1-1/2-inch thick radial ice.

The extreme enviornmental condition of an 1-1/2-inch radially thick iced antenna results in effectively closing the open structure to the wind. This greatly increases the wind force on the antenna. Since there is greater surface area to the Open Array, there is also an increase in the total weight of the ice load over the FA7202 Beacon Antenna. To best distribute these increased loads, the mounting of the Open Array on the ASR utilizes the existing mounting holes as well as an additional support structure.

This back structure will attach to the Open Array with three additional supports along the top 3-inch diameter tube, as well as four additional points along the bottom channel. These additional supports terminated to a common horizontal member which was supported by 3 pairs of vertical angle supports into the ASR reflector support structure. (See figure 4-1). The impact of this mounting arrangement on the ASR is included in the Structural Analysis performed by RF systems that is presented in Appendix C.

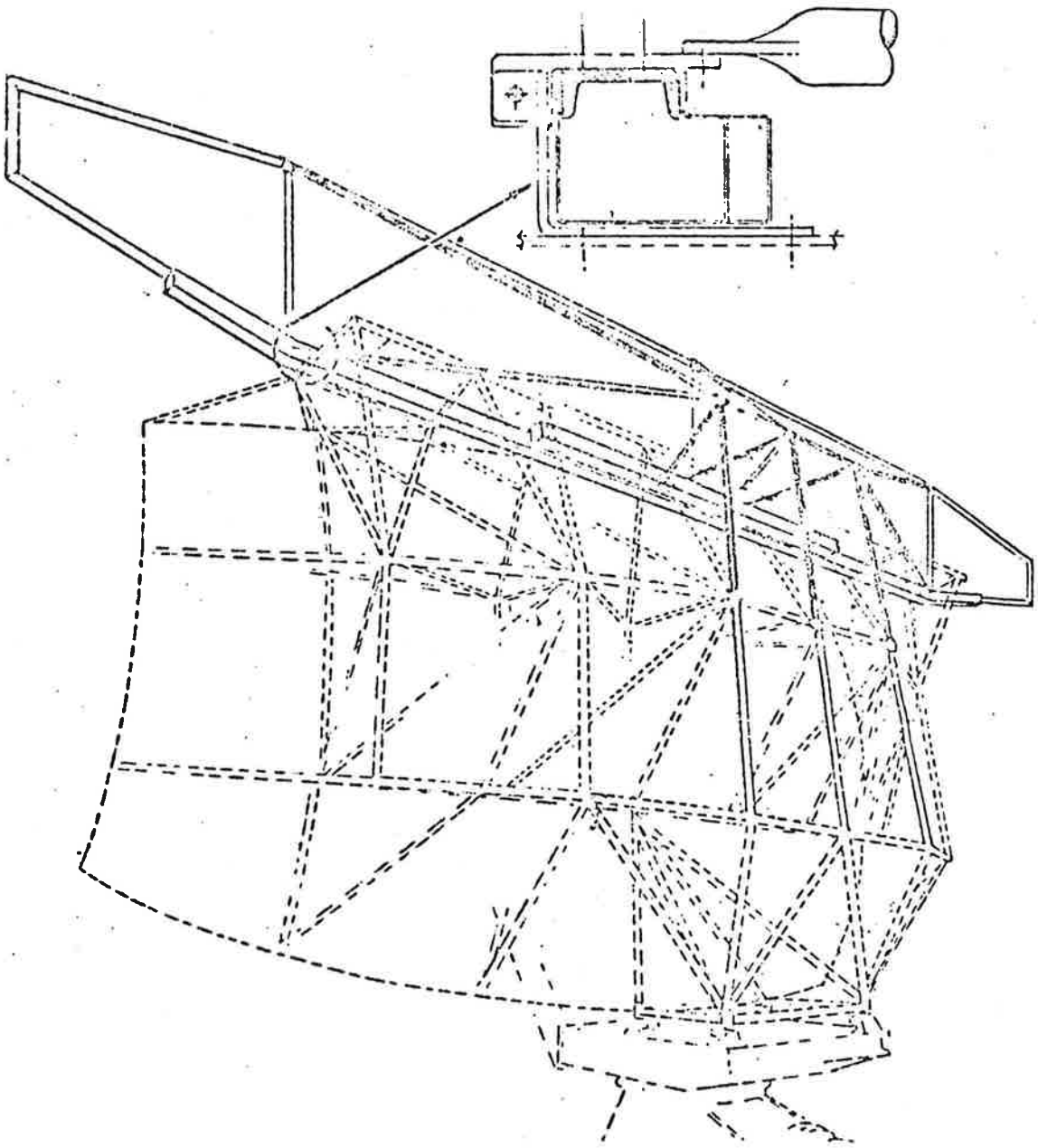

Figure 4-1. ASR Mounting

Analysis for Survival and Operating Conditions

To determine the loads which the wind applies on the existing FA7202 Beacon and ASR, and the 4-foot x 26-foot Open Array and ASR in both the iced and un-iced consitions, a detailed wind-loading analysis was performed by Applied Technology Associates (Consulting Engineers) and is presented in Appendix B. The derivations of the wind loading formulas used in the calculations and the governing parameters used in selecting the drag coefficients are included there. The existing beacon system, including the ASR antenna, are analyzed first for the survival, and then operating conditions. The 4-foot x 26-foot Open Array and ASR antenna are then analyzed for survival and operating conditions. An operating 85 knot wind, without ice condition, is then analyzed for both systems. The last condition is included because of the very low probability of seeing both 1-1/2-inch ice buildup and 85 knot winds.

The following are the calculations used to determine the wind force and overturning moments at the interface between antennas and the ASR bearing, as well as the azimuth torque due to rotation and orientation.

WIND LOAD ON 7202 BEACON

(survival condition)

$$P = 1/2\rho \, (CD_1A_1 + CD_2A_2) \, V^2$$

$$P = .5 \, (.00238) \, \{(1.75) \, (23.2) + (1.05) \, (21)\} \, (220^2)$$

$$P = 3670 \text{ lbs}$$

P = Wind Load (lbs)

ρ = Mass density of Air (lb sec^2/ft^4); slugs

C_D = Drag Coefficient

A = Projected Area (ft^2)

V = Wind Velocity (ft/sec)

NOTE: There are two drag coefficients and projected areas specified. These refer to the tops and middle section of the Beacon Antenna which have different aspect ratios when treated as individual elements. It is felt this approach provides a more accurate model for drag calculations and is carried through all the FA 7202 Beacon calculations.

WIND LOAD SURVIVAL CONDITION
FOR ASR ANTENNA

$P = 1/2\rho\ (C_D AV)^2$

$P = .5\ (.00239)\ (1.4)\ (113)\ (220)^2$

$P = 9100$ lbs

The resulting overturning moments at the antenna's interface and pedestal bearing, due to the survival conditions, are calculated below.

OVERTURNING MOMENT AT ANTENNA'S INTERFACE

$M = LP$

$M = 1.0\ (3670)$

$M = 3670$ ft-lbs

M = Overturning moment (ft-lb)

L = Moment Arm (ft)

P = Wind Load (lbs)

OVERTURNING MOMENT AT PEDESTAL BEARING

$$M = M_{BEACON} + M_{ASR}$$

$$M_T = 10.66\ (3670) + 5.66\ (9100)$$

$$M_T = 39200 + 51500$$

$$M_T = 90700\ \text{ft-lbs}$$

The maximum operating specification of 85 knot winds with 1-1/2-inch radial ice occur during 15 RPM rotation. The rotating of the antenna system causes a resultant torque at its vertical center line. This torque is due to the relative differences in wind velocity seen by opposite ends of the rotating antenna, as well as the various angles of attack of the wind on the antenna surfaces producing a lift type effect.

In addition, the total wind force on the rotating system is now also a function of the rotation of the FA7202 Beacon and ASR. The difference between this rotational induced wind force and static non-rotating wind force, however, is small in this case, due to the relatively low rotational speed. The calculations for the rotating system's wind force, azimuth torque, and overturning moment at the antenna's interface and ASR bearing are shown below.

WIND LOAD (OPERATING CONDITION) ON 7202 BEACON ANTENNA

$$P = C_D \rho/2 \; h \; (2R) \; (V^2 + \frac{W^2R^2}{3})$$

$$P = \rho/2 \cdot (C_{D_1} \times h_1 \times 2R_1 \; (V^2 + \frac{W^2R_1^2}{3}) + C_{D_2} \times h_2 \times 2R_2 \; (V^2 + \frac{W^2R_2^2}{3})$$

$$- C_{D_2} \times h_2 \times 2 \; (R_2 - R_1) \; (V^2 + \frac{W^2R_2^2}{3}))$$

$$P = .001189 \; (1.75 \times 1.667 \times 14 \; (146.7^2 + 1/3 \; (\frac{15 \times 6.28}{60})^2 \; (7^2))$$

$$+ (1.05 \times 1.5 \times 28 \; (146.7^2 + 1/3 \; (\frac{15 \times 6.28}{60})^2 \; (14^2))$$

$$-(1.05 \times 1.5 \times 14 \; (146.7^2 + 1/3 \; (\frac{15 \times 6.28}{60})^2 \; (7^2)$$

$$P = .001189 \; (880431 + 956178 - 475423)$$

$$P = 1618 \text{ lbs}$$

P = Wind Load

h = Height of antenna (ft)

w = Rotation Velocity (rad/sec)

R = Radius (ft)

V = Wind Velocity (ft/sec)

ρ = Mass density of Air (lb sec^2/ft^4); slugs

C_D = Drag Coefficient

WIND LOAD (OPERATING CONDITION) ON ASR ANTENNA

$$P = C_D \rho/2 \; h \; (2R) \; (V^2 + \frac{\omega^2 R^2}{3})$$

$$P = 1.4 \; (.001189) \; (8) \; (2 \times 8.75) \; (146.7^2 + 1/3 \; (\frac{15 \times 6.28}{60})^2 \; (8.75^2))$$

$$P = 5000 \text{ lb}$$

OVERTURNING MOMENT AT ANTENNA INTERFACE

$$M = LP$$

$$M = 1 \; (1618)$$

$$M = 1618 \text{ ft-lbs}$$

where M = overturning moment (ft-lb)

L = Moment arm (ft)

P = Wind load (lbs)

OVERTURNING MOMENT AT ASR BEARING

$$M_{TOTAL} = M_{BEACON} + M_{ASR}$$

$$M_T = 10.66 \; (16.8) + 5.66 \; (5000)$$

$$M_T = 17200 + 28300$$

$$M_T = 45500 \text{ ft-lbs}$$

The total azimuth torque on the antenna system is due to the sum of FA 7202 Beacon and ASR Antenna components. The center portion on the beacon is only considered in the orientation to the wind calculation. It is felt that the path of the Air Stream necessary for the torque inducing pressure distribution to occur would only exist in this area due to the box located on the bottom. The outer portions of the antenna are likely to only have two-dimensional

flow, therefore, no resulting torque. The rotational induced azimuth torque calculation uses the worst case wind orientation, antenna surface normal to wind direction. Where $\beta = 90^{o}$ in the figure below.

The following are the calculations for the maximum azimuth torque on the FA 7202 Beacon due to the rotation and antenna angle with respect to the wind.

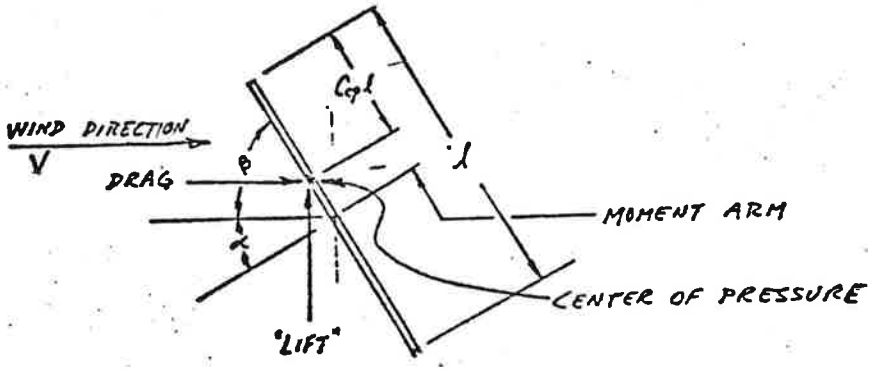

AZIMUTH TORQUE FROM 7202 BEACON ROTATING AT 15 RPM

$$M_Z = C_D \rho/2Vh \frac{4R^3}{3} V_o \omega$$

$$M_Z = \rho/2 \left(C_{D_1} \times h_1 \times \frac{4R^3}{3} + C_{D_2} \times h_2 \times 4 \left(\frac{R_2^3 - R_1^3}{3}\right)\right) (V \times \omega)$$

$$M_Z = .001189 \left(1.75 \times 1.667 \times \frac{4 \times 7^3}{60} + 1.05 \times 1.5 \times 4/3 \left(14^3 - 7^3\right)\right)$$

$$\left(146.7 \times \frac{15 \times 6.28}{60}\right)$$

$$M_Z = 1745 \text{ ft-lbs}$$

The calculations for the orientation to the wind induced torque follow. The moment equation is derived here starting with the three basic aerodynamic equations:

$$\text{Drag Force} = \frac{1}{2}\rho C_D A_D V^2$$

$$\text{Lift Force} = \frac{1}{2}\rho C_L A_L V^2$$

$$\text{Moment Arm} = \frac{\ell}{2} - C_{cp}\ell = (.5-C_{cp})$$

The lift force is actually a force in the horizontal direction acting perpendicular to the drag force.

Moment (Neglecting Rotation)

$$M_Z = (1/2\rho C_P A_D V^2)(\ell)(.5-C_{cp})(\cos\alpha)+(1/2\rho C_L A_L V^2)(\ell)(.5-C_{cp})\sin\alpha$$

$$A_D = h\ell\cos\alpha$$

$$A_L = h\ell\sin\alpha$$

$$M_Z = \frac{1}{2}\rho C_D h\ell^2\cos^2\alpha V^2(.5-C_{cp}) + \frac{1}{2}\rho C_L h\ell^2\sin^2\alpha V^2(.5-C_{cp})$$

$$M_Z = \frac{1}{2}\rho h\ell^2 V^2 (C_D\cos^2\alpha + C_L\sin^2\alpha)(.5-C_{cp})$$

$$M_Z = \frac{1}{2}\rho h\ell^2 V^2 f(a)*$$

*The coefficients of drag, lift, and center of pressure are functions of the angle of attack as shown in ASCE Report 3269 "Wind Forces on Structures:" Page 1144. The graphs from that reference (reproduced below) shows this for various aspect ratios $(\lambda)_0$. The final equation is therefore written as previously shown.

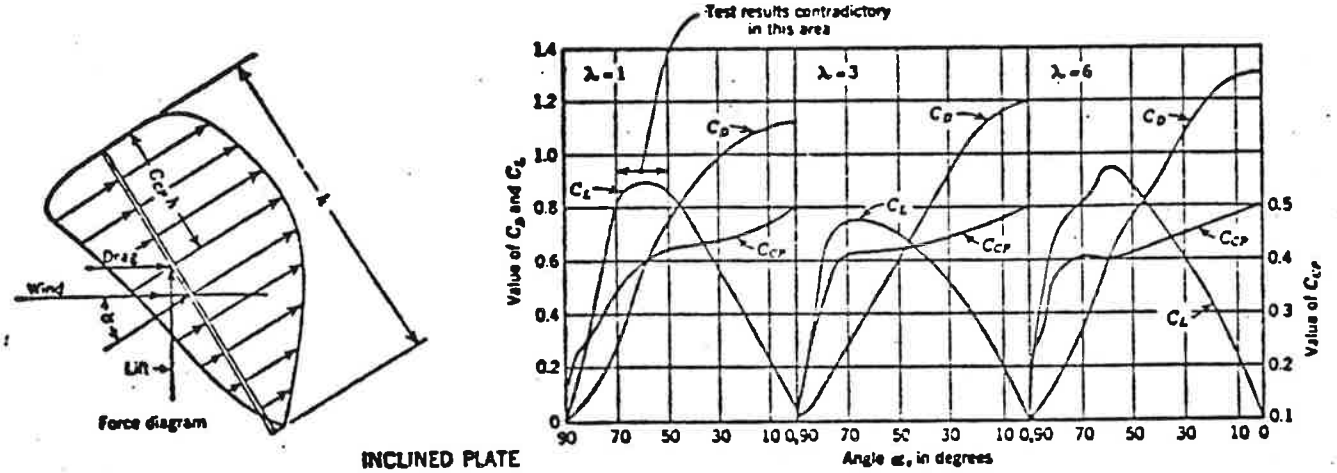

WIND PRESSURES ON ELEMENTARY BODIES

For $\lambda = 6$ and an initial C_D of 1.3 at $\alpha = 0$, the table below lists the values of f (α) against α.

For the central portion of the Beacon $\lambda = 8.4$, however, the f (λ) values for $\lambda = 6$ are used in the calculation.

α	f(α)
0^o	0
10^o	.0254
20^o	.0442
30^o	.0408
40^o	.0594
50^o	.0750
60^o	.0847
70^o	.0753
80^o	.0955
90^o	0

The following is the calculation for orientation torque:

AZIMUTH TORQUE FROM NO. 7202 BEACON DUE TO ORIENTATION

$M_Z = 1/2\ \rho h l^2 v^2\ f\ (\alpha)$

$M_Z = (.001189\ (1.667)\ (14^2)\ (146.7^2)\ (.0442)$

$M_Z = 325$ ft-lb

M_Z = Azimuth Torque (ft-lb)

l = Lengths of Antenna (ft)

$F(\alpha)$ = Orientation Factor

NOTE: The orientation factor for $\alpha = 20^{\circ}$ was used in the calculation. This is the angle for which the total torque on a flat plate of $\lambda = 6$ is maximized. As α increases, the orientation torque would increase. However, the rotational drag would decrease since it also is a function of orientation in the effect it has on the drag coefficient.

TOTAL AZIMUTH TORQUE FROM 7202 BEACON ANTENNA

$M_{Z_{TOTAL}} = M_{Z_{VELOCITY}} + M_{Z_{ORIENTATION}}$

$M_Z = 1745 + 325$

$M_Z = 2070$ ft-lbs

Similar calculations can be made for ASR antenna. The results of such calculations are presented below.

AZIMUTH TORQUE DUE TO ASR ROTATING AT 15 RPM

$$M_Z = C_D \rho/2 \; h \frac{4R^3}{3} V_o \omega$$

$$M_Z = 1.4 \; (.001189) \; (7) \; \left(\frac{4 \times 8.75^3}{3}\right) \; (146.7) \; \left(\frac{15 \times 6.28}{60}\right)$$

$$M_Z = 2350 \text{ ft-lb}$$

AZIMUTH TORQUE DUE TO ASR ORIENTATION

$$M_Z = 1/2 \; \rho h l^2 v^2 \; f(\alpha)$$

$$M_Z = .001189 \; (7) \; (17.5)^2 \; (146.7^2) \; (.0442)$$

$$M_Z = 2400 \text{ ft-lb}$$

TOTAL AZIMUTH TORQUE FROM ASR ANTENNA

$$M_{Z_{TOTAL}} = M_{Z_{VELOCITY}} + M_{Z_{ORIENTATION}}$$

$$M_Z = 2350 + 2400$$

$$M_Z = 4750 \text{ ft-lb}$$

TOTAL AZIMUTH TORQUE ON ASR-BEACON SYSTEM

$$M_{Z_{SYSTEM}} = M_{Z_{\substack{TOTAL \\ 7202}}} + M_{Z_{\substack{TOTAL \\ ASR}}}$$

$$M_Z = 2070 + 4750$$

$$M_Z = 6820 \text{ ft-lb}$$

The following are the calculations for wind loading and overturning moments due to 4-foot by 26-foot Open Array for the survival condition of 1-1/2-inch thick radial ice and 130 knot wind. Under these iced conditions, the Open Array is effectively closed and can be treated as a flat plate.

WIND LOAD (SURVIVAL CONDITION) 4' x 26' OPEN ARRAY

$$P = 1/2\ \rho\ C_D A\ V^2$$

$$P = .5\ (.00238)\ (1.3)\ (97)\ (220)^2$$

$$P = 7257 \text{ lbs}$$

OVERTURNING MOMENT AT ANTENNAS' INTERFACE

$$M = PL$$

$$M = 7257\ (2)$$

$$M = 14514 \text{ ft-lb}$$

OVERTURNING MOMENT AT ASR PEDESTAL BEARING

$$M_{TOTAL} = M_{4' \times 28'} + M_{ASR}$$

$$M_T = 7257\ (11.66) + 5.66\ (9100)$$

$$M_T = 84500 + 51500$$

$$M_T = 136{,}000 \text{ ft-lb}$$

The calculations for the wind loading and overturning moments of the 4-foot by 26-foot Open Array for the operating conditions

of 1-1/2-inch thick radial ice and 85 knot winds are shown below. The wind load calculation uses a rectangular model 4-foot by 26-foot and subtracts the wind load area at the truncated ends of the antenna.

WIND LOAD (OPERATING CONDITION) FOR 4' x 26' OPEN ARRAY

$$P = 1/2\ \rho\ C_D\ A_V^2$$

$$P = .001189\ (1.3)\ (97)\ (146.7^2)$$

$$P = 3215 \text{ lbs}$$

OVERTURNING MOMENT AT ANTENNAS' INTERFACE

$$M = PL$$

$$M = 3215\ (2)$$

$$M = 6430 \text{ ft-lb}$$

OVERTURNING MOMENT AT ASR BEARING

$$M_{TOTAL} = M_{4' \times 28'} + M_{ASR}$$

$$M_T = 3215\ (11.66) + 5.66\ (5000)$$

$$M_T = 37500 - 28300$$

$$M_T = 65800 \text{ ft-lb}$$

The total azimuth torque due to the fully iced 4-foot by 26-foot Open Array is the combination of the rotational induced torque and the orientation to the wind torque. The calculations for these two effects follow. These calculations are similar to

those employed for the Beacon Antenna where the maximum total is at $\alpha = 20^{o}$ and $\beta = 70^{o}$.

AZIMUTH TORQUE FROM 4' x 26' OPEN ARRAY ROTATING AT 15 RPM

$$M_Z = 2/3\ C_D\ \rho\ h\ R^3\ V\ \omega$$

$$M_Z = .66\ (1.06)\ (.00238)\ (4)\ (14^3)\ (146)\ \left(\frac{15\ (16.28)}{60}\right)$$

$$M_Z = 4185\ \text{ft-lb}$$

AZIMUTH TORQUE FROM 4' x 26' OPEN ARRAY DUE TO ORIENTATION

$$M_Z = 1/2\ C_D\ \rho\ h\ l^2 v^2$$

$$M_Z = .5\ (.0442)\ (.00238)\ (4)\ (28^2)\ (146)^2$$

$$M_Z = 3515\ \text{ft-lb}$$

TOTAL AZIMUTH TORQUE FROM 4' x 26' OPEN ARRAY

$$M_{Z_{TOTAL}} = M_{Z_{ORIENTATION}} + M_{Z_{ROTATION}}$$

$$M_Z = 3515 + 4185$$

$$M_Z = 7700\ \text{ft-lbs}$$

TOTAL AZIMUTH TORQUE ON 4' x 26" ARRAY AND ASR SYSTEM

$$M_{Z_{TOTAL}} = M_{t_{4' \times 28'}} + M_{Z_{ASR}}$$

$$M_T = 7700 + 4750$$

$$M_T = 12{,}450\ \text{ft-lb}$$

The extreme operating conditions of 85 knot wind and 1-1/2-inch thick ice are very remote conditions in most geographic locations. A condition of extreme winds, however, is a possibility in most areas. The following calculations are for wind drag on an uniced 4' x 26' Open Array rotating at 15 RPM. The derivation of the formulas used are present in the wind analysis in the appendix.

WIND LOAD (OPERATING CONDITION, 85 KNOTS NO ICE) for 4' x 26' OPEN ARRAY

$$P_Y = C_D \rho/2 \phi \ 83V^2 + 4212.6 \omega^2$$

$$P_Y = 1.2 \times .001189 \times .364 \ (83 \times 146.7^2 + 4212.6 \ (\frac{15 \ (6.28)}{60})^2$$

$$P_Y = 933 \text{ lb}$$

NOTE: This is the drag due to the vertical members of the array only. The wind drag of the other member must be added. In order to estimate the other member contribution to the wind force, the antenna is first assumed to be an open rectangle. The wind load is calculated and the vertical member contribution to this shape is subtracted, leaving the drag due to the rest of the antenna. This resultant is then added to the drag due to the vertical members on the tapered (true design) antenna. This gives the total drag on the antenna.

WIND DRAG ON 4' x 26' RECTANGULAR MODEL

$$P_Y = C_D \rho/2 \ h \ \phi \ (2R) \ (V^2 + \frac{\omega^2 R^2}{3})$$

$$P_Y = \rho/2 \ (V^2 \ r\omega^2 R^2) \ (C_{D_1} \times \phi \times h_1 \times L + C_{D_2} \times h_2 \times L + C_3 \times h_3 \times L)$$

$$P_Y = .001189\ (146.7^2 + \frac{(1.57^2)(14)^2}{3}\ (1.2 \times .364 \times 42/12 \times 28$$

$$+ 1.2 \times 3/12 \times 28 + 1.6 \times 5/12 \times 28)$$

$$P_Y = 1861 \text{ lb}$$

WIND DRAG FOR VERTICAL MEMBERS ONLY ON RECTANGULAR MODEL

$$P_Y = \rho/2\ (h)\ (\phi)\ (2R)\ (V^2 + \frac{\omega^2 R^2}{3})$$

$$P_Y = \rho/2\ (x^2 + \frac{\omega^2 R^2}{3})\ (C_{D_1} \times \phi \times h_1)$$

$$P_Y = .001189\ (146.7^2 + \frac{(1.57)^2(14^2)}{3}\ (1.2 \times .364 \times \frac{42}{12} \times 28)$$

$$P_Y = 1103 \text{ lbs}$$

RESULTANT WIND LOAD FOR RECTANGULAR OPEN MODEL

$$P_{Y_R} = P_{Y_{TOTAL}} - P_{Y_{VERTICAL}}$$

$$P_{Y_R} = 1861 - 1103$$

$$P_{Y_R} = 758 \text{ lb}$$

TOTAL WIND DRAG ON 4' x 26' OPEN ARRAY

$$P_Y = P_{VERTICAL} + P_{OTHER}$$

$$P_Y = 933 + 758$$

$$P_Y = 1691 \text{ lbs}$$

The azimuth torque due to the 4-foot by 26-foot open array rotation in the 85 knot winds is calculated below. Due to the open construction of the antenna, there is not a significant orientation factor and it is therefore not included. The derivation of the following equations is presented in the appendix.

AZIMUTH TORQUE DUE TO 4' x 26' OPEN ARRAYS ROTATION (85 KNOT WINDS, NO ICE) FOR VERTICAL MEMBERS ONLY

$$M_Z = C_D \rho/2 \phi (8425) (Y_o \omega)$$

$$M_Z = 1.2 \left(\frac{0023}{2}\right) (.364) (8425) (146.7) \left(\frac{15 \times 6.28}{60}\right)$$

$$M_Z = 1008 \text{ ft-lbs}$$

The above torque is the vertical member contribution, including those at the tapered ends to which the torque of the other members must be added. The rectangular model for determining the other members contribution to the total torque on the antenna is employed by subtracting the contributions of its vertical member, as in the wind force analysis. The total moment on the antenna is therefore as calculated.

TOTAL AZIMUTH TORQUE DUE TO 4' x 26' ANTENNA

$$M_Z = M_{Z_{\substack{\text{VERTICAL} \\ \text{NUMBER}}}} + M_{Z_{\substack{\text{OTHER MEMBERS} \\ \text{RECTANGULAR MODEL}}}}$$

$$M_Z = 1008 + 1052$$

$$M_Z = 2060 \text{ ft-lbs}$$

NOTE: The moment due to the other members is calculated in the appendicized wind load analysis page 5.1 and 5.2.

The wind loading on the ASR for the operation conditions without ice is as follows:

WIND DRAG ON ASR (OPERATING CONDITION, 85 KNOT WIND, NO ICE)

$$P = C_D \rho/2 \; h \; (2R) \; (V^2 + \frac{\omega^2 R^2}{3})$$

$$P = 1.1 \; (.001189) \; (8) \; 2 \times 8.75) \; (146.7^2 + 1/3 \; (\frac{15 \times 6.28}{60})^2 \; (8.75)^2)$$

$$P = 3940 \text{ lbs}$$

The total overturning moment at 4-foot by 26-foot antennas' interface and ASR bearing are calculated below.

OVERTURNING MOMENT AT ANTENNAS' INTERFACE

$$M = PL$$

$$M = 1691 \; (2)$$

$$M = 3382 \text{ ft-lb}$$

OVERTURNING MOMENT AT ASR BEARING

$$M_{TOTAL} = M_{ASR} + M_{4' \times 28'}$$

$$M_T = 5.66 \; (3940) + 11.66 \; (1691)$$

$$M_T = 22300 + 19700$$

$$M_T = 42000 \text{ ft-lbs}$$

It should be noted that a small ice buildup on the ASR reflector mesh would effectively close it, greatly increasing the drag. However, small ice buildups (up to 1/2-inch) on the 4-foot by 26-foot Open Array have only small effects on its total drag.

The azimuth torque due to the 85 knot wind on the uniced ASR is calculated below. The equation is derived in the appendicies wind load analysis.

AZIMUTH TORQUE FROM UNICED ASR DURING MAXIMUM OPERATING CONDITIONS

$$M_Z = C_D \phi \, 8/2 \, \frac{4R^3}{3} \, H \, V_o \, \omega$$

$$M_Z = 1.1 \; (.0023/2) \; (4/3) \; (8.75)^3 \; (8) \; (.46.7) \; \left(\frac{15 \times 6.28}{60}\right)$$

$$M_Z = 2130 \text{ ft-lbs}$$

The overturning moment at the bearing for an uniced 7202 Beacon and ASR is as follows:

TOTAL OVERTURNING MOMENT AT ASR BEARING FOR THE 85 KNOT UNICED OPERATING CONDITION

$$M_{TOTAL} = M_{BEACON} + M_{ASR}$$

$$M_T = 966 \; (1618) + 5.66 \; (3940)$$

$$M_T = 17500 + 22400$$

$$M_T = 39{,}900 \text{ ft-lbs}$$

Summary

From the results of the wind load analysis, see table 3-5, it can be concluded that for maximum iced survival and operating conditions, the total loads applied at the antennas' interface and the ASR pedestal bearing are greater for the 4' x 26' Open Array, see tables 3-6 and 3-7. The effect these increased loads have on the ASR drive system and reflector are discussed in Section VI.B. and V.C., respectively. For the uniced conditions

between the two extremes, the difference between the loads will gradually increase with up to approximately 1/2-inch ice buildup. From that point up, the increase in load of the 4-foot by 26-foot antenna over the 7202 Beacon becomes significant.

Table 3-5. SUMMARY OF WIND LOADS IN POUNDS

Condition	7202 Beacon	4' x 26' Open Array	ASR Antenna
Survival Condition	3670	7257	9100
Maximum Operating (Iced)	1618	3215	5000
Maximum Operating (Un-iced)	1618	1691	3940

Table 3-6. SUMMARY OF OVERTURNING MOMENTS AT ANTENNA INTERFACE AND ASR BEARING IN FOOT POUNDS

Condition	7202 at ASR Interface	7202 & ASR at Bearing	4' x 26' at ASR Interface	4' x 26' & ASR at Bearing
Survival Condition	3670	90,700	14,514	136,000
Maximum Operating (Iced)	1618	45,500	6,430	65,800
Maximum Operating (Un-iced)	16.8	39,900	3,389	42,000

Table 3-7. SUMMARY OF AZIMUTH TORQUE DUE TO WIND LOAD IN FOOT POUNDS

Condition	7202 Beacon	4' x 26' Open Array	ASR Antenna
Maximum Operating (Iced)	2070	7700	4750
Maximum Operating (Un-iced)	2070	2060	2130

Structural Analysis

The design of the 4-foot by 26-foot Open Array has been structurally analyzed and has been shown to have sufficient strength and rigidity to meet the survival and operation requirements. This analysis is included in the appendices. The impact of the 4-foot by 26-foot Open Array mounted to the top of the ASR for the operating and survival conditions, as well as its impact on the ARSR boom, for the chin mounting configuration are included in the aforementioned analysis. The results of the structural analysis along with the design approach are presented below for 4-foot by 26-foot Open Array and ASR. The ARSR boom mounting is considered in Section IV.

The material used throughout the welded antenna and mounting structures is aluminum alloy 6061-T6 which has a yield strength of 35,000 PSI. However, annealing occurs in the welded zones that will cause a decrease in yield strength. In these areas, 15,000 PSI is used in the analysis. This number is conservative since the American Welding Society Text Volume IV records a 22,000 PSI yield strength for 6061-T6 heli-arc welded, using 4043 weld rod. A margin of safety of 1.2 using 15 KSI yield strength is effectively a margin of safety of 1.75 using the documented 22 KSI yield strength.

The mounting of the 4-foot by 26 foot Open Array to the ASR is an exposed environmental condition. The structure therefore must be capable of withstanding without permanent deformation the wind induced loads in the worse case environment. To provide additional support to the Open Array a back-up structure is employed of the configuration shown in figure 4-2. With this back-up structure a minimum margin of safety of 1.21 for the open array structure is calculated for the survival conditions. These conditions consist of 130 knot winds with 1.5 inches radial ice (specific gravity = .9) covering the entire 4-foot by 26-foot antenna.

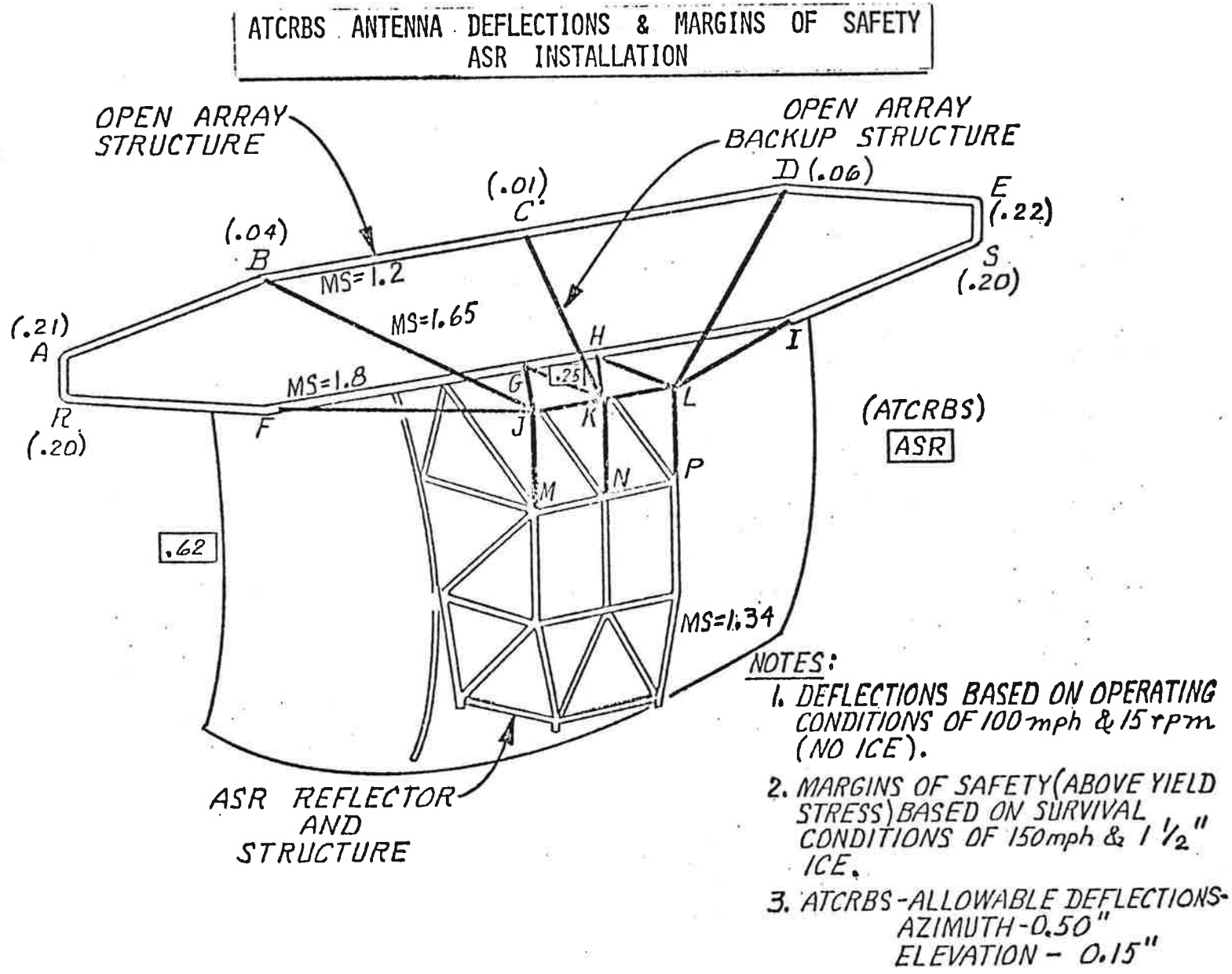

Figure 4-2. Open Array Back-up Structure

The minimum margin of safety exists in the 3-inch diameter tube, running horizontally across the top of the open array antenna.

The minimum margins of safety for the ASR and open array support structures are 1.34 and 1.65, respectivley. The minimum M.S. for the ASR occurs in the lower most rear vertical member in the second vertical truss section from the centerline of the antenna. This is member "DL" on page 20 of the appendicized structural analysis. The open array support structure members with the 1.65 M.S. are the long diagonal tubes supportint the top of the outer ends of the 4-foot by 26-foot structure.

The initial design approach for mounting the 4-foot by 26-foot Open Array on the ASR was to utilize a spaceframe support technique. This would entail mounting a 16-foot long support of triangular cross section to the rear of the Open Array. In turn, supporting this at its rear point with vertical members from the 3 center trusses of the ASR structure. This design, although offering excellent strength and rigidity, also offered too much weight and surface area. The latter was undesirable from a wind and ice loading standpoint.

A second approach was undertaken to design a mounting structure that would utilize a greater portion of the allowable deflections available in the Open Array design. This structure, as seen in figure 4-2, consists of 3 pairs of 2 x 2 x 3/16 structural angles connecting to the three central trusses of the ASR7. They join to a common horizontal 2-inch by 1/8-inch wall tube which in turn has four members, also 2-inch by 1/8-inch wall tubes connecting to the ATCRBS lower channel. The structure is completed by 4 diagonals, one to each of the top and bottom horizontal members, 8 feet from the centerline and by a 2-inch by 1/8-inch wall centerline support from the top of the ATCRBS to the common horizontal member. The mounting arrangement utilizes the existing mounting pads on the top of the ASR structure.

Under the operating conditions of 85 knot winds, without ice, the deflections of the 4-foot by 26-foot Open Array and ASR were calculated to be within the allowable limits. The extreme operating conditions of 1-1/2-inch ice formation on the Antenna with the simultaneous occurrance of 85 knot winds would appear to deflect the antenna beyond the operating deflection limits. However, this calculation is conservative since it does not consider the stiffness that 0.9 specific gravity ice would add to the ASR reflector mesh or the antenna support structure. However, the survival calculation did consider both 130 knot wind and ice 1-1/2-inch thick to prove structural integrity. Extreme winds can occur in most locations and is therefore included along with the rotational effects in the deflection calculations.

For the conditions of 85 knot wind and 15 rpm, the Open Array was analyzed and will deflect .013 maximum whereas the limiting deflection specification is .015 inches. The deflection calculated in the azimuth plane was .215 inches, where .500 was the specification limit. The wind load distribution on the rotating antenna causes a torque which deflects the antenna tips .014 inches with respect to one another. The deflection limit on this condition is .30 inches.

The deflections for the conditions of 85 knot winds during 15 rpm on the ASR are as follows. The centerline deflection is .266 inches where .375 maximum is specified. In the azimuth plane, deflection is .618 inches, the maximum allowable is .750 inches. The limiting conditions for this ASR deflections are calculated from information given in the ASR 5 specification.

It should be emphasized at this point that for the structural analysis calculations for the ASR, pinned joints are assumed in the three main vertical trusses considered. It does not include the diagonal members between these trusses or the outboard trussed members. The welded construction of the antenna are frame members, which add stiffness, but at some tradeoff

of the transfer of moment loads. Therefore, the overall analysis is conservative and smaller deflections and larger margins of safety are anticipated.

Vortex Shedding Considerations

An analysis of the induced vibration caused by vortex shedding on the 0.625-inch diameter tuned reflectors was performed. The major conclusions resulting from this study are, that although resonant stresses and deflections result from this phenomena, no significant effect on the structure or performance of the antenna will occur.

The resonant frequency of the tuned reflector is calculated first by treating it as fixed end beam.

$$F_N = \frac{22.2}{2\pi} \sqrt{\frac{EIg}{WL^3}}$$

$$F_N = \frac{22.4}{6.28} \sqrt{\frac{3.0 \times 10^6 \ (.004) \ (386)}{.4(40^3)}}$$

$$F_N = 48 \text{ cps}$$

where F_N = Natural Frequency, cps

W = Weight, lbs

E = Modulus of Elasticity, psi

L = Length, inch

g = gravity vector, in lb/sec^2

I = Moment of Inertia, in^4

By equating the naturel frequency of the tuned reflector to the vortex shedding induced frequency, the critical wind velocity can be determined as shown below. (REF. Lienhard, J.H. "Synopsis of Lift, Drag and Vortex Frequency Data for Rigid Circular Cylinders", Washington State University College of Engineering, Research Division, Bulletin 300, 1966).

$$F_v = \frac{SV}{d}$$

$$\frac{F_v d}{S} = V$$

$$\frac{48(.052)}{.21} = V$$

$$11.88 \text{ ft/sec} = V$$

$$8.08 \text{ mph} = V$$

where F_v = Vortex Shedding Frequency, cps

S = Strouhal Number, Dimensionless

V = Wind Velocity, ft/sec

d = Tuned reflector diameter, ft

NOTE: The Strouhal Number used in the equations is a property of the reflector's cross-section and is related to its drag coefficient. It can be considered constant for the Reynolds Numbers experienced during the operating and survival ranges of wind velocity. (REF. ASCE Report No. 3269 Wind Forces on Structures.)

The calculated critical wind velocity of 8 mph, which produces the induced resonant frequency, is well within the operational range. However, this does not present a deflection nor a working

stress problem. This is because the exciting force, induced by vortex shedding, is of relatively small magnitude. The calculations for the force of the vortex shedding excitation follow. (REF. Den Hartog, J.P., "Mechanical Vibration," Fourth Edition.)

$$F_K = 1/2\ \rho\ V^2 A \sin \omega t$$

$$F_K = .00255\ (8.08)^2\ \left(\frac{(.625(40)}{144}\right) \sin \omega$$

$$F_K = .029 \sin \omega t$$

where F_K = Vortex shedding force

ρ = Density Air, $sec^2 lb/ft^4$

V = Velocity, mph

A = Projected area ft^2

The fixed end reflector could, therefore, be excited with a force of $F_x = .029$ lb sin ωt. Having a total weight of 0.4 lbs, the acceleration and amplitude of deflection of the reflector is calculated as:

$$g_s = \frac{F}{W}$$

$$g_s = \frac{.029}{0.4}$$

$$g_s = .072$$

where F = Exciting force, lbs

W = Weight, lbs

g_s = Acceleration

$$D.A. = \frac{19.6(G)}{F_N^2}$$

$$D.A. = \frac{19.6(.072)}{(48)^2}$$

$$D.A. = .00061\text{-inch}$$

$$A = .0003\text{-inch}$$

where D.A. = Double amplitude, inches

A = Amplitude, inches

Assuming a very conservative transmissibility of 100 maximum through the reflector, a double amplitude of .061 inches will exist at mid-span along with a 7.2 "G" acceleration. The corresponding stress at this point would be as follows:

$$S = \frac{32EC}{L^2} \quad (100A)$$

$$S = \frac{32\ (3 \times 10^6)\ (.312)}{40^2} \quad (.03)$$

$$S = 562 \text{ psi}$$

where S = Stress, psi

E = Modulus of elasticity, psi

L = Length, in

C = Distance to extreme fiber from center, in

A = Amplitude, in

The resulting stress of 562 psi, induced by the vortex shedding phenomena, is extremely low in this case and would allow for a safety factor of 28 in the fiberglass reflector. The rod deflection of .03 in is within the acceptable limits necessary for electrical performance.

To assure that the vortex shedding does not present a problem at the higher harmonics of the fundamental frequency, calculations similar to above were conducted with the results showing that higher stresses, but lower reflector deflection, would occur.

The following figures illustrate the waveform that the tuned reflector would take at the various harmonics. Included are the transmissibilities and natural frequency coefficients (an) used in the calculations. It can be seen that the deflections decrease with increasing harmonics. Note, however, that the slope of the deflection is greater with increasing harmonics causing the highest stresses in the reflector material.

		Transmittability	Coefficient (An)*
Fundamental Frequency		100	22.4
1st Harmonic		60	61.7
2nd		40	121
3rd		20	200
4th		10	298
5th		5	388

(*Ref: Den Hartog, J.P., Mechanical Vibration

$$F_{HARMONIC} = An \sqrt{\frac{EIg}{WL^3}}$$

For example, the fourth harmonic of the reflector would have a natural frequency of 400 cps which corresponds to a critical wind velocity of 70 mph. The vortex shedding force would be

2.17 lbs or 5.4 "G"'s. Assuming a conservative transmissibility of 20, a 108 "G" acceleration and 0.0064-inch deflection will occur in each quarter length of the reflector. This will stress the rod to 1,900 psi which still allows for an adequate margin of safety of 8.25.

For the maximum survival specification of 130 knot winds, the respective vortex induced frequency would be the fifth harmonic. The natural frequency of the reflector would be 826 cps. The vortex shedding force would be 9.3 lbs or 23.2 "G"'s. Using a transmissibility of 5 for this harmonic, the deflection and stress would calculate to .0003 inches and 5730 lbs, respectively, at each sixth length of the reflector. This allows for a 2.8 margin of safety.

In conclusion, as wind velocity increases, vortex shedding critical frequencies increase and excite the tube at harmonics of its fundamental frequency. At each of these harmonics of the 44 Hz fundamental, vibrational deflections are not significant enough to affect electrical or structural performance of the antenna. The conclusion, as previously mentioned, is that vortex shedding presents no problem to the antenna design.

ATCRBS/ASR INTERFACE ANALYSIS

Status of Existing ASR Information

In order to determine the impact, if any, of the open array on existing ASR systems, a portion of the Phase I study was devoted to a search for information on key portions of the ASR antenna. From the standpoint of direct replacement concept, presumably, a new antenna can be added without structural analysis of the ASR. However, under the conditions of large ice formations, as previously discussed, the open array is not equivalent to the FA7202. In fact, wind and dead loads will be greater, consequently, there was a need for a study of key portions of the ASR antenna to insure both safe operation of ATCRBS and ASR and to assess the effect, if any, on the operational capabilities of the ASR.

The specific portions of the ASR which received attention in connection with this study included the reflector, bearing, drive system and rotary joint. The tasks taken in connection with this portion of the study included:

- Visits to NAFEC to inspect ASR-5, ASR-4, and ASR-7 sites.
- Search and requests for fabrication drawings
- Discussion with Kaydon Company, supplier of the bearing for ASR-5
- Attempts at discussion with USEM, manufacturer of the motor drive system
- Study of the existing rotary joint from technical manuals, drawings and discussions with Kevlin Mfg. (developed rotary joint for ASR with two L-band channels for FAA).

Visits to NAFEC. This task included several visits to NAFEC, prior to, and during, the study program to inspect the ASR sites and also to make specific measurements on the ASR-7 site. The ASR-7 site has been constructed as a facility for testing the E-scan antenna. It is our understanding that the open array antenna if developed, will be installed on this site for field tests. The measurements which

were performed on the ASR-7 consisted mainly of determining specific lengths, thicknesses and sizes of the structural members of the ASR reflector. A complete set of measurements were performed in order to insure that sufficient information was available to fully analyze any aspect of the reflector. In addition, photographs were taken of both the reflector, pedestal, and other portions of the system. Although drawings were available of some ASR sites, it was felt that measurements of the ASR-7 should be made to insure that there were no apparent differences between the reflector designs. From the measurements taken, we concluded that the ASR reflectors were more or less the same in design.

Figure 5-1 shows the drawings prepared to indicate the results of the measurements performed on the ASR-7 at NAFEC. This information was supplied to RF Systems in order that they could perform an analysis of the ASR reflector.

Search or Request for Drawings. A listed number of fabrication drawings were obtained on microfilm of the ASR-5 system. These drawings were employed initially for preliminary information on the reflector. Subsequently, the measurements performed at NAFEC verified that the ASR-7 and 5 reflector were very similar in design. Consequently, little use was made of these drawings beyond the initial preliminary evaluation.

Discussions with the Bearing Supplier. Early in the study program, based on information supplied on some drawings, and other information gained from the technical manuals for the ASR-5, we determined that Kaydon Co. supplied the bearings for the ASR-5 system. During the Phase I study, a number of phone conversations were held with the Kaydon engineering people and a substantial amount of information has been gathered with regard to the capabilities of this bearing. This information will be discussed in a subsequent section. It was

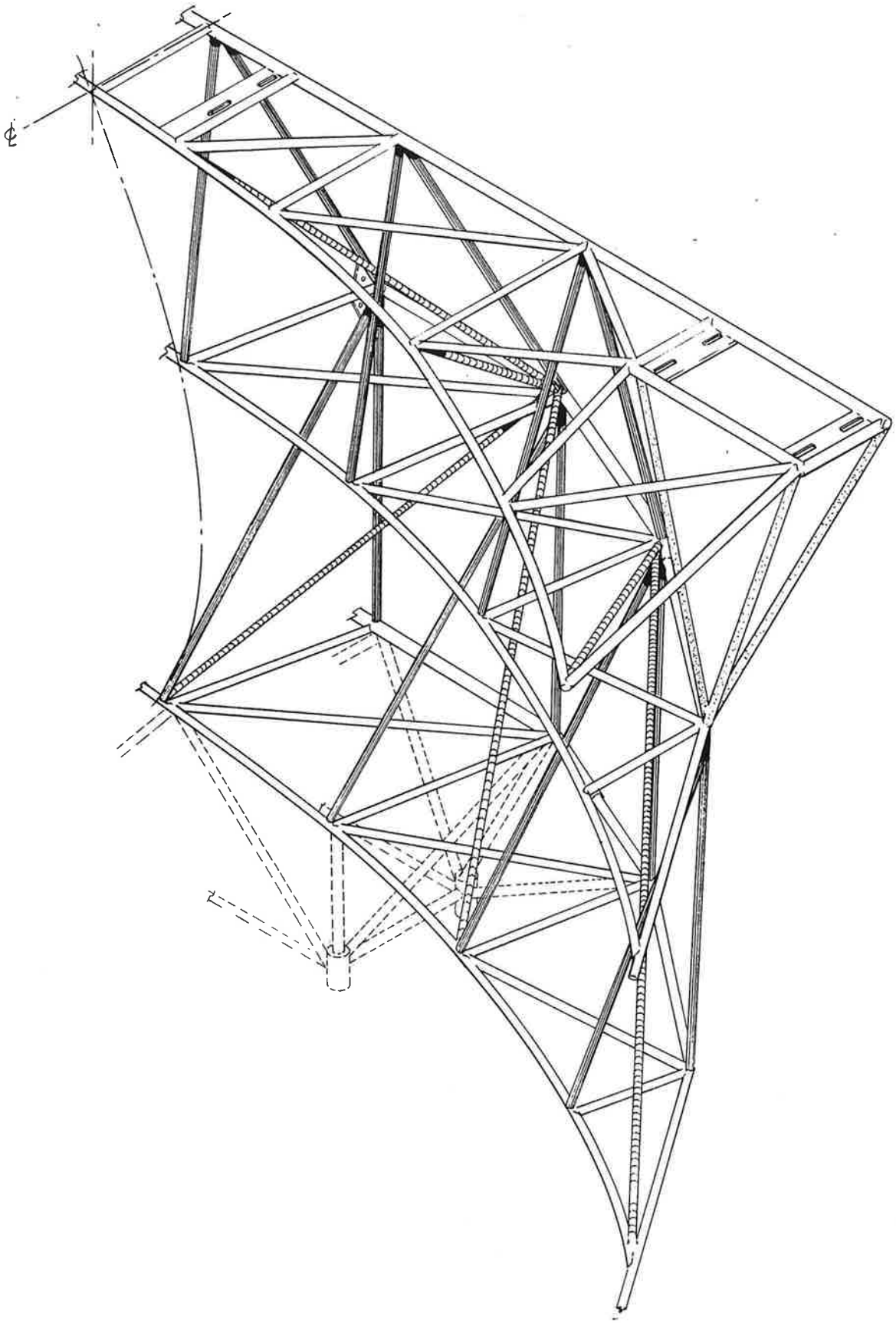

Figure 5-1. Drawings of ASR-7 Structure (Sheet 1 of 3)

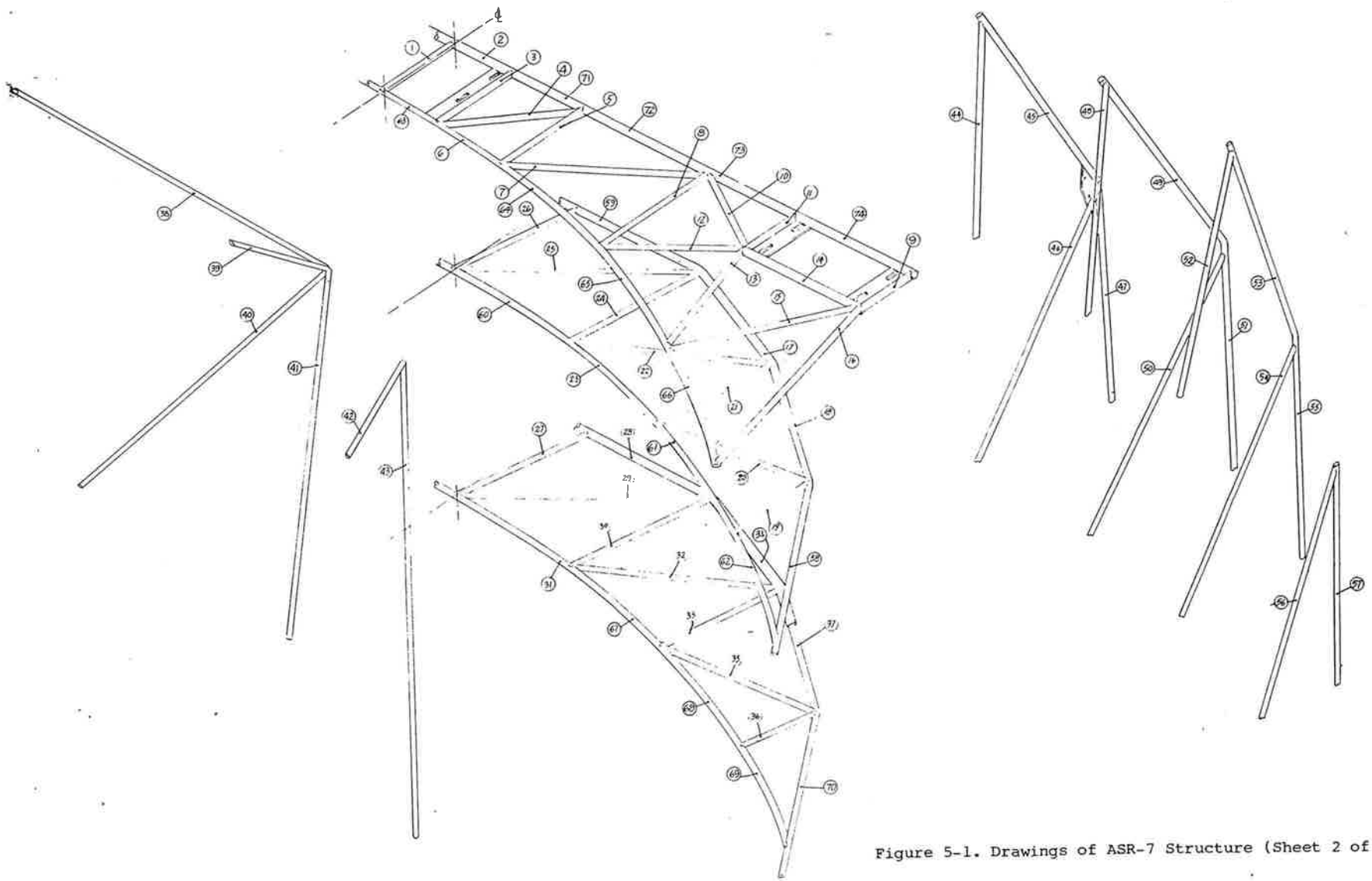

Figure 5-1. Drawings of ASR-7 Structure (Sheet 2 of 3)

No.	LENGHT	DIA.	THK
1	15.5	1.50	.125
2	12.25	1.50	.125
3	16.312	1.50	.125
4	20.0	1.50	.125
5	17.982	1.50	.125
6	14.09	1.50	.125
7	30.0	1.50	.125
8	25.223	1.25	.083
9	12.5	1.50	.125
10	19.0	1.50	.125
11	12.50	1.25	.125
12	21.0	1.25	.083
13	27.0	1.50	.083
14	24.0	1.50	.125
15	28.0	1.25	.083
16	42.0	1.00	.065
17	29.0	1.50	.125/.083
18	17/16=33	1.50/1.25	.125/.083
19	16.5	1.50	.083
20	25.5	1.25	.125
21	23.5	1.50	.083
22	29.5	1.50	.125
23	27.5	1.25	.125
24	28.5	1.50	.083
25	36.0	1.50	.125
26	26.0	1.50	.125
27	22.59	1.50	.125
28	26.34	1.50	.125
29	36.0	1.50	.125
30	28.06	1.50	.125
31	27.0	1.25	.125
32	29.5	1.25	.083
33	22.96	1.50	.083
34	29.00	1.50	.125
35	25.5	1.50	.125
36	15.76	1.00	.065
37	16/17=33	1.50/1.25	.125/.083
38	59	1.50	.125
39	67	1.50	.125
40	46	1.50	.125
41	52.5	1.50	.125
42	64.0	1.25	.083
43	52.5	1.25	.083
44	35.0	1.50	.125
45	44.5	1.50	.125
46	38.0	1.50	.125
47	36.5	2.00	.125
48	35.0	1.50	.125
49	44.0	1.50	.125
50	40.0	2.00	.25
51	34.0	2.00	.25
52	35.5	1.25	.083
53	38.0	1.25	.083
54	37.0	1.25	.083
55	35.0	1.25	.083
56	35.0	1.25	.083
57	34.5	1.25	.083
58	39.0	1.25	.083
59	26.34	1.50	.125
60	27.0	1.50	.125
61	29.5	1.50	.125
62	27.5	1.50	.125
63	12.25	1.50	.125
64	27.5	1.50	.125
65	29.0	1.50	.125
66	27.5	1.50	.125
67	27.5	1.50	.125
68	29.5	1.50	.125
69	27.5	1.50	.125
70	39.0	1.25	.083
71	14.09	1.50	.125
72	26.34	1.50	.125
73	17.09	1.50	.125
74	24.5	1.50	.125

Figure 5-1. Drawings of ASR-7 Structure (Sheet 3 of 3)

also discovered early in the Phase I study that USEM manufactures the motor drive system for the ASR-5. We have attempted to conduct discussions with the USEM personnel, but have had limited success in determining the performance of the motor. We believe that the information is available but that USEM personnel were reluctant to discuss details on this design. We would suggest that prior to the conclusion of Phase II, that additional discussions be held to determine more specifically the information of the motor drive system. However, based on the information that we have available, we have reached preliminary conclusions which are discussed in a subsequent section.

Study Relating to Rotary Joint. A study was also made of the existing rotary joint through technical manuals and drawings, and discussions with Kevlin Mfg. In the phone conversations with Kevlin Manufacturing Co., we have established the availability of this design for use in the ATCRBS system. An outline drawing has been requested of the existing design and a request for budgetary cost has been made. These estimates, however, were not available at the time of submission of this report.

Present System

The present system consists of the FA7202 antenna mounted directly on top of the ASR antenna. The FA7202 consists of a 1-1/2 ft. by 28 ft. line array; it weighs 340 lbs. Although recent ASR specifications call for the ASR to support the beacon antenna of only 340 lbs., we believe that the ASR antenna can support a greater weight load. We believe this is to be true on a basis of the requirement that the antenna will support, without permanent deformation, 1-1/2 in. of radial ice on all its surface. This amounts to several tons of ice load. Analyses which we have performed during the study verified this conclusion. According to Mr. Kleiman, of TSC, in so far as the record shows,

only one failure on the ASR has been recorded. There are at present approximately 200 of these systems in operation. In so far as the pedestal is concerned, the design appears quite rugged. It utilizes a four point contact bearing with a 19 in. pitch diameter, manufactured by Kaydon Bearing.

Discussions with various personnel in FAA have indicated that the service life of these bearings is significantly longer than specification. The drive uses an ac, three phase, five horsepower motor. We believe from calculations that this motor is somewhat marginal with regard to maintaining a constant rpm in heavy winds. In fact, in discussions with some FAA and TSC personnel, we have been informed that decelerations of those systems has indeed been observed in heavy wind conditions.

Summary of Interface Analysis

Figure 5-2 summarizes the results of the interface analysis. This analysis has included the effects of both operating and non-operating conditions on the proposed configuration of a 4 ft by 26 ft open array on top of the existing ASR. For the non-operating requirement, of 150 mile per hour winds and 1-1/2 inches of ice, studies show that both the ATCRBS open array and ASR antenna would survive without permanent deformation under conditions of full icing on both antennas. We believe this to be the crucial test in so far as acceptability of the open array is concerned without a heater system.

The operating requirement consists of wind velocities up to a maximum of 100 mph and ice thickness up to 1-1/2 of radial ice. Our study indicates that most combinations of ice and wind are acceptable in so far as operation is concerned, except for some extreme conditions involving a combination of ice and wind. In the marginal condition shown on the graph, the conservative estimates indicate that reflector deflections would exceed specifications in so far as the ASR is concerned.

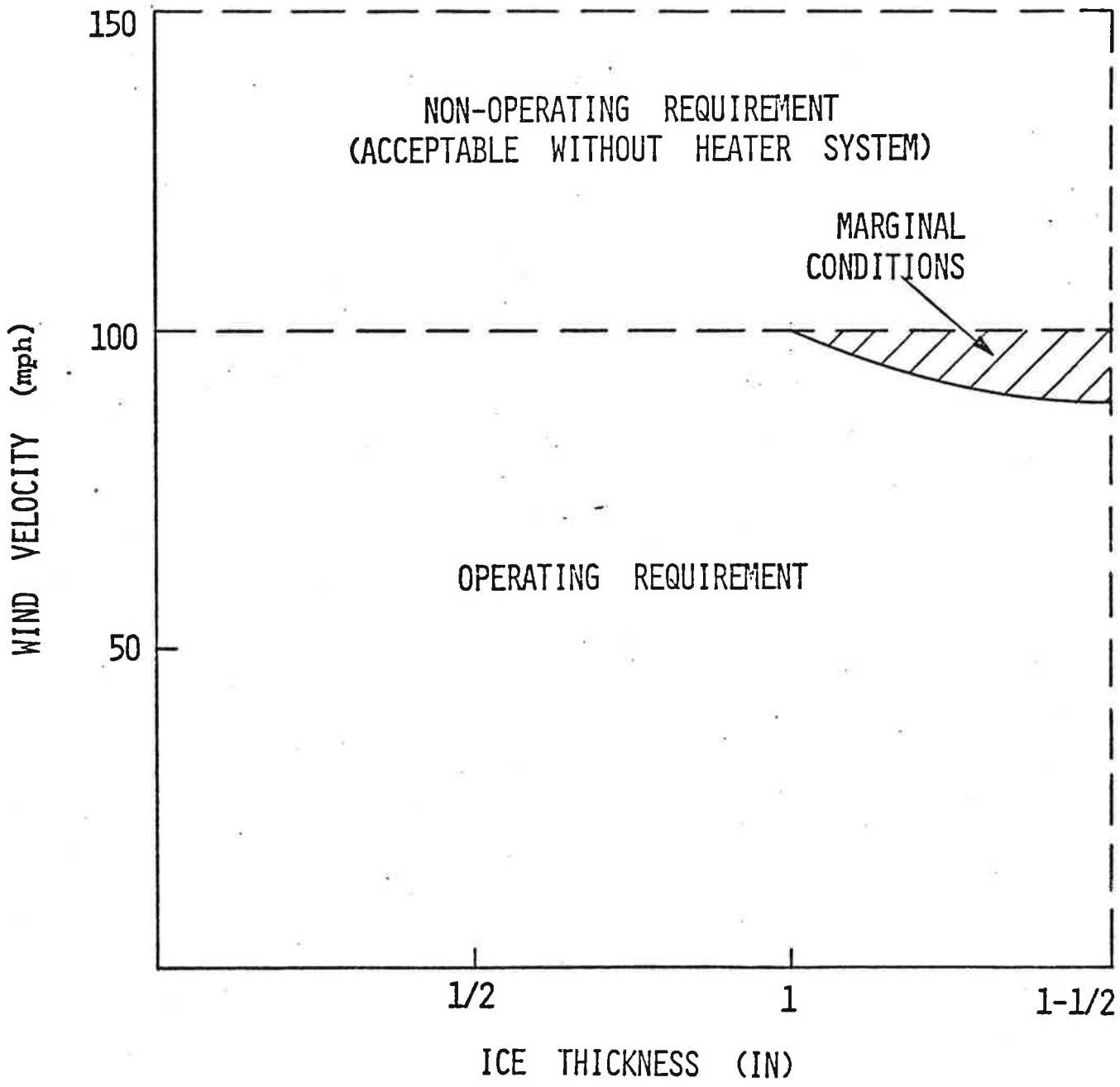

Figure 5-2. ATCRBS/ASR Interface Analysis - Summary

Additional effects would include increased loads on the bearing and on the motor drive. Outside of the marginal conditional area there will still be some loads greater than those existing in the present system. However, we do not believe these loads to be serious, and we do not expect that they would affect the bearing life significantly or motor capacity in ability to drive the ASR reflector.

It should be noted that the open array will perform with no degradation to the ASR in operating conditions of 1/2 in. radial ice and 100 mph winds. This conclusion is reached in the following manner. Without any ice coating to all, the open array antenna is exactly equivalent in loads to the FA7202 antenna. With as much as 1/2 inch of ice, the additional cross section of the open array antenna is small enough so that additional loads are negligible. But there will, however, be some additional weight load. With ice loads greater than 1/2 inch and extending beyond 1 inch of ice, then the exposed area of the open array to windloading will be significantly greater. Consequently, loads will exceed those which exist in the present case.

Impact on Reflector

Analyses on the reflector consisted of two specific tasks. First, determination of loads on specific structural members under conditions of total load, of 150 mph winds and dead load caused by 1-1/2 inches of ice on both ATCRBS and ASR to determine margins of safety relative to the yield point of the particular members. Second, the calculation of deflection at the reflector tips under operating conditions of 100 mph winds. Specific details regarding the structural analysis are contained in Appendix C. The following is a summary of the results.

Figure 5-3 describes the assumed structural model employed to compute margins of safety in deflections. This model is

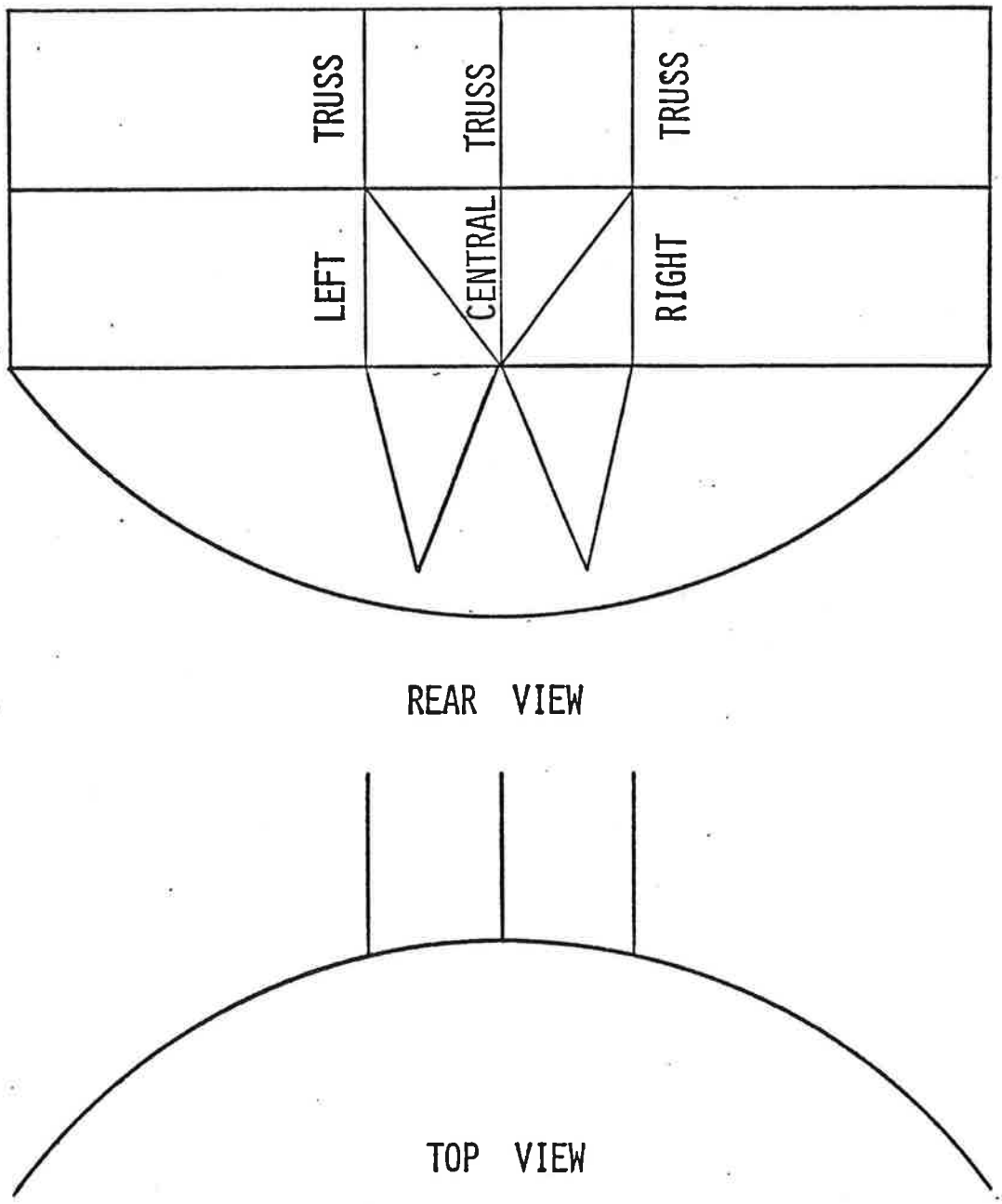

Figure 5-3. Impact Analysis - Deflection Model Employed

a conservative simplification of the actual structure to permit rapid results to be obtained within the time frame of schedule. The model chosen ignores the rigidity normally provided by the missing portions of the structure, particularly the horizontal trusses. Generally, models of this type yield margins of safety and deflections which are conservative by about a factor of two to one. Consequently, in cases where we have computed deflections to be of the order of the maximum permitted in the specification, the actual deflections will not exceed the specification.

Figure 5-4 summarizes the results of the structural analysis which was performed. Indicated in the figure are the deflections and lowest margins of safety for the open array, support structure and the ASR reflector. In the non-operating condition, the member with the lowest margin of safety is the lower member in the rear vertical truss, which carries a large portion of the live and dead load into the pedestal. For this member, a margin of safety was calculated to be 1.34. Other members of the structure were checked and found to have larger margins of safety. Deflections at the upper edge of the reflector were computed by determining the deflection on the load for the central vertical truss. The deflections were found to be less than the specification for the ASR-8.

In a similar manner, the deflection of the three central trusses was computed and the difference in deflection used to calculate expected tip deflection. These deflections were found to be less than the ASR-8 specification and within the specification outlined in the TSC design constraints. These stated that deflection be held to a value low enough to insure pointing errors within the radar beam of less than 1/2 degree.

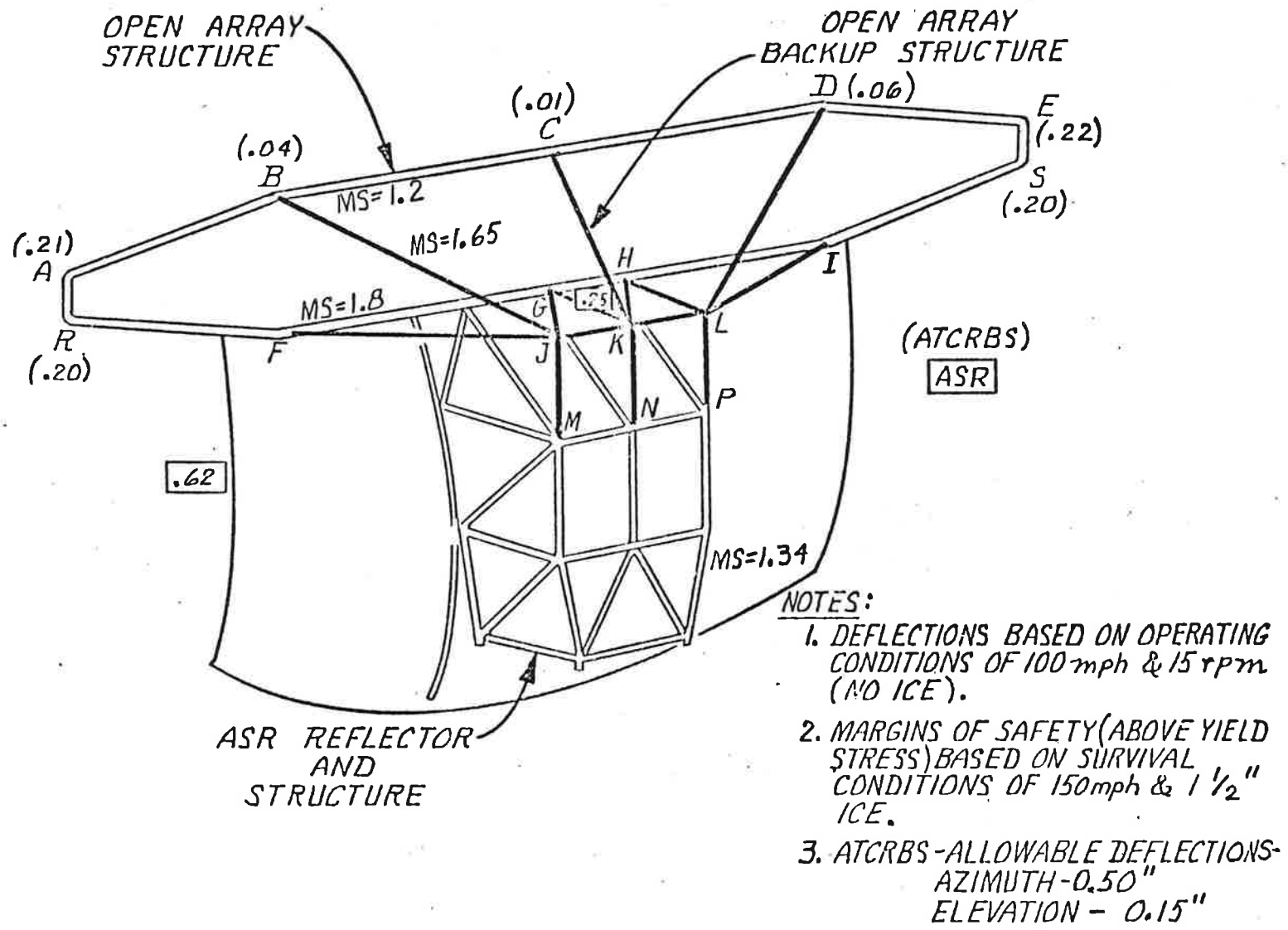

Figure 5-4. ATCRBS Antenna Deflections and Margins of Safety ASR Installation

ATCRBS/ARSR STRUCTURAL DESIGN

Mounting Arrangement

Three different mountings of the 4 ft x 26 ft open array to the ARSR-2 reflector were outlined in the original proposal. These consisted of a top mounted direct replacement of the FA7202 beacon antenna, a back mounted configuration attached near the top of the ARSR Reflector Support structure, and a chin mounted design located beneath the reflector boom. Of the three configurations, the boom mounting offers the most straight-forward approach. The chin mount configuration would not require structural modification to the radome or lenghly system down-time for installation. The ATCRBS and counter weight structure would be bolted to the ARSR without the need for elaborate hoisting equipment. There is sufficient clearance for rotation without removal of obstacles such as guard rails. The lower most part of the ATCRBS would be 6 ft from the floor.

The major obstacles associated with the first two configurations are briefly presented below.

The first configuration would involve raising the height of the radome with an additional structure to achieve sufficient mounting clearance. This is undesirable since it would entail lengthly system down-time. The second configuration would require a system change since the scanning of the beacon and ARSR would be 180° out of phase.

The structural impact of the open array on the ARSR in the chin mounted position is analysed in the RF Systems Structural Analysis included in the Appendixes. The results of this analysis are presented in Part B.

The chin mounting of the ATCRBS 4 ft x 26 ft open array on the ARSR is not exposed to environmental extremes due to the radome enclosure. This allows for mounting with only minimal structural

back up as shown in figure 6-1. The 4 ft x 26 ft open array is located approximately 15 feet from the center of rotation of the ARSR. At which point, the top horizontal member of the ATCRBS is located 1 foot from the bottom of the boom. The mounting structure between the boom and open array is fabricated of flat bar and 2-1/4 inch diameter 1/16 wall aluminum tube. Connection to the ATCRBS antenna is made at four pick up points located on the top horizontal member, at 14 inches and 8 feet on both sides of the antenna center line. Two additional pick up points are provided on the lower channel 8 feet on each side of center. The inner points are tied into the boom by 2 vertical and 2 horizontal members; the outer points, by long diagonals terminating on the bottom member of the boom 7-1/2 feet behind the ATCRBS antenna.

The structural analysis shows that the added weight of the 4 ft x 26 ft open array and back up structure will cause an additional deflection of .047 inch in the ARSR boom at the focal point. The deflections in the ATCRBS are negligible. The margin of safety of the loads on the boom is 16.4.

In order that the dynamic loads on the ARSR are balanced a counter weight is added to the system. By correctly locating this weight, the dynamic imbalance during rotation of the ARSR caused by the open arrays weight can be neutralized. This is done at a tradeoff of increasing the total thrust load to the bearing. From the bearing standpoint however, the increase in thrust load would have less effect on bearing life than the associated increase in moment load. The 614 pound counter weigbt will be located 64-3/4 inches from the center of rotation. The counter weight will be mounted to the intermediate carriage which the boom and reflector attach to. Mounted in this manner, the reflector does not see additional loads, and therefore no further analysis is required.

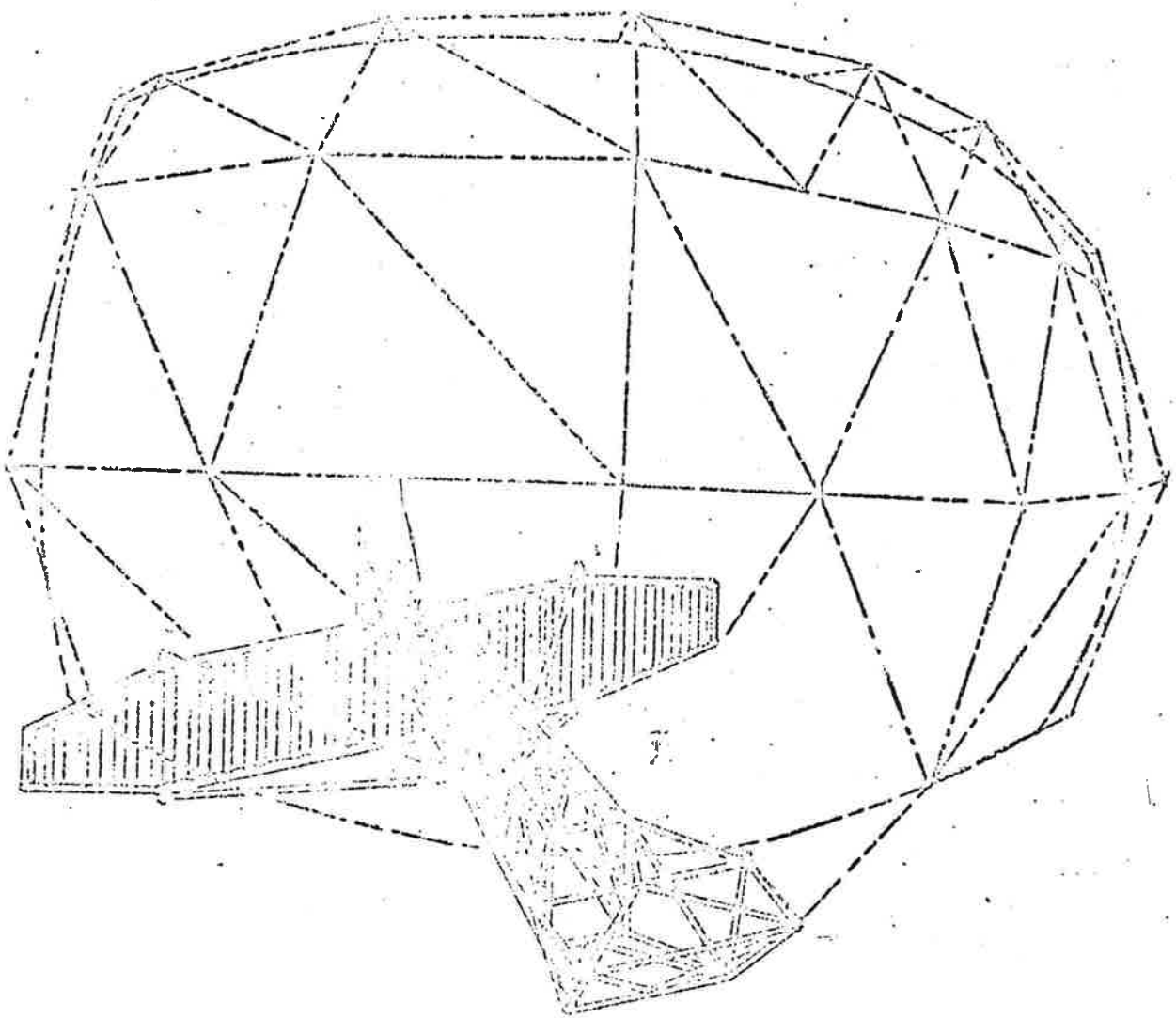

Figure 6-1. Chin Mounted Configuration for ARSR

COST BENEFIT STUDIES - VERTICAL SIZE VERSUS COST

ASR Case

With regard to cost benefit studies, the primary parameter of interest in the open array is vertical aperture, since this parameter controls the degree of vertical lobing. Studies have shown that a four foot aperture is a direct replacement for the FA7202 from the standpoint of windloads, but the question arises as to the use of larger vertical apertures and its impact on existing systems. Several questions of interest are:

- What is the largest vertical aperture that will eliminate all lobing effects over the elevation angles of interest?
- Are there any parameter tradeoffs that can be made to achieve a greater height, such as a change in aspect ratio?
- Is the greater height technically feasible from the standpoint of ATCRBS antenna design and impact on the existing ASR?
- Are there any quantative steps in cost as antenna height is increased?

Maximum Vertical Height. Figure 7-1 shows the vertical lobing envelope size at 2^{o} elevation as a function of aperture height. The calculation assumes dry sandy loam as the ground reflection characteristic. This computation was performed using figure 2-10 as a basis which was presented in Section II. It should be noted that a 1-1/2 foot aperture corresponding to the FA7202 antenna yields a 19 dB envelope, whereas a 4 feet (open-array) provides a 10.5 dB envelope, a reduction of nearly 50%. The 8 foot aperture (E-Scan antenna) provides even greater improvement, reducing the envelope to 3.5 dB.

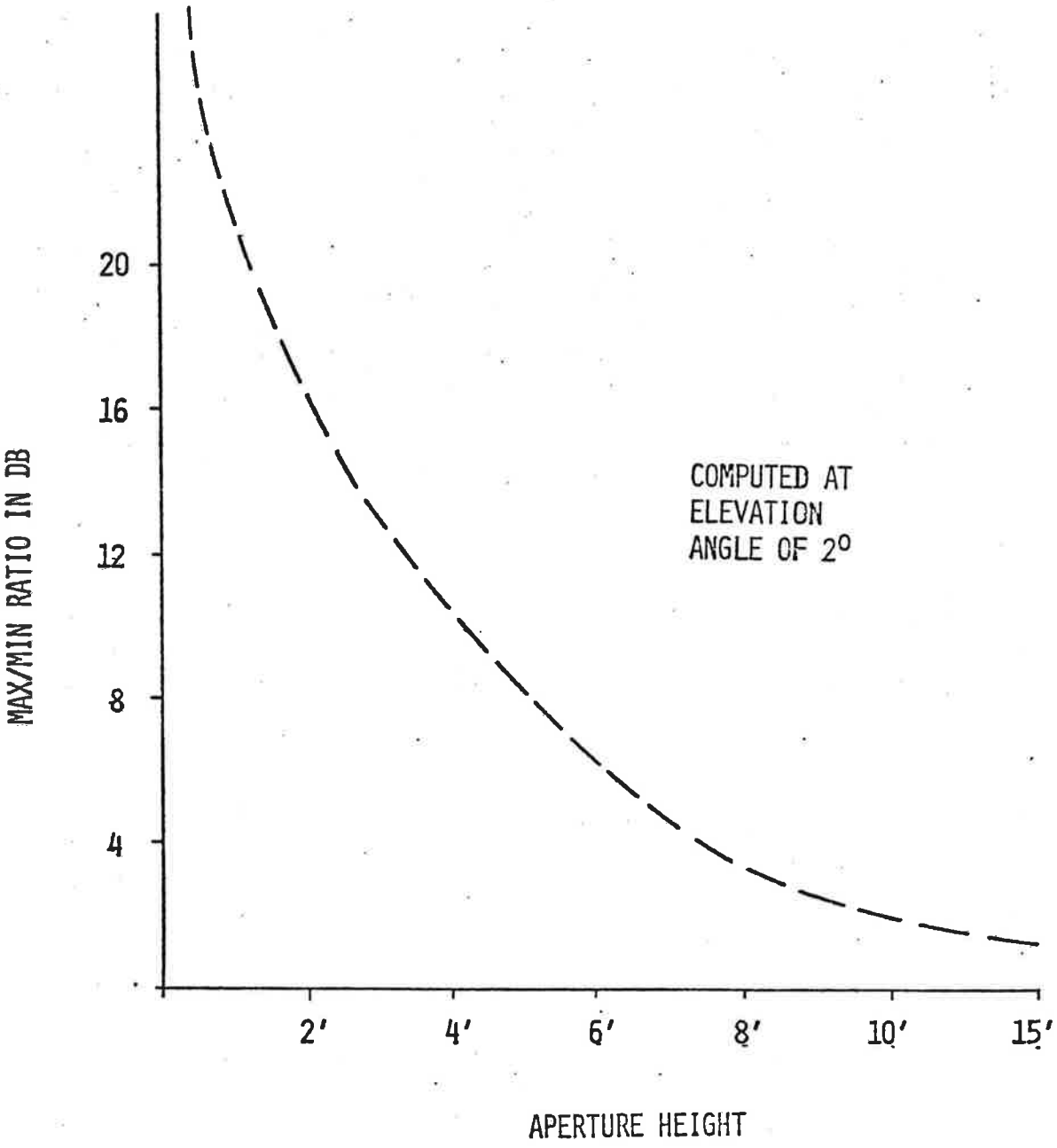

Figure 7-1. Vertical Lobing Envelope Size vs. Aperture Height

From the graph, it is concluded that the maximum aperture size that needs to be considered for the ASR is 15 feet; this reduces the envelope to zero. Beyond this height, a lobing problem ceases to exist. From the standpoint of a practical system, it does not seem sensible to consider the 15 foot case because perfect uniformity of signal level is usually not required. In fact, the elevation pattern without vertical lobing has some ripple associated with the synthesis of the pattern, and typically has a 3 dB variation of signal. Therefore, it would seem that a vertical lobing envelope of 3 dB at 2^{o} would be practical limit with regard to performance requirements. This would dictate the use of a maximum aperture size of 8 to 10 feet.

Tradeoff of Antenna Parameters. One method of achieving a larger than 4 foot vertical aperture would be to reduce the antenna size in azimuth. For example, from considerations of windload, a 4 ft by 26 ft aperture would be about equivalent to an 8 ft by 14 ft aperture. The major effect of this change would be to cut the system resolution capability in azimuth by 50%. Admittedly, reduction of vertical lobing will improve system resolution when the aircraft are located in pattern nulls. Nevertheless, when the antenna aperture is reduced by 50%, the system resolution is bound to be seriously affected. As traffic loads increase, the desirability of a 28 ft aperture will become more evident.

Feasibility of Increased Vertical Aperture. From the standpoint of the ATCRBS antenna, the feasibility of a vertical aperture larger than 4 feet is well established (8 foot apertures are currently used in the E-scan electronic scan antenna and in the antenna for the DABS Experimental Facility) at Hazeltine. The real issue concerns the allowable limits with regard to weight and windloads imposed on the

existing ASR antenna. In sites where ice loads will not be present, a 6 ft or 8 ft vertical aperture may be feasible with tolerable effects on the existing system. In sites where occurances of 1-1/2 inches of ice will take place, either upgrading of the ASR to permit these ice loads would be required or alternatively, a heater system could be employed to de-ice the ATCRBS antenna. Another possibility would be to employ a radome in these select sites.

Use of a 8 ft or possibly even a 6 ft aperture on sites where 1-1/2 in. of ice is expected without one of the above steps is not advised because analyses show that margins of safety in the structure would be unacceptable at the non-operating condition of 150 mph winds, and 1-1/2 in of ice. If the specification is reduced to 1/2 in of ice and 150 mph winds, then it appears that use of a 6 ft or 8 ft antenna is feasible without the above mentioned provisions.

Quantum Steps in Cost. For sites where ice is not the problem, then the only cost factors for a 6 ft or 8 ft antenna are those associated with the larger ATCRBS antenna height and possibly the need for a more powerful motor, if deceleration in high winds is not acceptable. For sites where large amounts of ice are expected, (1/2 in of ice or greater) some significant changes are required, namely upgrading of ASR, or the installation of a heater system, or the use of a radome. Upgrading of ASR would means reinforcement of the backup structure, particularly the main trusswork connected to the pedestal. The motor should be replaced with one of a larger capacity. The bearing may have to be replaced to permit greater static loads. Installation of a heater system in the ATCRBS antenna is feasible but power requirements imposed on the site to maintain an ice-free condition

would be severe, and on the order of 15 to 30 kilowatts. Installation of a radome (35 foot) would permit an 8 ft aperture to be employed without a heater or without upgrading the ASR antenna. However, the tower foundation may need reinforcement.

ARSR Case

For the ARSR, we can also raise similar questions, namely;

- o What is the largest vertical aperture that will eliminate all lobing effects over the elevation angles of interest?
- o Are there any parameter tradeoffs that can be made to achieve the greater antenna height such as a change in aspect ratio?
- o Is the greater height technically feasible from the standpoint of ATCRBS antenna design, and impact on the existing ARSR system?
- o Are there any quantum steps in cost as antenna height is increased?

Maximum Vertical Height. In the ARSR case, presumably one is interested perhaps down to as small as 1^{o} elevation. Figure 7-2 shows the envelope size as a function of antenna height for this case. Here array aperture heights of 16 to 20 feet could be considered from the standpoint of performance improvement, because of the low elevation angle requirement. For best performance, (3 dB ripple is a practical limit) a 20 foot array aperture would be desirable.

Tradeoff Parameters. The ARSR uses a radome, therefore, changing the aspect ratio to achieve greater aperture height with constant windload is not an issue in this application.

lobing down to the 3 dB limit. The real problem is the impact of such an aperture on the existing systems. Hazeltine has chosen the 4 ft high aperture in order to permit installation with safe operation in all ASR sites and for commonality, we have suggested the same antenna for ARSR. If strict commonality is not of the utmost importance, then we would suggest a family of three antennas very common in design(would use the same dipoles, structural design, and azimuth networks) consisting of a 4 ft, 6 ft, and 8 or 10 ft high antennas. In this manner, for each site, one may select the best antenna. For example,

1. 4 ft antenna - used on northern most ASR sites where ice is a problem with no changes to ASR.
2. 6 ft antenna - used on most ASR sites with possibly a heavier motor in very windy regions.
3. 8 ft antenna - used for ARSR. Also can be used on ASR sites if a radome is installed, or possibly a heater system employed along with a heavier motor.

SITE CONFIGURATION AND IMPLEMENTATION PLAN

The Hazeltine open array antenna we believe provides a very simple solution in so far as site implementation is concerned. The antenna is light weight and is easy to handle. It is capable of being assembled at the site with a minimum of time and effort. The antenna design will use existing mounting holes. No changes are required to the existing radar systems such as structural reinforcement of the reflector or modifications to the pedestals. All new mounting points will utilize adaptor hardware to avoid the need for welding or modifying existing antenna structures.

Because of the simplicity of the approach, minimum downtime will be required. Installation can be easily accomplished within an 8 hour period, preferably during low traffic times, such as 12 to 8 a.m.

ASR

The general procedure of installation of the open array on the ASR site would consist of the following steps:

- o The open array and the omni antennas would be uncrated and assembled on the site. The backup structure for the open array directional antenna will also be assembled to the antenna on the ground.
- o The adaptor hardware needed to interface the backup structure of the open array with the rear truss work of the ASR would be installed.
- o The existing FA-7202 antenna and companion omni would be removed from their mounting locations.

- The antenna would be lifted and bolted into place.

- The three main vertical struts which attach the backup structure of the open array to the rear truss work of the ASR would be installed.

- RF cables would be connected.

- The omni would be installed on the existing pole in the corner of the tower platform.

ARSR

The procedure for installing the open array on the ARSR would consist of the following steps:

- The open array and omni would be uncrated at the base of the tower.

- The ARSR tower design includes provision for removing several panels of the tower floor. From inspections at the site, it appears that a 12 foot by 18 foot section of the tower floor can be easily removed.

- Large antenna sections can be lifted up from the ground, directly up through this opening, as the tower design includes provisions for permitting this type of installation.

- The antenna can either be hoisted in sections or first assembled on the ground and then lifted up into the tower.

- The hardware required to adapt to the boom is then installed on the radar feed boom.

- The antenna is lifted in place, possibly by manual means and installed on the boom.

- Adjustments will be provided to permit the antenna to be leveled.

- The counterweights and associated structure are then installed on the rear portion of the reflector chassis.

o The omni antenna is then installed by lifting it to place under the radome roof and installing adaptor hardware to the existing radome ceiling.

o Cables are then connected to complete the installation.

Alternate Configuration for ARSR

Three configurations have been considered for this site. We have chosen the chin mounted array because we believe it to be the simplest and most attractive approach. The other alternatives consisted of mounting the open array antenna on top of the ARSR reflector or back to back with the ARSR reflector. With regard to mounting the open array on top of the ARSR reflector, measurements have been done and inspections of the site have been made which have led us to conclude that the existing radome would have to be raised by at least two feet to permit this installation arrangement. Lifting up the radome is possible in that an additional ring, consisting of steel truss work can be installed on the tower to increase the height of the radome by the required two feet. However, we believe that such an installation would require a fairly substantial amount of downtime. Either the radome would have to be removed and lowered to the ground in order to permit the ring to be installed rather quickly, then the radome lifted back into place; or the existing radome would have to be jacked up in place and the steel truss work installed in sections. In either case, the downtime is considered to be very significant. In addition, the cost associated with this modification would be substantial. In view of the expense and downtime required, we have decided not to recommend this approach, although recognizing that electrically, it provides very nearly the best electrical approach, particularly from the standpoint of SLS operation.

We have also considered the back to back arrangement, that is, mounting the antenna on the back of the ARSR reflector. This approach would provide a very attractive mechanical solution from the standpoint of interfacing with the reflector and also minimizing downtime. However, it imposes system complications which we believe are extensive and which would require modificationtions to the electrical system for the ARSR. The problem imposed is that beacon replies will be phased 180^{o} in azimuth with respect to radar replies as a result of the misalignment of the two beams for the radar and beacon system. Although we have not thoroughly investigated this approach, we believe that this complication is not tolerable, nor do we believe the modifications to be simple enough to be attractive. Consequently, we did not consider this approach any furhter.

Monopulse Performance

The open-array antenna will include azimuth networks in order to provide near optimum monopulse difference pattern performance, hence, no modifications are required so far as the antenna design is concerned to provide monopulse capability. From a systems standpoint, however, there will be a need to modify or replace the existing rotary joint on both ASR and ARSR to provide the full monopulse capability. For most sites, the rotary joints which presently are utilized have only a single channel at L-band. The monopulse operation will require that these rotary joints have two channels at L-band. We understand from discussions with engineering personnel at NAFEC that a new rotary joint will be installed on the recently constructed ASR-7 site, which presumably is the site on which the Hazeltine open-array antenna will be installed.

In our search for rotary joints with two channels at L-band, we have discovered that Kevlin Manufacturing Co. has developed a rotary joint for FAA use. It is our understanding that this rotary joint may be the one to be procured for installation

on the ASR-7. This rotary joint contains two L-band channels and three S-band channels for the ASR radar. If additional rotary joints are required, we will investigate the availability of these units from Kevlin, or possibly alternate manufacturers who have also devleoped a similar rotary joint. In our discussions with Kevlin, we understand that the rotary joint which they have developed is quite easily installed on ASR sites. Its mechanical configuration is designed to retrofit in the existing flange arrangement in the ASR pedestal.

The precise specifications for a dual L-band channel rotary joint to be used in a monopulse system will, of course, depend on the system requirements imposed by the system designer. It appears from the present performance achievable in rotary joints that in regard to phase and transmission characteristics that existing rotary joint technology will be sufficient to meet the monopulse requirements.

For the ARSR site, if monopulse is required, a dual channel L-band rotary joint will also have to be provided. In our visits to NAFEC, we have learned that at least one ARSR site now has a dual L-band channel joint. This site is at Elwood located in the vicinity of NAFEC test facility. The design of this rotary joint did not appear to be identical to the ASR rotary joint developed by Kevlin, and at the present time we do not know who has developed this particular unit. Presumably, additional units can be procured for the ARSR sites to provide the dual channel capability. We also understand that newer ASR and ARSR sites have requirements for rotary joints which include additional L-band channels for upgrading of the beacon system. In these cases, the requirements for modifying the rotary joint disappears.

Maintainability

The antenna design will include maximum flexibility with regard to maintainability and replcement of individual components. The antenna consists basically of many small units of dipoles, cables and networks. Each unit is individually packaged and capable of being removed from the antenna. Dipoles are removable on an individual basis from the array structure by removing several screws. It is recommended that dipole spares be provided with each antenna in case of breakage during installation or perhaps after installation. Although individual networks are capable of being replaced, it does not appear from a reliability standpoint that this would be necessary, consequently, these networks will not be made replaceable in so far as replacement while the open-array is installed on the ASR or ARSR. If replacement is necessary, the antenna can be removed and disassembled within a shop area and individual components in the network replaced.

ANTENNA TEST FACILITIES

A two-stage program of antenna testing is planned. The first stage will be a part of the antenna development cycle and will allow adjustment and optimization of the antenna design for best antenna patterns. The second stage will be a final series of pattern measurements on the final antenna.

For the first stage of antenna testing, the Hazeltine Smithtown antenna test facility will be used. Adjustment and optimization of the antenna can be efficiently accomplished here. For high-quality pattern measurement the antenna will be tested on the upper roof and a directive L-band source antenna will be used to avoid spurious reflections. Since the 1000-foot test range is less than the $2D^2/\lambda$ distance of the ATCRBS antenna, the antenna will be refocused by the addition of short sections to the azimuth cables.

For the second stage of pattern testing, a test range equal to or longer than the $2D^2/\lambda$ distance will be used in order to obtain conclusive patterns of the final antenna configuration. The 1900-foot ESSCO range in Concord, Mass. is longer than the 1750-foot $2D^2/\lambda$ distance of the ATCRBS antenna. This range is a flat (ground-image) range and has an 80-foot-high tower on which the ATCRBS antenna can be mounted for high-quality pattern measurements. A directive L-band source antenna can be used to avoid spurious reflections. It is our plan to use the ESSCO range for the second stage of antenna testing.

Antenna patterns to be measured include 360° azimuth patterns (conical cuts) at various elevation angles, and elevation patterns at various azimuth angles. Sum patterns will be measured at 1030 and 1090 MHz and difference patterns at 1090 MHz. There will also be patterns measured in the cross polarization. Gain and input impedance of the antenna will be measured. The omni

SLS antenna will also be tested at Smithtown for azimuth and elevation patterns, gain and impedance, at 1030 MHz.

The program of antenna testing outlined above is expected to provide an opportunity to optimize the antenna performance and to thoroughly evaluate the antenna before delivery of the antenna to NAFEC for field tests.

HEATER SYSTEM

The design study for the prevention of ice formation and buildup on the antenna structure was initiated to insure that the reflector deflection of the ASR operational conditions (85 Knot winds with 1-1/2 inches ice) would be within specification. Adequate structural integrity of the antenna under these loads as well as the survival conditions has been established. The thermal analysis is presented in Appendix D and briefly summarized in the following paragraphs.

To establish a realistic baseline for the thermal calculations, several authoritative reference sources on meteorological data were utilized. Based on this data, which included precipitation rates, liquid water content, icing conditions and wind velocity, the total heat energy required to keep the antenna ice free at different ambient temperatures was calculated. The total heat energy consists of the melt energy and the energy to offset convective cooling of the wind. Calculations show that the total energy required if efficiently used is about 16 kw for the design conditions established. These conditions are 30 mph winds, a liquid water content of .64 gm/in^3, and a deposition rate of 1.5 inches in a 3 hour period.

To accomplish the required heating, two approaches were considered. The first approach utilizes electrical heater wires which are mounted on the surface of the .625 inch and 2 inch diameter tubes. This approach places the heat at the surface of ice formation and provides for efficient use of heating power. The alternate method utilizes the tubular antenna structure as a heat exchanger. This method involves passing heated air through the antenna frame with air blowers. Using this arrangement, which is practical due to the antenna tubular design, the input power required would be approximately 25 kW.

Although the application of ice prevention equipment to antennas and radomes is technically feasible, it inherently causes the antenna mechanical design to be more complex and thus more costly. In the open array antenna, ice prevention would increase the material cost by virture of heaters, controls, blowers, etc. Fabrication, assembly and maintenance would be more costly due to the provisions for heaters or air flow. Finally, each installation would require an additional 16 to 25 Kw of power to provide heater and/or blower power when required. After reviewing the above factors and realizing that the antenna can structurally survive, without permanent deformation, all specified operational and non-operational requirements without heaters, their elimination from consideration is strongly recommended.

GROWTH POTENTIAL

Additional Uses for 4 x 26 Open Array

A possible application for the 4 x 26 foot open array that was not covered earlier in this report is those ARSR sites that employ military radar antennas. In some cases these antennas do not employ radomes, and it may be desirable to replace the existing ATCRBS antenna with a new antenna having substantially no greater windage. In other cases there are radomes, but the radar antenna reflector may be smaller than the civil ARSR-2 reflector and may leave room for the new antenna above the reflector without raising the radome. In both of these cases it is likely that the omni SLS antenna could be located just above the main antenna for minimum differential in the periodicity of the vertical-lobing patterns.

Another possible application for the 4 x 26 foot open array would be to a separate-site installation where only the beacon antenna would be present. With the small windage of this antenna, a small pedestal and lightweight tower could be considered. Also, the drive motor requirements would be minimized; this would be particularly significant where accurate slaving to the radar antenna on a nearby site was needed.

Open Arrays with Larger Vertical Aperture

The 4 x 26 foot open array is being developed to mount on an existing ASR reflector and pedestal without substantially increasing the windage beyond that of the present ATCRBS antenna. However, for other situations that do not have this constraint a vertical aperture larger than 4 feet may be desirable. An

open array with a larger vertical aperture (for example, an 8 x 28 foot open array) could easily be developed using many of the components of the 4 x 26 foot open array.

One situation where an open array with a larger vertical aperture can be considered is an ASR installation where an increase in the windage might be tolerated, either by having less extreme environmental requirements or by using a heavier pedestal and structure. These possibilities were discussed in an earlier section of this report.

Another situation in which an open array with a larger vertical aperture may be appropriate is with the very large FPS-35 military radar antenna used at certain ARSR sites. In this case, the pedestal and radar antenna structure are probably strong enough to permit a moderate increase in windage over that of the existing ATCRBS antenna.

For the civil ARSR-2, it was noted earlier in this report that a convenient location for the 4 x 26 open array was the "chin" mounting under the radar feed boom. The 4 x 26 open array is light weight and can be supported from the existing feed boom with little additional structure. However, an array with a larger vertical aperture could also be used in this location, probably having as much as an 8 foot vertical aperture. Although the low-windage feature of the open array is not needed inside the ARSR-2 radome, the open-array structure is light weight and therefore is attractive for this application. If an 8 x 28 foot open array were available, it would be appropriate to consider it for the ARSR-2 chin location.

For the planned ARSR-3 installation, an 8 x 28 foot open array on top of the radar reflector appears feasible. Assuming that the ARSR-3 employs a 65 foot diameter radome as requested by the FAA, there appears to be ample room below the top of the

radome for both an 8 x 28 open array and an 8 foot omni antenna. The extra space between the top of the radome and the beacon antennas is desirable to minimize the effect of the radome on the performance of the beacon antennas.

Another possible application for an open array with a large vertical aperture would be to a separate-site installation where only the beacon antenna would be present. Here the reduced windage of the open-array structure would permit a large vertical aperture to be used without requiring a very heavy pedestal and a very powerful drive motor. For example, it is probable that an 8 x 28 open array could use the existing ASR pedestal design. Whether an ASR drive motor would also be adequate where accurate slaving to the radar on a nearby site was needed is a question. In any case, the open array would require a much less powerful motor than a solid antenna.

In summary, an open array with a larger vertical aperture (such as an 8 x 28 open array) has a number of possible applications. It can easily be developed using the experience gained in developing the 4 x 26 open array, as well as using many of its components.

Capability for Difference SLS

In ATCRBS the SLS signal is typically radiated from an omni antenna located just above the main antenna. With an omni pattern, the SLS antenna can be stationary and can be mounted separately from the rotating antenna. Also, an omni pattern gives complete coverage for suppression of false targets caused by reflection from nearby buildings (improved SLS). One problem of the separate omni SLS antenna is that, because it is not located at the same height as the main antenna, the vertical-lobing periodicity is different from that of the main antenna. This can degrade the performance of the SLS.

The E-scan circular cylindrical array for ATCRBS provides an omni SLS pattern that radiates from the same vertical aperture that radiates the directive pattern. This "integral" omni SLS pattern gives ideal SLS performance independent of vertical lobing.

Military IFF antennas commonly provide an integral SLS pattern which employs a difference pattern having sidelobes with filled-in nulls that cover the sum-pattern sidelobes at all angles. This pattern can be obtained simply by transforming the existing symmetrical excitation into an antisymmetrical excitation with a hybrid junction. Usually there is also an SLS pattern radiated toward the rear by means of a small "back-fill" radiator on the back of the antenna, to cover the antenna backlobe. These SLS patterns are "integral" and give SLS performance independent of vertical lobing. These patterns do not give complete coverage for suppression of false targets caused by reflection from nearby buildings. They also result in "beam sharpening" because the difference pattern peaks suppress transponders outside of a narrow angle in azimuth. Beam sharpening is desired in IFF systems but not necessarily in ATCRBS.

As described earlier in this report, the "chin" location for the 4 x 26 open array under the feed boom of the ARSR-2 is recommended as the simplest installation. However, the omni SLS antenna would be located above the radar reflector, far above the 4 x 26 ATCRBS antenna. This will increase the differential in the periodicity of the vertical-lobing patterns of the two antennas. It is estimated that above 2° elevation angle, the vertical variations in relative signal of the main antenna and the omni antenna will be less than they are at present because of the increase to the 4 foot vertical aperture in the new antennas. However, below 2° elevation, the variations in relative signal will be greater

because of the very large separation of the two antennas in this case. Of course, at all elevation angles the variations in each individual signal will be much less with the two new antennas. Thus, ATCRBS will clearly be improved by the new antennas above 2^{o} elevation. However, below 2^{o} the net effect on the system is not easy to predict, and could be a degradation. With still larger vertical apertures the same kind of results are obtained, but the "crossover" angle becomes lower than 2^{o} elevation.

Consider now a 4 x 26 open array having a difference SLS pattern, and using the "chin" location under the ARSR-2 feed boom. Since the difference SLS pattern is "integral" the SLS performance will be independent of vertical lobing. In addition, of course, the vertical lobing will be much less with the new antennas than with the existing antennas because of the increased vertical aperture of the new antenna. Thus in both of these aspects the new antennas would clearly be an improvement over the existing antennas.

However, there are two questions about this use of difference SLS that should be answered. One concerns the "beam sharpening" that would result. It is believed that in the typical ARSR site, beam sharpening would not be handicap because typically there are substantially more replies to an ARSR interrogator than are needed. It is possible that beam sharpening would actually prove to be beneficial for an ARSR site.

The other question is the lack of complete SLS pattern coverage for suppression of false targets caused by reflection from nearby buildings. While the backfill SLS radiation will cover the rear area, the regions to each side of the ATCRBS antenna may not be covered, and false targets from reflections in these side directions may not be suppressed. It is believed likely that many ARSR sites do not have significant building reflections. Therefore, these sites would not be handicapped by the lack of complete SLS pattern coverage. Even on those sites where building

reflections are present, false targets might be suppressed by appropriate orientation of the backfull antenna or by use of an additional SLS antenna specifically for this purpose. The backfull antenna would be located behind the ARSR radar reflector.

It appears from the above considerations that difference SLS with a "chin" mounted 4 x 26 (or 8 x 28) open array is an attractive possibility for many ARSR sites. Implementation of difference SLS presently is not included in the development of the 4 x 28 open array but could be incorporated by a modification to the azimuth network. Figure 11-1 indicates how this might be done by inserting an electronic switch in one of the difference channels within the azimuth network. During transmission, the switch would provide an SLS difference pattern, while during reception the switch would provide the monopulse difference pattern having low sidelobes. If monopulse was not used at a particular site, the switch could be omitted and the difference SLS connection made permanently.

Figure 11-2 indicates how the circuitry around the rotary joint might be arranged. If the rotary joint was at the lower location it would have two ATCRBS channels, or one channel if monopulse was not used. The SLS switch and the difference channel switch would be located in the antenna and would be controlled through slip rings. Hazeltine has produced many IFF antennas having SLS switches above the rotary joint; high-reliability performance is obtained. If the rotary joint was at the upper location it would leave the SLS switch below the rotary joint, permitting servicing without shutting down the radar.

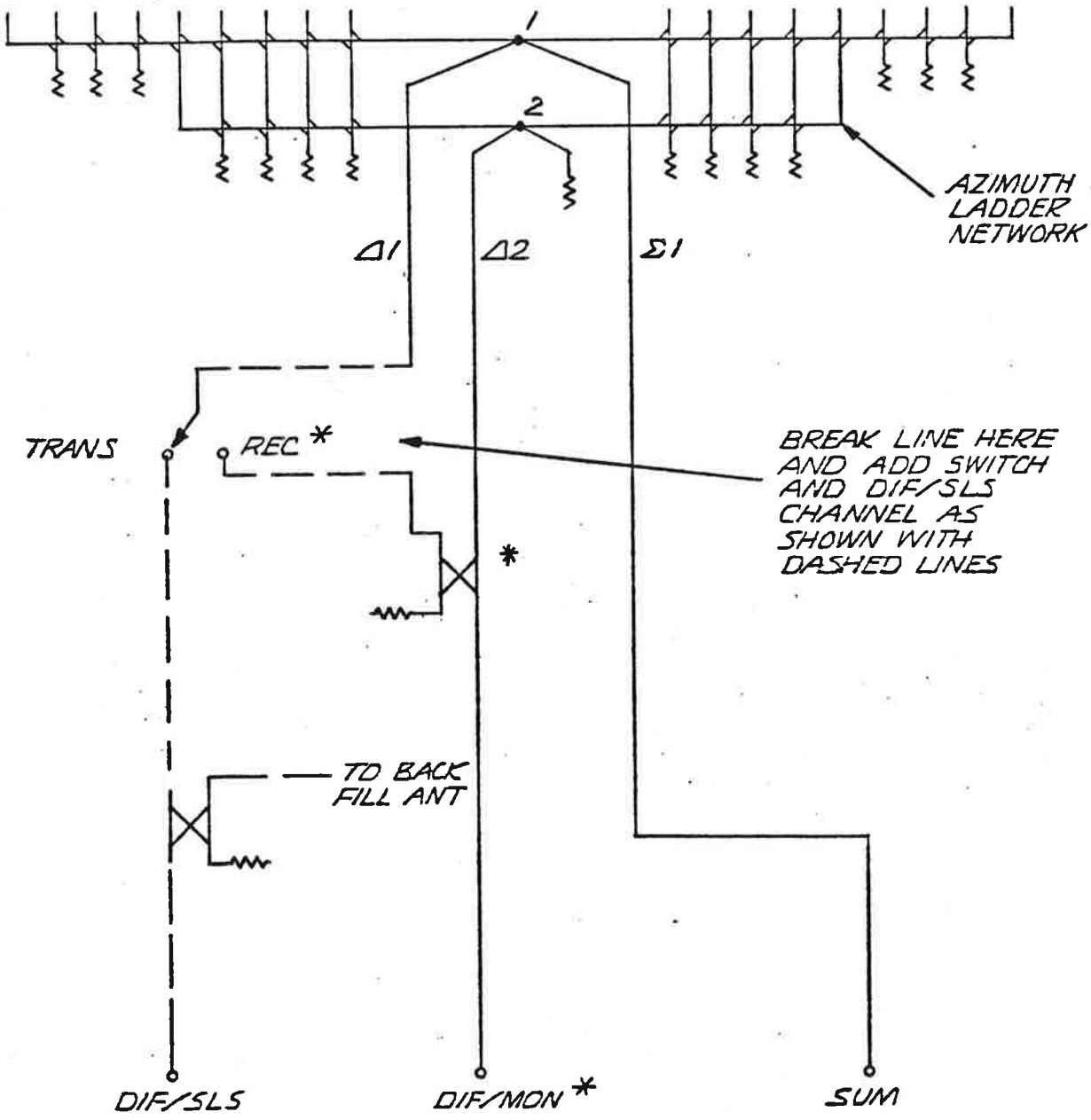

* OMIT IF MONOPULSE IS NOT USED.

Figure 11-1. Modification to Azimuth Network for Addition of Difference SLS

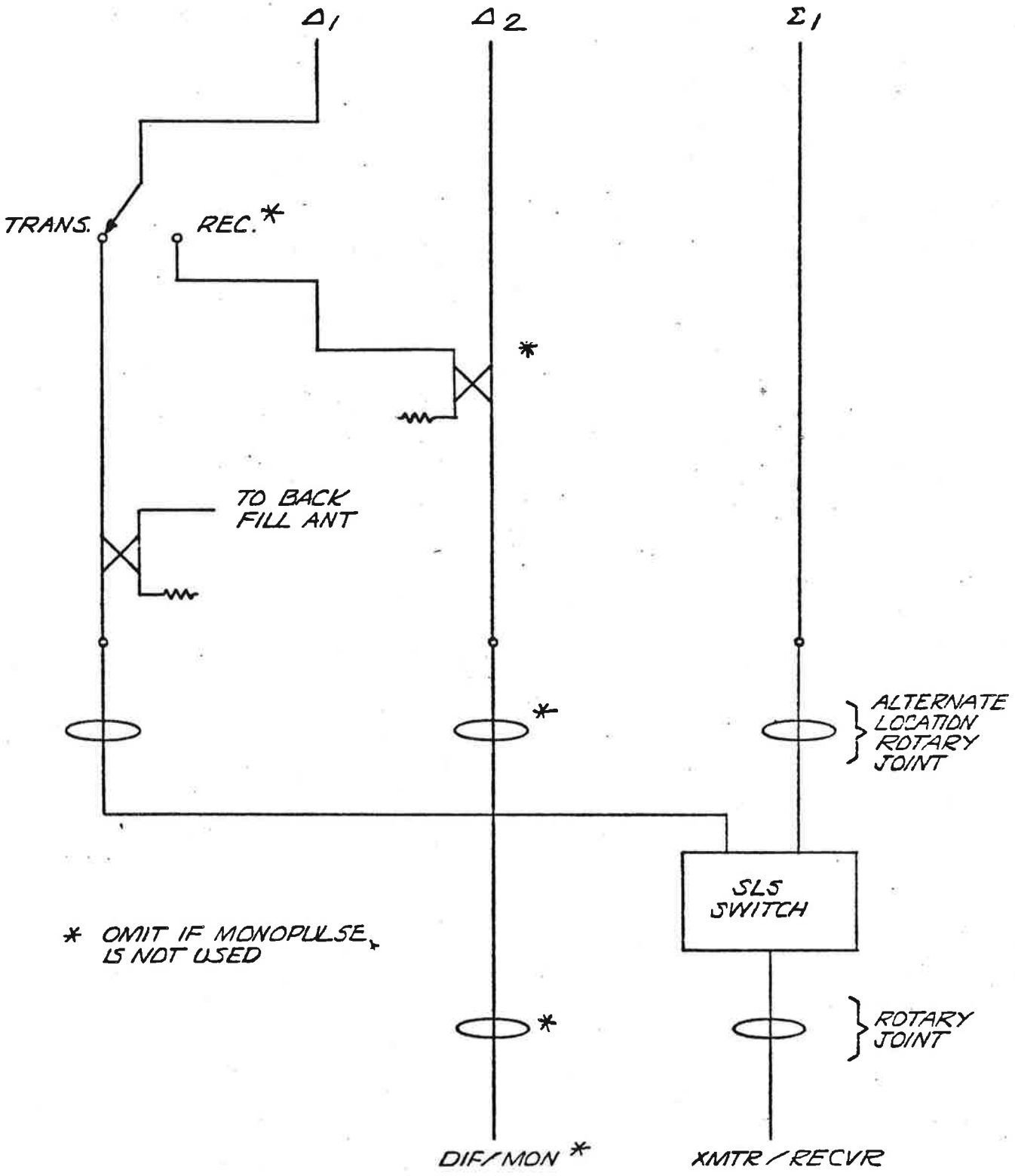

Figure 11-2. Possible Circuit Arrangements for Addition of Difference SLS

DELIVERABLE ITEMS

Table 12-1 lists the proposed performance specifications for the engineering model to be delivered; table 12-2 shows the estimated monopulse performance characteristics of the antenna as presently configured. Additional details on the specifics of the Phase II program are fully discussed in our original proposal, Report 3-5303, Vol. II.

During Phase II, the development phase of the program, Hazeltine will deliver the items listed below. Refer to Program Schedule, figure 12-1.

1. A 4 foot x 26 foot Open Array Antenna, including all components required to radiate a shaped beam in elevation and simultaneous sum and difference beams in azimuth. The array will weight less than 400 lbs. including Backup Structure, and will mount directly to the ASR reflector. The array will be fabricated and tested in accordance with the requirements of Item 5, Section C, Part VI, of the contract.
2. A Backup Structure for installing the Open Array Antenna on the ASR including all necessary hardware.
3. One Low Pass Filter installed in the Open Array Antenna on the sum channel.
4. One 4 foot high Omni Array Antenna. The antenna will be fabricated and tested in accordance with the requirements of Item 5, Section C, Part VI of the contract.
5. Labor and materials necessary for installing both the Open Array Antenna and the Omni Antenna on the ASR-7 at NAFEC.
6. RF Cabling from the antennas to the transmitter and receiver building.

7. A Factory Test Plan and performance of tests, in accordance with the requirements of Item 6, Section C, Part VI of the contract.

8. A Field Test Plan and engineering field services, in accodance with Item 7, Section C, Part VI of the contact.

9. An Instruction Manual, prepared in accordance with the requirements of Item 8, Section C, Part VI of the contract.

10. Preliminary Production Specifications, prepared in accordance with the requirements of Item 9, Section C, Part VI of the contract.

11. Oral Technical Briefings as required by Item 10, Section C, Part VI.

12. A Master Program Schedule and Monthly Progress Reports as required by Item 11, Section C, Part VI.

13. A Master Cost Schedule and Monthly Cost Reports and required by Item 12, Section C, Part VI.

14. A Final Technical Report as required by Item 12, Section C, Part VI.

Table 12-1. Performance Specification

Parameter	Ref. Para.	TSC Spec	H/C Calculated	H/C Design Goal
Directional Pattern Gain	1.4.1	21 dB	21.7 dB	>21 dB
Azimuth Beamwidth 1030 MHz				
horizon (3dB)	1.4.2	2.1° to 2.6°	2.3°	2.1° to 2.6°
horizon (10dB)	1.4.2	<4.5°	4.1°	<4.5°
from -2° to +25°	1.4.2	horizon ±15%	-	horizon ±15%
Azimuth Sidelobes 1030 MHz				
-2° to 0° elev.	1.4.2	-15 dB	-33dB (error free)	-15 dB
0° to 5° elev.	1.4.2	-20 dB	"	-21 dB
+5° to 25° elev.	1.4.2	-15 dB	"	-25 dB
Azimuth backlobes	1.4.2	-21 dB	-25 dB	-21 dB

Table 12-1. Performance Specification

Parameter	Ref. Para	TSC Spec	H/C Calculated	H/C Design Goal
Azimuth beamwidth 1090 MHz	1.4.6	same as 1030	-	same as 1030
Azimuth sidelobes 1090 MHz	1.4.6	same as 1030	-	same as 1030
Elevation Pattern 1030 MHz				
Beam nose	1.4.4 (Rev)*	$<+10^{\circ}$	$+13^{\circ}$	$\leq 13^{\circ}$
Min power $+1^{\circ}$ to $+5^{\circ}$ elev.	1.4.4	-5 dB	-5 dB	-5 dB
Max power -1° elev.	1.4.4	-7.5 dB	-7.6 dB	-7.5 dB
Max power $<-9^{\circ}$ elev.	1.4.4	-21 dB	-24 dB	-20 dB
Ripple $+5^{\circ}$ to $+30^{\circ}$ elev.	-	-	2.2 dB	3.0 dB
Elevation Pattern 1090 MHz	1.4.6	same as 1030	-	same as 1030
Directional beam skew lower 3dB point to $+25^{\circ}$	1.4.5	$\pm 0.3^{\circ}$	-	$\pm 0.3^{\circ}$
Directional beam squint 1030/1090 lower 3dB point to $+25^{\circ}$	1.4.8	$\pm 0.2^{\circ}$	-	$\pm 0.2^{\circ}$
Cross polarized radiation				
1030 MHz -2° to $+25^{\circ}$	1.4.3	<-15 dB	-20 dB	<-15 dB
1090 MHz	1.4.7	<-15 dB	-20 dB	<-15 dB
VSWR	-	-	-	1.5:1
E.M.I. Filter				
Insertion loss	1.6			
1015 to 1105 MHz	1.6	<1.0 dB	-	<1.0 dB
Attenuation	1.6			
1250 to 11,0000 MHz	1.6	>50 dB	-	>50 dB
VSWR	-	-	-	1.25:1

*1.4.4. As revised in contract DOT-TSC-598, page 3, dated April 25, 1973.

Table 12-1. Performance Specification (Cont)

Parameter	Ref. Para	TSC Spec	H/C Calculated	H/C Design Goal
Omni Pattern Uniformity	-	-	±1.5 dB	±1.75 dB
Elev. Pattern Relative to directional	1.4.9	matched		matched ±2 dB
VSWR	-	-	-	1.5:1
Cross Polarization	-	-	-	<-15 dB

Table 12-2. Estimated Monopulse Performance Characteristics

Parameter	Lincoln Laboratory Recommendation	H/C Calculation	H/C Performance Estimate
Sum Gain	20 dB	21.7 dB	21.0 dB
Peak Az. Sidelobes (0^o to 35^o elev.)	21 dB	33 dB (error free)	
Volt. Av. Sidelobes (20^o Az sector) (0^o to 35^o elev.)	-30 dB	-30 dB	-28 dB
Slope	3 dB/deg.	1.3 dB/deg	1.25 dB/deg.
nominal Σ/Δ crossover	3 dB	3 dB	3 dB
Δ/Σ linearity (best lin. fit)	±2%	±6%*	±8%
Δ/Σ slope variation 0^o to 10^o elev.	±2%	-	±4%
10^o to 35^o elev.	±20%	-	±25%
Σ-Δ phase	$\pm 10^o$	-	$\pm 10^o$
Δ Null depth (0^o to 35^o	$\geq$30 dB	-	$\geq$30 dB
Null position (0^o - 10^o elev.)	$\pm 0.02^o$	-	$\pm 0.2^o$
	$\pm 0.02^o$	-	
Rotating Joint Δchannel	Yes	-	Yes
Amplitude unbalance	0.2 dB	-	0.2 dB
Phase unbalance	5^o	-	5^o

*Calculated and measured value for DABS experimental antenna.

APPENDIX A

ANTENNA PATTERNS